COMMUNICATION

Fiber and Monomer Recovery from an Amine-Cured Epoxy Composite Using Molten NaOH-KOH

Received 00th January 20xx,
Accepted 00th January 20xx

DOI: 10.1039/x0xx00000x

Y. Justin Lim,[a§] Zehan Yu,[b§] Valeriy Cherepakhin,[a] Travis J. Williams,[a*] Steven R. Nutt[b*]

We report a rapid route to reclaim carbon fiber (CF) fabric and monomeric chemicals from amine-epoxy CF-reinforced polymer (CFRP) composites. We use a reaction that occurs in molten NaOH-KOH eutectic to selectively cleave aryl ether and amine linkages, which involves two temperature-dependant mechanisms. Bisphenol-A is isolated in up to quantitative yields, and recovered CF fabric is remanufactured into 2nd-generation CFRPs.

Carbon fiber-reinforced polymer (CFRP) composites comprise carbon fibers (CFs) embedded in a polymer matrix. They exhibit exceptional strength-to-weight and stiffness-to-weight ratios and fatigue resistance, making them excellent for aerospace applications. The carbon fiber market is expected to grow at a rate of > 8% annually, and the demand is expected to outstrip the global supply by 2030.[1] In recent years, composite recycling has garnered increasing attention because of the value that can be reclaimed from composite matrices and fibers. However, thermoset CFRPs used in aerospace manufacturing are cured irreversibly, rendering the matrix insoluble/inert, which presents a challenge for recycling. Recent advances in solvolysis have opened promising routes to recover both fibers and monomers from CFRP waste:[2, 3] in fact, we previously introduced oxidative processes to recover clean fibers from benzoxazine[4] and amine-epoxy CFRPs.[5-10] These methods respectively enable the recovery of bisphenol F tetracarboxylate via hydride abstraction[4] and bisphenol A (BPA) via oxygen atom transfer.[6] The academic community's interest in CFRP recycling is also growing, as we've witnessed an increase in composite recycling publications in just the last year. Some of these approaches accomplish full dissolution of the matrix, but most struggle with the collection of organic monomers.[11] While many technologies exist to recover oligomeric/polymeric material from composite matrices, our interviews with resin manufacturers indicate that the market will only appreciate known, existing monomers as matrix recyclates. This is necessary (1) fully to characterize the materials, (2) to assure manufacturers of product consistency, and (3) to drop into existing supply chains.

The introduction of hydroxide-based methods has been a major advancement in amine-cured epoxy CFRP recycling was.[12-16] We find hydroxide-based strategies to be particularly interesting because of their ability to remove the matrix from the fibers and the potential to recover monomeric chemicals in high yields. Herein, we introduce a new hydroxide-based, solvent-free method that is the first to recover both CF fabrics and organic monomers: BPA and for the first time the linking diamine. Compared to the current state of the art, as summarized in Table S1, this method eliminates the flammability and explosivity risks associated with organic solvents under pressure (e.g., toluene, THF, and dioxane)[12, 13, 16] at high temperatures (< 340 °C).[14, 15] Furthermore, higher temperature techniques have resulted in the degradation of organic products, and conversely, lower temperature techniques (160-190 °C) take up to 24 hours to complete while being unable to recover amine recyclates from thermoset composite substrates.[12, 13, 16] Our method is advantageous because it can recover clean fibers and monomers efficiently (220°C, 0.5 hours), thus reducing energy costs, and does not require the use of metal catalysts, therefore avoiding the threat of resource depletion.[12, 13, 16] Additionally, the ability to recover both BPA and diamines provides a valuable economic incentive.

Our process enables near-quantitative recovery of BPA from an aerospace epoxy composite (T_g > 175 °C) with concurrent collection of the linking diamine in high yields (59%). In the case of a diamine with a sulfone bond such as 3,3'-

[a] *Loker Hydrocarbon Research Institute, Wrigley Institute of Environmental Studies, and Department of Chemistry, University of Southern California, 837 Bloom Walk, Los Angeles, California, 90089, USA*
[b] *MC Gill Composites Center, Mork Family Department of Chemical Engineering and Material Science, University of Southern California, 3651 Watt Way, Los Angeles, California, 90089, USA*
[§] *Co-first author.*
[*] *Co-corresponding author.*
† Electronic Supplementary Information (ESI) available

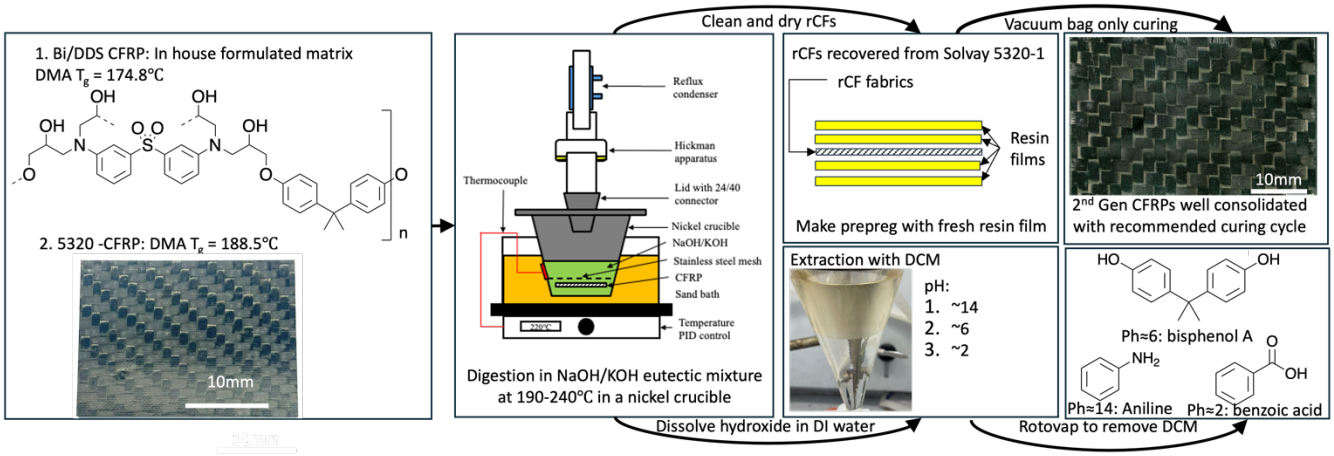

Scheme 1 NaOH-KOH eutectic recycling process for recovering and reusing CFs and monomeric chemicals from amine-epoxy CFRPs

diaminodiphenylsulfone (3,3'-DDS), the collected amines consist of aniline and 3-aminophenol. Finally, we demonstrate that the recovered fibers can be used to produce second-generation CFRPs. Key findings from this study reveal an unreported 1,2-hydride shift during matrix degradation, conservation/recovery of the diamine monomer, and characterization of the surface chemistry of recovered fibers and understanding how that impacts the loss in short beam shear strength (SBS) of second-generation composites.

We tested our method on two separate CFRPs: first, Bi/DDS panels (T_g = 175 ℃) produced using a resin formulated in-house, comprising the diglycidyl ether of bisphenol A (DGEBA) and 3,3'-DDS (Scheme 1). Second, 5320-1 CFRP laminates (T_g = 189 ℃) were produced from commercial resin films (Solvay 5320-1) to demonstrate our method on aerospace material. Once fully cured, Bi/DDS and 5320-1 CFRPs were cut to coupons for digestion.

We use a 1:1 NaOH-KOH eutectic that serves as a solvent and reagent to accomplish CFRP matrix cleavage. The eutectic leverages a relatively low melting point (170 ℃), low volatility, and high reactivity.[17] In preparation, CFRPs produced from Bi/DDS are treated with an organic solvent to swell the matrix. Benzyl alcohol was selected as the pre-treatment solvent due to its effectiveness in swelling and environmental friendliness (Section 3a, SI). After pretreatment at 185 ℃ for 5 hours, Bi/DDS CFRPs are then digested using NaOH-KOH eutectic in a 100 mL nickel crucible equipped with a Hickman distillation head (Scheme 1). Reactions were performed at 190-240 ℃ for 15 minutes to 7 hours in a PID-controlled sand bath (section 3b(SI) and Table S5). Then, CFs were washed, dried, and weighed to calculate the matrix conversion (Table S6). We found pretreatment has a profound effect on the matrix dissolution rate as the matrix decomposition ratio of the pretreated CFRPs is greater than that of untreated ones (Table S6, entries 1-8, and Figure S5). We then compared matrix dissolution rates after three hours and found the effect is more apparent at lower temperatures: 89% vs. 6% at 190 ℃ and 99% vs. 47% at 240 ℃. We rationalize the efficacy of benzyl alcohol pretreatment as causing matrix swelling and extensive delamination of the composites (Figure S3), thus facilitating hydroxide diffusion between plies and accelerating matrix digestion. We then determined the treatment duration of the pretreated Bi/DDS CFRPs at different temperatures to be 7 hours at 190 ℃ to 15 minutes at 240 ℃ (Figure S6), and therefore selected 220 ℃ for 30 min as our optimized conditions for its reasonable duration, preservation of CF properties, and milder temperature.

CF fabrics can then be readily recovered and compared to virgin fabrics using SEM, XPS, and tensile tests. Based on SEM images (Figures 1, S10, and S11), the recovered CFs appeared clean and undamaged. XPS C(1s) spectroscopy shows that the C-O concentration on CF surface decreased, indicating diminution of the sizing functionalities of the fibers, as shown in Figure 2. As expected, an XPS surface elemental composition study (Table S8) showed that hydroxide treatment decreases the O/C ratio. Single-fiber tensile strength data (Figures S14, Tables S9-S14) showed that the recovered CFs retain > 92% of the strength and > 99% modulus of the virgin material.

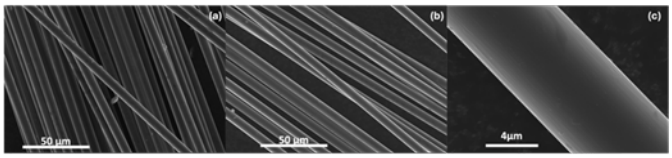

Figure 1 SEM images of fresh (a) and recycled CFs at 220℃ (b,c)

After examination of the fibers, we used the recovered fabrics as substrates to produce 2nd generation CFRPs. Figure S8 illustrates the remanufacturing process with CF fabric recovered from a 5320-1 CFRP: first, 5320-1 samples (50.8 x 38.1 mm) are digested in 140 g NaOH-KOH eutectic mixture (20 hrs, 220 ℃). Recovered CF fabrics are washed successively with acetone, deionized water, and dimethyl sulfoxide. After drying, fabrics are combined with fresh Solvay 5320-1 resin film and cured. Cross-sections of the resulting second-generation CFRPs were polished and examined with a microscope, showing complete consolidation (Figure S9) and demonstrating the viability of direct remanufacturing of CF fabric from molten NaOH-KOH conditions. Table S7 shows SBS test results of remanufactured and first-generation 5320-1 CFRPs. SBS values of remanufactured 5320-1 CFRP decreased by 23.7% compared to first-generation, indicating weaker adhesion strength

between resin and recycled CFs. This is consistent with the diminution of sizing functionality, as observed by XPS.

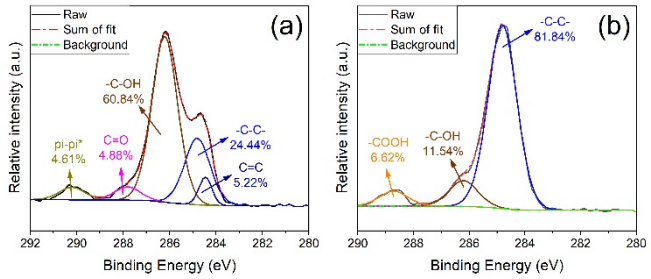

Figure 2 XPS C(1s) high resolution spectra of fresh (a) and recycled CFs at 220 ˚C (b)

However sizing can be restored by nitric acid treatment.[18, 19]

We then analyzed matrix degradation products, which enabled us to develop a monomer recovery procedure (Scheme 1 and Figure S15) for recovery of bisphenol A, benzoic acid, aniline, and 3-aminophenol. In the case of pretreated CFRPs, a pH-controlled extraction from the post-digestion melt provides bisphenol A (86% molar yield). The hydroxide digestion of untreated CFRPs (250-280 ℃, Table S20) gives bisphenol A (92-99%), aniline (< 30%), and 3-aminophenol (< 37%). ^{1}H NMR spectra of the crude products, as isolated by simple extraction, are shown in Figure 3. Although this separation procedure works well, note that the proposed technique consumes a considerable amount of water, acid, and/or hydroxide. To address this concern, we demonstrated ion exchange chromatography as an alternative strategy to isolate BPA (Section 8, SI). Ion exchange chromatography has proven to be advantageous in this situation, because it minimizes the amount of water and acid needed to isolate BPA, while enabling up to 91 mol% recovery of hydroxide (Table S18), determined by titration (section 8, SI).

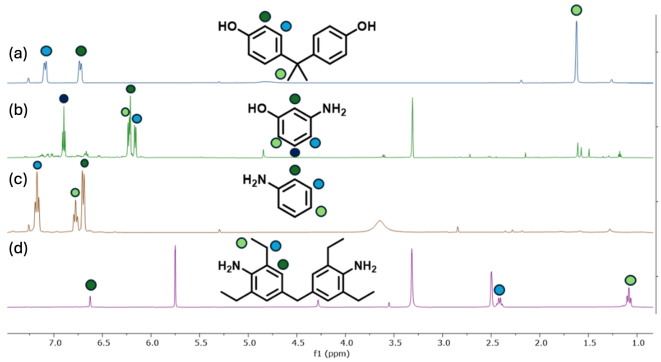

Figure 3 ^{1}H NMR spectra of isolated aniline (a), BPA (b) and 3-aminophenol (c) from unpretreated Bi/DDS sample digestions and MDEA (d) from Bi/MDEA digestion

To account for the formation of BPA, we explored the possibility of three chemical mechanisms: an intermediate epoxide (recently characterized independently by Skrydstrup and Beckham),[12, 13] E2 elimination, or a 1,2-hydride (Scheme 3). A model degradation study was conducted to probe this with our conditions. We found that reactivity between Model 1 and NaOH-KOH is consistent with two of the possible mechanisms: intermediate epoxide[12, 13] and 1,2-hydride shift. Formation of 3-butoxypropane-1,2-diol (detected by LC-MS) from Model 1 at 150 ℃ favors the epoxide-mediated step. However, at higher temperature (180 ℃), Model 1 generates 1-butoxypropan-2-on, suggesting the 1,2-hydride shift path. The presence of the ketone was confirmed with the annotated ^{1}H NMR, ^{13}C NMR,

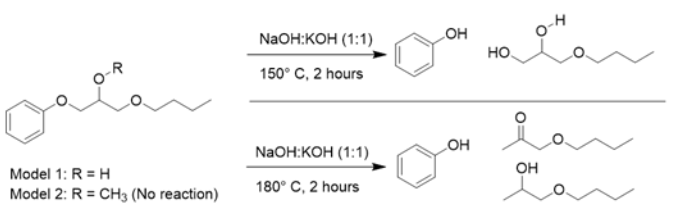

Scheme 2 Degradation of model compounds with NaOH-KOH

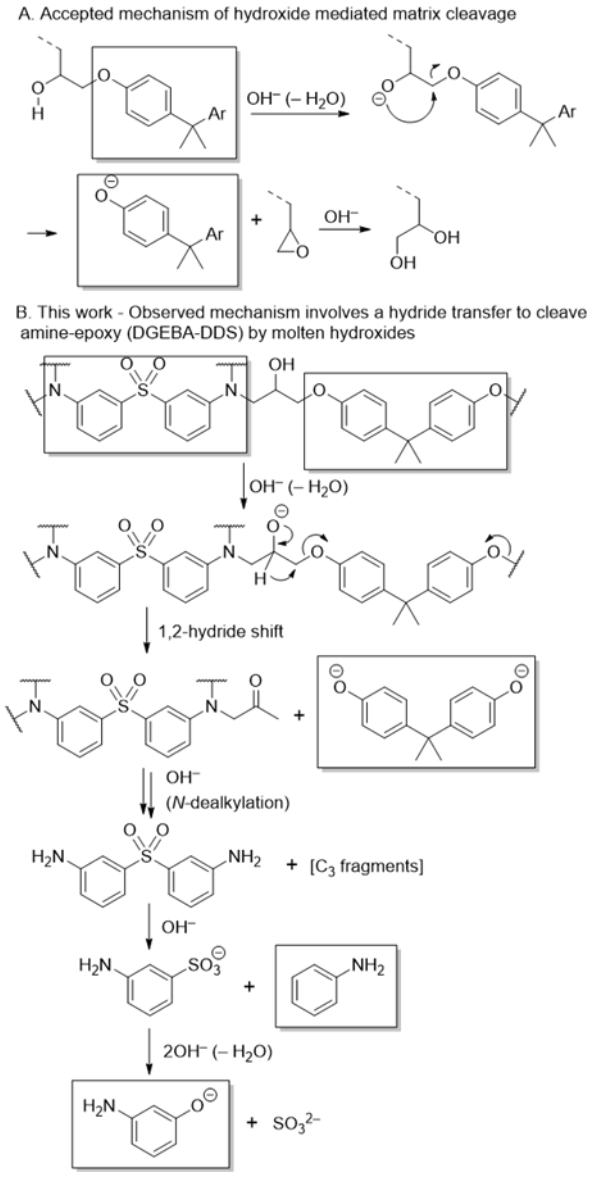

Scheme 1 Hydroxide-driven cleavage of CFRP matrices

HMBC, and HSQC data in section 11b of the SI. Additionally, no reactivity was observed with the *O*-methylated Model 2 (180 ℃). This finding highlights the necessity of the intermediate

alkoxide for aryl ether cleavage and diminishes the likelihood of an E2 path. We then rationalize the formation of amine products such as aniline and 3-aminophenol from a hydroxide-driven *N*-dealkylation of 3,3'-DDS and aryl sulfone bond cleavage. Also, the absence of 3,3'-DDS in the matrix digest is consistent with the known instability of sulfone groups to molten hydroxide.[20, 21] We then performed an experiment to confirm the instability of the sulfone by putting 3,3'-DDS under molten hydroxide conditions. Here we observed that upon heating to 190 ˚C, the sulfone cleaved apart (Section 13, SI). To achieve recovery of the diamine monomer at respectable yields we recommend digesting thermoset systems without sulfone bonds. We demonstrate this in Sections 2c and 3f (SI) by manufacturing and digesting a resin system cured by the diamine monomer 4,4'-Methylenebis(2,6-diethylaniline) (MDEA). In this experiment, we confirmed that diamines without sulfones can be conserved (^{1}H NMR, ^{13}C NMR, MALDI, Figure S39-43) and recovered at high yields (59%, Table S22). The ^{1}H NMR spectra of the recovered diamine is shown in Figure 3. Finally, simple extraction of the pretreated reaction's acidic compounds reveals the presence of benzoic acid which can be explained by apparent hydroxide-driven benzyl alcohol dehydrogenation left over from pretreatment.[22]

In sum, this work accomplishes recovery/remanufacturing of CF fabric from aerospace composites and recovers monomers from the matrix itself. This method selectively deconstructs DGEBA-DDS/MDEA matrices to saleable monomeric units, BPA, aniline, 3-aminophenol, and MDEA. The efficient reaction degrades pretreated CFRP matrices fully within 30 minutes. Recovered CFs retain their woven architecture and tensile strength (> 92%). Despite changes to the surface chemistry of the recycled fiber fabric, we show the remanufacturing of rCF sheets isolated from hydroxide-based matrix cleavage. SBS of second-generation CFRPs were then characterized. Furthermore, we show mechanistic variation in chemical polymer cleavage depending on temperature, an insight that we are presently working to exploit.

Conflicts of interest

Williams is the founder of Closed Composites, a start-up aiming to commercialize composite materials recycling.

Data availability

The data supporting this article have been included as part of Supplementary Information.

Acknowledgement

This work is sponsored by the MC Gill Composites Center at USC and the National Science Foundation (CMMI-2134658). and TJW thanks NSF for BRITE award sponsorship (CMMI-2227649). We thank the NSF (CHE-2018740, DBI-0821671, CHE-0840366), the NIH (S10 RR25432), and USC Research and Innovation Instrumentation Awards for analytical tools. Huntsman Corporation and Solvay generously donated epoxy, amine curing agent, and prepreg used in this study. We thank Professor Ajit Mal and his student Fadhel Alsaffar for SBS characterization. We thank Qixuan Chang for SEM analyisis and Tom Czyszczon-Burton for XPS characterization. We thank Wendy Fei for experimental preparation.

Notes and references

1. J. Zhang, V. S. Chevali, H. Wang and C.-H. Wang, *Composites Part B: Engineering*, 2020, **193**, 108053.
2. C. A. Navarro, C. R. Giffin, B. Zhang, Z. Yu, S. R. Nutt and T. J. Williams, *Materials Horizons*, 2020, **7**, 2479-2486.
3. S. K. Kristensen, A. Ahrens, B. S. Donslund and T. Skrydstrup, *ACS Organic & Inorganic Au*, 2024.
4. J. N. Lo, S. R. Nutt and T. J. Williams, *ACS sustainable chemistry & engineering*, 2018, **6**, 7227-7231.
5. C. A. Navarro, Y. Ma, K. H. Michael, H. M. Breunig, S. R. Nutt and T. J. Williams, *Green Chemistry*, 2021, **23**, 6356-6360.
6. C. A. Navarro, E. A. Kedzie, Y. Ma, K. H. Michael, S. R. Nutt and T. J. Williams, *Topics in catalysis*, 2018, **61**, 704-709.
7. Z. Yu, Y. J. Lim, T. Williams and S. Nutt, *Green Chemistry*, 2023, **25**, 7058-7061.
8. Y. Ma, C. A. Navarro, T. J. Williams and S. R. Nutt, *Polymer degradation and stability*, 2020, **175**, 109125.
9. Y. Ma, D. Kim and S. R. Nutt, *Polymer Degradation and Stability*, 2017, **146**, 240-249.
10. C. Olivar, Z. Yu, B. Miller, M. Tangalos, C. B. Jenkinson, S. R. Nutt, B. R. Oakley, C. C. Wang and T. J. Williams, *Journal of the American Chemical Society*, 2024.
11. N. F. Torkaman, W. Bremser and R. Wilhelm, *ACS Sustainable Chemistry & Engineering*, 2024, **12**, 7668-7682.
12. R. C. DiPucchio, K. R. Stevenson, C. W. Lahive, W. E. Michener and G. T. Beckham, *ACS Sustainable Chemistry & Engineering*, 2023, **11**, 16946-16954.
13. H. Sun, A. Ahrens, G. M. F. Batista, B. S. Donslund, A. K. Ravn, E. V. Schwibinger, A. Nova and T. Skrydstrup, *Green Chemistry*, 2024, **26**, 815-824.
14. W. Nie, J. Liu, W. Liu, J. Wang and T. Tang, *Polymer Degradation and Stability*, 2015, **111**, 247-256.
15. J. TAKAHASHI and T. WAJIMA, *International Journal of the Society of Materials Engineering for Resources*, 2022, **25**, 85-89.
16. T. Skrydstrup, A. Ahrens, A. Bonde, H. Sun, N. Wittig, A. Sommerfelt, S. Frølich and H. Birkedal, 2022.
17. H. Otto and R. Seward, *Journal of Chemical & Engineering Data*, 1964, **9**, 507-508.
18. J. Jang and H. Yang, *Journal of materials science*, 2000, **35**, 2297-2303.
19. T. A. Langston and R. D. Granata, *Journal of composite materials*, 2014, **48**, 259-276.
20. C. K. Ingold and J. A. Jessop, *Journal of the Chemical Society (Resumed)*, 1930, 708-713.
21. D. F. Othmer and C. E. Leyes, *Industrial & Engineering Chemistry*, 1941, **33**, 158-169.
22. E. E. Reid, H. Worthington and A. W. Larchar, *Journal of the American Chemical Society*, 1939, **61**, 99-101.

Fiber and Monomer Recovery from an Amine-cured Epoxy Composite using Molten NaOH-KOH

Y. Justin Lim,[a§] Zehan Yu,[b§] Valeriy Cherepakhin,[a] Travis J. Williams,[a*] and Steven R. Nutt[b*]

[a] *Loker Hydrocarbon Research Institute, Wrigley Institute for Environment and Sustainability, and Department of Chemistry, University of Southern California*

[b] *Department of Chemical Engineering and Materials Science, University of Southern California*

[§] Co-first Author

[*]Co-Corresponding Author: travisw@usc.edu

[*]Co-Corresponding Author: nutt@usc.edu

Table of contents:

        - Benzoic acid isolation
7. **Unpretreated composite degradation components**
8. **Ion exchange chromatography**
9. **Bi/MDEA neat resin degradation component**
    a. Organic base extract from dichloromethane
        - MDEA isolation
    b. Organic neutral extract from dichloromethane
        - Bisphenol A isolation
10. **Reaction yields**
    a. Determination of unit polymer
    b. Verification of proposed unit polymer using CHNS elemental analysis
    c. Reaction yields of degradation components from Bi/DDS sample digestion
    d. Reaction yields of degradation components from Bi/MDEA sample digestion
11. **Model 1 synthesis and degradation reactions**
    a. Synthesis of Model 1
    b. Degradation of Model 1 at 180 ˚C
    c. Degradation of Model 1 at 150 ˚C
12. **Model 2 synthesis and degradation reactions**
    a. Synthesis of Model 2
    b. Degradation of Model 2 at 180 ˚C
    c. Degradation of Model 2 at 150 ˚C
13. **3,3’-DDS degradation experiments**

1. **Literature review on the current state of the art of alkali and molten salt-based amine-epoxy recycling strategies**

Table S1. Summary of alkali-based recycling strategies in literature.

Ref	Reagents		Temperature (ºC)	Pressurized	Treatment duration (hours)	Monomer recovery
This work	**NaOH/KOH eutectic salt**		**190-240**	**N**	**0.25-7**	**BPA, amines**
Yan. et al[1]	1-propanol	KOH	280-340	Y	1-5	N/A
Liu. et al[2]	phenol	KOH	300-325	Y	0.5-3	N/A
Jiang. et al[3]	polyethylene glycol	KOH	160	N	3.3	N/A
Zhao.et al[4]	MEA	KOH	160	N	1.5	N/A
DiPucchio.et al[5]	Organic solvents	KOtBu/KOH	140-160	Y	24-48	BPA, amines*
Ahrens.et al[6]	Organic solvents	triphos-Ru-TMM	160	Y	24	BPA
Sun.et al[7]	Organic solvents	NaOH	190	Y	24	BPA
Takahashi.et al[8]	Molten NaOH salt		250-350	N	1-1.5	N/A
Wu.et al[9]	$KCl/ZnCl_2$ eutectic salt	TiO_2	350	N	1.5	N/A
Ren.et al[10]	Molten Na_2CO_3/NaOH		350-400	N	2	N/A
Nie.et al[11]	Molten KOH salt		285-350	N	0.5-2	N/A

***: Amine recovery reported from molecular models and thermoplastics**

2. **General Procedure**

a. Fabrication of Bi/DDS amine-epoxy CFRP

Matrix of Bi/DDS amine-epoxy CFRPs was formulated using diglycidyl ether of bisphenol A (17.95 g, epoxy equivalent weight (EEW) = 187 g/eq; Araldite GY6010, Huntsman) and 3,3-diaminodiphenyl sulfone (6.05 g, amine hydrogen equivalent weight (AHEW) = 63 g/eq, ARADUR 9719-1, Hunstman). The mixing ratio of amine and epoxy was 100%, and the amounts of reagents (g) were calculated using EEW and AHEW. Amine and epoxy were hand-mixed in an aluminum jar for 10 min. Then, the mixture was heated and vacuum degassed in a vacuum oven at 120 ℃ until the mixture became clean and homogenous.

Resin films were then prepared on a Wabash hot press. Resin mixture (4.5 g) was spread on a 203 x 203 mm release film (Airtech, Release Ease 236 TFNP) preheated to 60 ℃ on the hot press. Then, two resin films were attached to pre-cut CF fabrics (203 x 203 mm, 2 x 2 twill, FiberGlast 1069). Then, the stack was heated and pressed by the hot press at 60 ℃ with 0.1 tons force (18.8 Kpa) for 2 mins.

Cured Bi/DDS CFRP panels were then laminated via a vacuum bag-only process (VBO) using 4 layers of prepreg. The curing cycle was (1) 1.5 ℃ /min to 120 ℃, (2) hold at 120 ℃ for 3 hrs,

(3) 1.5 °C/min to 180 °C and (4) hold at 180 °C for 3 hrs. Fully cured Bi/DDS CFRP panels were cut into 50.8 x 10.2 mm samples on a water-jet cutter (ProtoMax, OMAX).

b. Fabrication of 5320-1 CFRP

5320-1 CFRPs were fabricated using commercial aerospace-grade resin film (Solvay CYCOM 5320-1). Resin films were cut into 203 x 203 mm. 2 layers of resin films were attached to pre-cut CF fabrics (203 x 203mm, 2 x 2 twill, FiberGlast 1069). Prepreg was fabricated by heating and pressing the stack on a hot press at 60 ℃ with 0.1 tons force (18.8 kPa) for 2 mins. After cooling down, release films of prepreg were peeled off, and an additional 2 layers of resin film were attached to the prepreg. Then, the stack was heated and pressed again on a hot press at 60 ℃ with 0.1 tons force (18.8 kPa) for 2 mins.

5320-1 CFRP panels were then laminated via the VBO process using 4 layers of prepreg. The curing cycle was (1) hold at 60 °C for 2 hrs, (2) 1 °C/min to 120 °C, (2) hold at 120 °C for 2 hrs, (3) 1.7 °C/min to 177 °C, and (4) hold at 177 at 120 °C for 2 hrs. Fully cured 5320-1 CFRP panels were cut into 50.8 x 38.1 mm samples on a water-jet cutter (ProtoMax, OMAX).

c. Fabrication of Bi/MDEA neat resin samples

Bi/MDEA neat resin samples were formulated using diglycidyl ether of bisphenol A (3.53 g, epoxy equivalent weight (EEW) = 187 g/eq; Araldite GY6010, Huntsman) and 4,4'- methylenebis (2,6-diethylaniline) (MDEA, 1.47 g, amine hydrogen equivalent weight (AHEW) = 78 g/eq, Sigma-Aldrich). The mixing ratio of amine and epoxy was 100%, and the amounts of reagents (g) were calculated using EEW and AHEW. Amine and epoxy were hand-mixed in an aluminum jar for 10 min. The mixture was then heated, and vacuum degassed in a vacuum oven at 120 ℃ until the mixture became clean and homogenous.

Resin mixture was then poured into cubic silicone molds (10 x 10 x10 mm), and transferred to a convection oven for curing. The curing cycle was (1) 1.5 °C /min to 120 °C, (2) hold at 120 °C for 3 hrs, (3) 1.5 °C/min to 180 °C and (4) hold at 180 °C for 3 hrs. Fully cured Bi/M-DEA neat resin cubes were ground using an electrical grinder.

d. Matrix content weight (W_m) percent measurement of Bi/DDS CFRPs

Matrix contents of CFRP samples were determined using the method described in ASTM D3171-22, Procedure B. Weights of CFRPs were first weighted to the nearest 0.0001 gram (Mi). Then, CFRPs were placed into a 100 mL 2-neck round bottom flask with sulfuric acid (50 mL, 95-98%). The flask was heated to 100 ℃ in an oil bath with magnetic stirring and a reflux condenser connected. Hydrogen peroxide (10 mL, 30%) was added to the flask each time at 1, 2, and 3 hrs of reactions. After 4 hrs, the flask was removed from the oil bath to cool to room temperature. CFs were filtered out and washed with DI water and acetone. Cleaned CFs were dried in a convection oven at 125 ℃ overnight and weighed again to the nearest 0.0001 gram (Mf). W_m is calculated using the following equation. Six measurements were taken on Bi/DDS CFRP, as shown in the Table S2.

$$W_m = \frac{(M_i - M_f)}{M_i} \times 100\%$$

Table S2. Summary of matrix content weight measurement of Bi/DDS CFRP.

Entry	M_i (g)	M_f (g)	W_m (%)
1	0.5825	0.2906	50.11
2	0.5591	0.2953	47.18
3	0.5746	0.2924	49.11
4	0.6379	0.3173	50.26
5	0.5567	0.3015	45.85
6	0.5541	0.3015	45.59
	Avg		48.02

e. T_g measurement of Bi/DDS and 5320-1 CFRPs

Glass transition temperatures (T_g) were measured on TA instrument Q800 DMA using a dual cantilever fixture following ASTM D 7028-07 standard. DMA samples (60 x 10 mm) were cut from fully cured Bi/DDS and 5320-1 CFRP panels on a water jet cutter (ProtoMax, OMAX). Heating rate, frequency, and strain amplitude were set as 5 ℃/min, 1 Hz, and 0.05%, respectively. Measurement started at 40 ℃ and ended at 250 ℃ (Bi/DDS CFRP) or 300 ℃ (5320-1 CFRPs), as shown in Figures S1-S2. T_g (onset of storage modulus), T_{loss}, and $T_{tan\delta}$ (temperatures at loss modulus and tanδ peaks) are summarized in Table S3.

Table S3. DMA T_g measurements of Bi/DDS and 5320-1 CFRPs.

CFRPs	T_g (℃)	T_{loss} (℃)	$T_{tan\delta}$ (℃)
Bi/DDS	174.84	182.00	184.01
5320-1	188.49	209.24	214.74

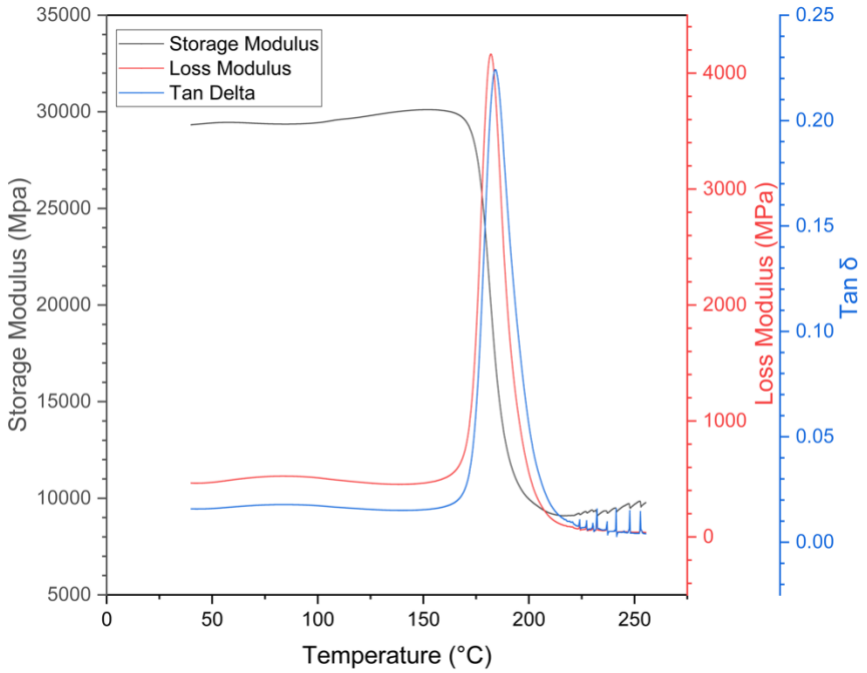

Figure S1. DMA T_g measurements of Bi/DDS CFRP

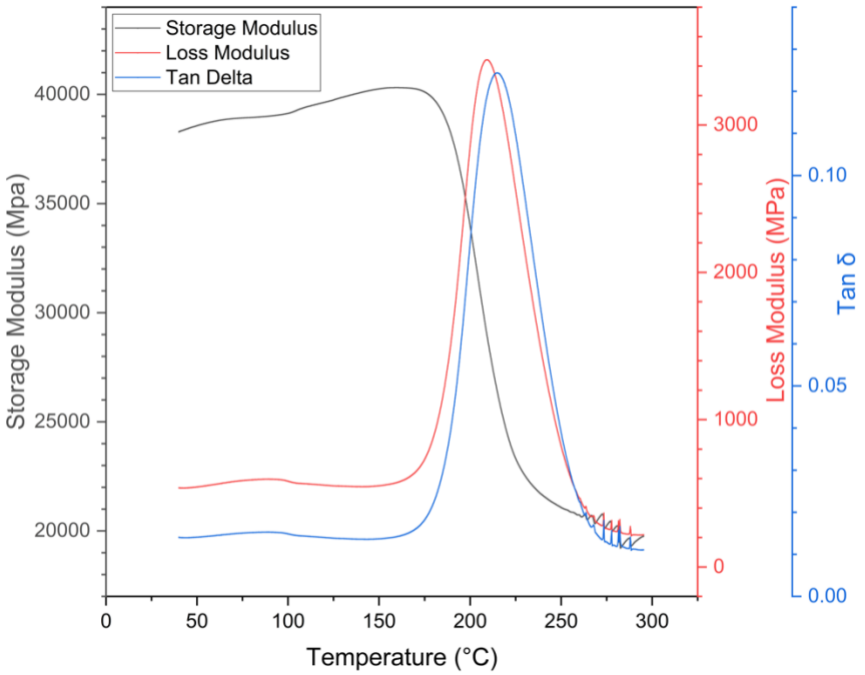

Figure S2. DMA T_g measurements of 5320-1 CFRP.

f. Chemical synthesis and analysis

All synthetic procedures were conducted in a chemical fume hood with exposure to air, unless otherwise indicated. Deuterated NMR solvents were purchased from Cambridge Isotopes Laboratories. Unless otherwise specified, sodium and potassium hydroxide salts and the other reagents are commonly available from major commercial suppliers (Macron Fine Chemicals and VWR chemicals). Other chemicals included benzyl alcohol (TCI America), dichloromethane (EMD Millipore), ethyl acetate (EMD Millipore), bisphenol A diglycidyl ether (Huntsman), 3,3'-diaminodiphenyl sulfone (Huntsman), sodium hydride (Acros Organics), 1-butanol (BeanTown Chemical), sulfuric acid (Supelco), hydrochloric acid (Sigma-Aldrich), hydrogen peroxide (EMD Millipore), iodomethane (Sigma-Aldrich), and glycidyl phenyl ether (Thermo Fisher Scientific Chemicals). These chemicals were used without further purification. Deionized water was purified in-house using a deionizer cartridge (Philadelphia Scientific).

NMR spectra were recorded on a Varian Mercury 400, Varian VNMRS 500, or VNMRS 600, spectrometers and processed using MestReNova. All chemical shifts are reported in units of ppm and referenced to the residual ^{1}H or ^{13}C solvent peak and line-listed according to (s) singlet, (bs) broad singlet, (d) doublet, (t) triplet, (dd) double doublet, etc. ^{13}C spectra are delimited by carbon peaks, not carbon count. Mass spectral data were acquired on an Agilent 6545 LC-QTOF instrument with electrospray set to positive ionization and a Bruker AutoFlex MALDI. IR data were acquired on a Thermo Fisher Nicolet 4700 FT-IR spectrometer.

Silica sulfuric acid catalysts were made in our labs. These catalysts were prepared by soaking 20 grams of silica-gel with 25 mL of concentrated sulfuric acid in a 100 mL beaker. Afterwards, the beaker was placed in a heated oil bath (130 °C) for one hour and was carefully monitored. After one hour had elapsed, the contents were transferred to a 250 mL round bottom flask and placed in a heated rotary evaporator (95 °C) for 30 minutes under reduced pressure. Finally, the contents of the flask were transferred to a glass jar and stored in a desiccator.

3. **Molten hydroxide digestion of CFRPs**

a. Pre-treatment of Bi/DDS CFRPs

A pre-treatment step was applied to Bi/DDS CFRP before molten hydroxide digestion. This process involved the use of organic solvents to swell the CFRP matrix to reduce the rate-limiting factor of diffusion. To effectively swell the matrix, pre-treatment temperatures need to be higher than T_g of CFRP, which requires pre-treatment agents with a boiling point > 190°C. Solvents with appropriate boiling points are summarized in Table S4, alongside their safety, health, and environmental assessments from the CHEM 21 solvent selection guide. *N*-Methyl-2-pyrrolidone (NMP) was excluded due to its significant health risks. Ethylene glycol and benzyl alcohol were selected and tested for pre-treating Bi/DDS CFRPs.

Table S4. Selection of solvents with desirable boiling point from CHEM 21 solvent guide.

Solvent	BP (ºC)	Safety Score	Health score	Env. score	Ranking
Benzyl alcohol	206	1	2	7	Problematic
Ethylene glycol	198	1	2	5	Recommended
NMP	202	1	9	7	Hazardous

A Bi/DDS CFRP sample (50.8 x 10.2 mm) was first weighted to the nearest 0.0001 gram (M_i) and then placed in a 50 mL single-neck round bottom flask with benzyl alcohol or ethylene glycol (25 mL). The flask was then heated to 185 °C with a reflux condenser connected. After 5 hours, the pre-treated Bi/DDS CFRP was retrieved and then prepared for hydroxide eutectic digestion. Light microscope images of pre-treated Bi/DDS CFRP samples in ethylene glycol and benzyl alcohol were shown in Figure S3 (b) and (c) respectively. Benzyl alcohol was selected as pr-treatment solvent as it clearly outperformed ethylene glycol, inducing more significant swelling of the CFRP matrix, as shown in the Figure S3.

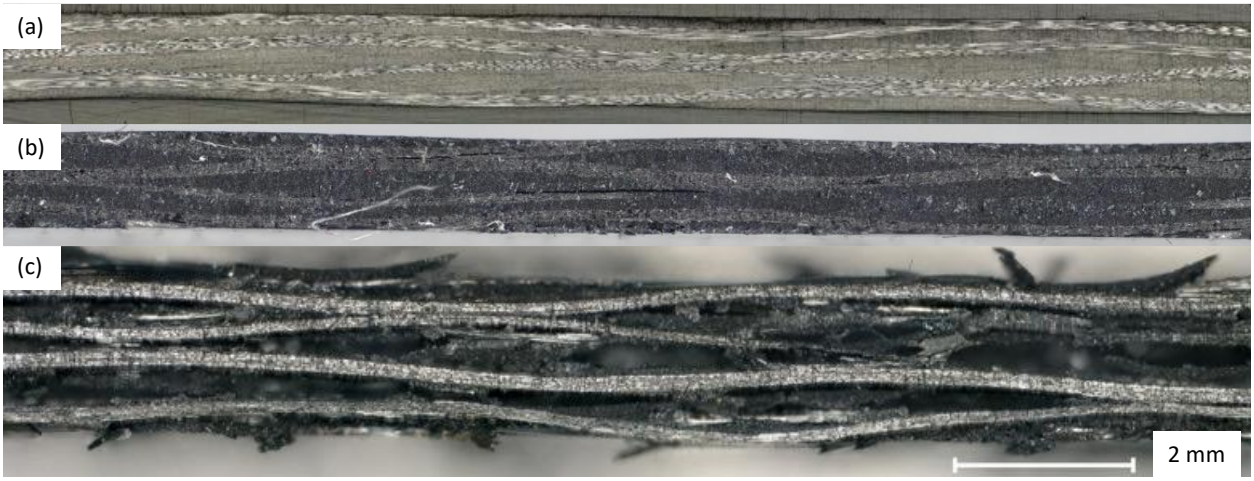

Figure S3. Cross-sectional images of Bi/DDS CFRPs before (a), after ethylene glycol (b) and benzyl alcohol (c) pre-treatment

b. Molten hydroxide digestion of Bi/DDS CFRPs

NaOH and KOH pellets were ground to a fine powder using a pill grinder. A mixture of NaOH and KOH (40 g, 1:1 molar) was placed in a 100 mL nickel crucible. A thermocouple was attached to the crucible using high-temperature tapes (flash breaker, Airtech). The crucible and hydroxide mixtures were then heated to pre-set temperatures in a sand bath. A pre-treated Bi/DDS CFRP was placed into the crucible. A stainless-steel mesh (304 stainless steel, 5 mesh, 46 mm diameter) was placed on top of the CFRP to ensure the sample was fully submerged in hydroxide mixtures. A customized stainless-steel lid with a 24/40 female joint was placed on top to connect a Hickman distillation apparatus to collect volatiles, as shown in Figure S4.

After a reaction period, the recycled CFs were taken out from molten hydroxide mixture and cooled to room temperature. The recycled CFs were washed with DI water and acetone three times and dried in a convection oven at 125 ℃ overnight. Dried CFs were weighted to the nearest 0.0001 gram. Hydroxide melts were subjected to extraction following the procedure described in Section S5. Table S5 summarizes the digestion experiments performed on Bi/DDS CFRPs.

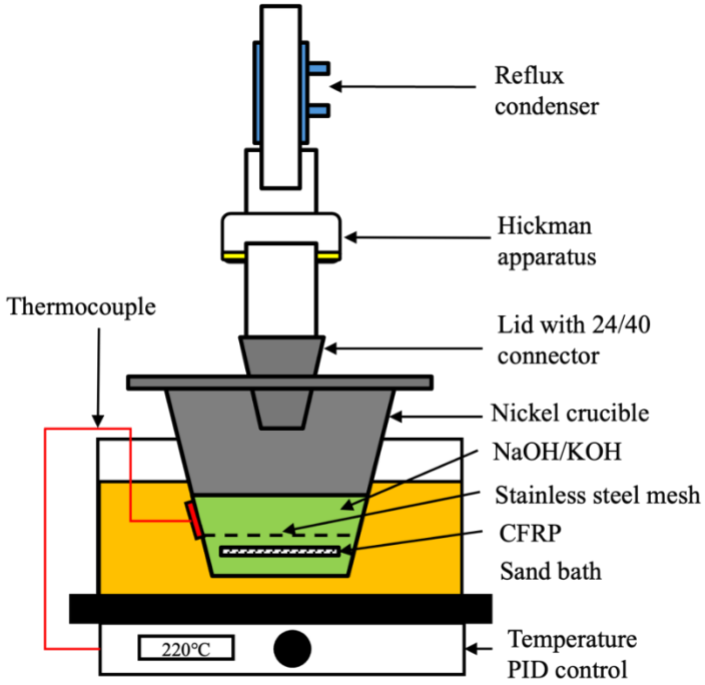

Figure S4. Schematic diagram of Bi/DDS CFRP decomposition setup

Table S5. Summary of Bi/DDS CFRP digestion experiments.

Entry	Substrate	$M_{eutectic}$ (g)	Temperature (°C)	Duration (hr)
1	Bi/DDS CFRPs	40	190	3
2			200	
3			220	
4			240	
5	Pre-treated Bi/DDS CFRPs		190	3
6			200	
7			220	
8			240	
9			240	0.25
10			220	0.25
11				0.5
12			200	0.5
13				1
14				4
15				5
16			190	1
17				4
18				5
19				6
20				7

c. Effect of pre-treatment on digestion efficiency

The purpose of pre-treatment is to use organic solvent to swell the cross-linked network of the matrix, inducing delamination, as shown in Figure S3, thus reducing the rate-limiting effect of diffusion. Entry 1-4 and 5-8 in Table S6 study the effect of the pre-treatment on resin decomposition ratio at different temperatures after 3hrs of digestion. Resin decomposition ratios (R_d) are calculated using matrix content weight (W_m), Bi/DDS CFRP weight (M_i), and recovered CF weight (M_d) as summarized in Table S6 and Figure S5:

$$R_d = \frac{M_i - M_d}{M_i \times W_m} \times 100\%$$

Table S6. Summary of the effect of pre-treatment on digestion efficiency.

Entry	M_i (g)	M_d (g)	R_d (%)
1	0.5798	0.5623	6.3
2	0.5849	0.5459	13.9
3	0.5672	0.4863	29.7
4	0.5616	0.4359	46.6
5	0.594	0.3417	88.5
6	0.5797	0.3228	92.3
7	0.5882	0.3062	99.8
8	0.5869	0.3075	99.1

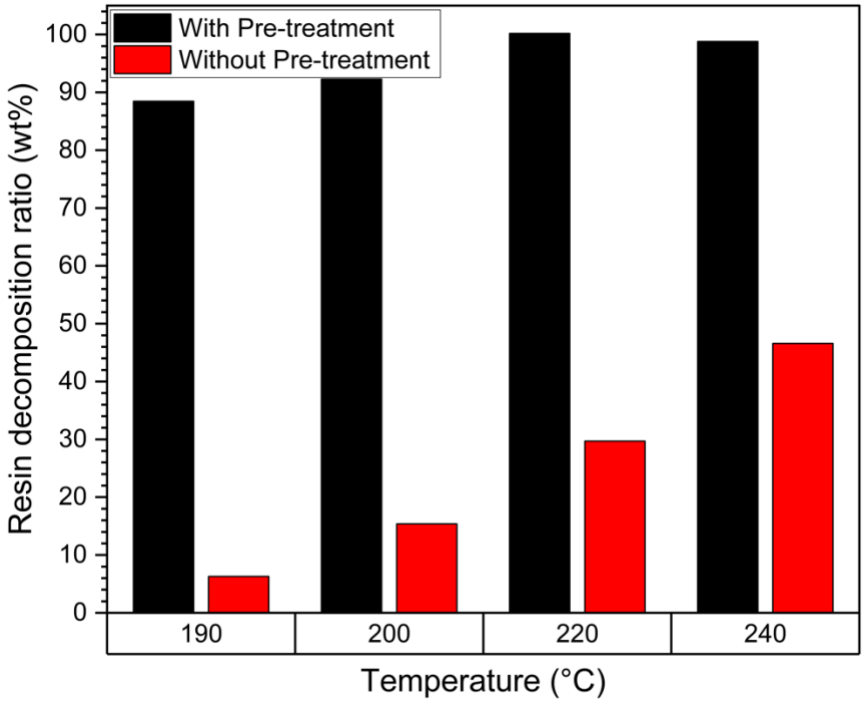

Figure S5. Effect of pre-treatment on matrix dissolution rate at different temperatures.

d. Digestion duration at different temperatures

Matrix dissolution time of Bi/DDS CFRPs were determined by performing reaction with incremental treatment duration as shown in Table S3, Entry 5-19. After each digestion, rCFs were cleaned, dried, and visually inspected for resin residues. The 240 and 220 ℃ reactions were monitored incrementally every 15 minutes. The 200 and 190 ℃ reactions were monitored incrementally every 60 minutes. The matrix dissolution times at selected temperatures are summarized in Figure S6.

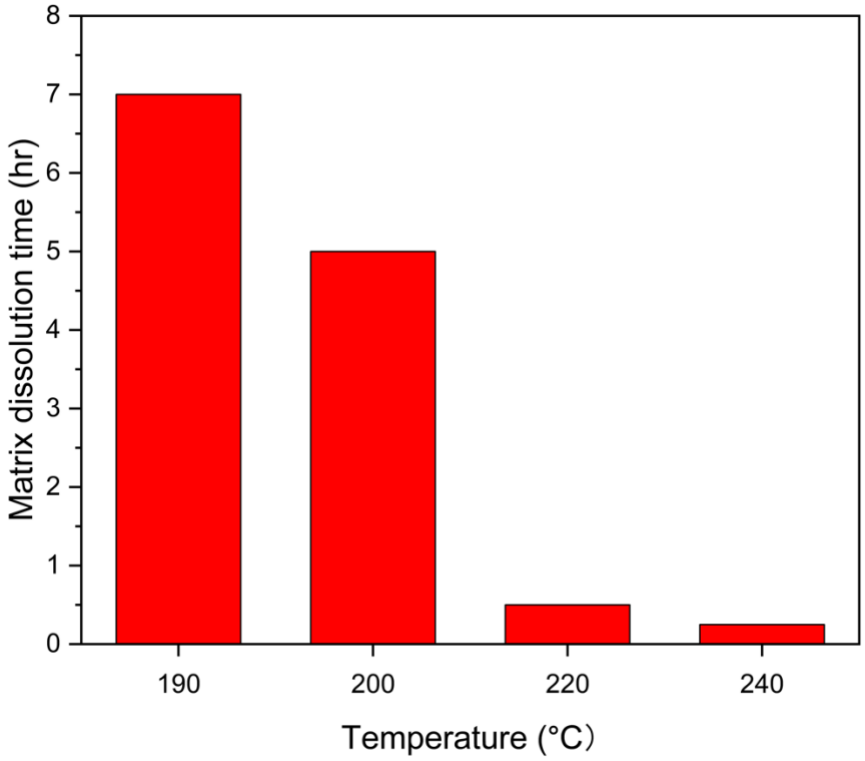

Figure S6. Matrix dissolution time of Pre-treated Bi/DDS CFRP at different temperatures.

e. Molten hydroxide digestion of 5320-1 CFRPs

A mixture of NaOH and KOH (140 g, 1:1 molar) powders were placed in a 100 mL nickel crucible. The crucible, with a nickel lid on top and a thermocouple attached, was then heated to 220 ℃ in a sand bath. A 5320-1 CFRP sample (50.8 x 38.1 mm) was placed into the crucible for digestion, as shown in Figure S7. After 20 hrs, recycled CFs were retrieved from the crucible and cooled to room temperature. Then, recycled CFs were washed with DI water, acetone, and dimethyl sulfoxide (DMSO) three times. Cleaned CFs were dried in a convection oven at 125 ℃ overnight. Dried CFs were used with fresh resin films to manufacture 2nd-Generation 5320-1 CFRPs, as described in Section S3 part (a).

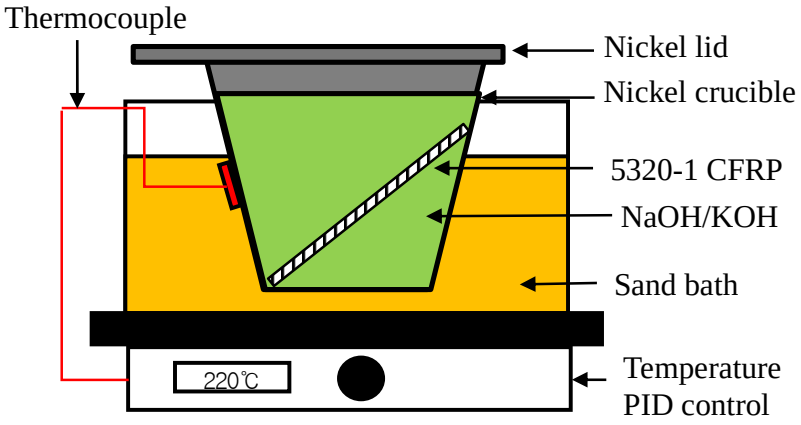

Figure S7. Schematic diagram of 5320-1 CFRP decomposition setup.

f. Molten hydroxide digestion of Bi/M-DEA neat resin samples

Digestion of unpretreated Bi/M-DEA neat resin was performed using a 15 g mixture of NaOH and KOH (40 g, 1:1 molar) placed in a 100 mL nickel crucible. The crucible and hydroxide mixture were heated to 260 ℃ in a sand bath. Pre-grounded Bi/M-DEA neat resin (0.2018 g) was placed into the crucible. A customized stainless-steel lid with a 24/40 female joint was placed on top to connect a Hickman distillation apparatus to collect volatiles, as shown in Figure S4. The resin was completely dissolved after 6 hours of reaction at 260 ℃.

4. **Manufacture 2nd Gen 5320-1 CFRPs using recovered CFs**

a. Fabrication of 2nd Gen 5320-1 CFRPs

As shown in Figure S8, recycled CFs (~50.8 x 38.1 mm) were combined with fresh resin film (50.8 x 38.1 mm, Solvay CYCOM 5320-1) to fabricate prepreg and 2nd generation 5320-1 CFRPs following the same procedure described in Section S1(b). A reference 5320-1 CFRP was made with fresh CFs (50.8 x 38.1 mm) as a benchmark for characterizing 2nd CFRPs.

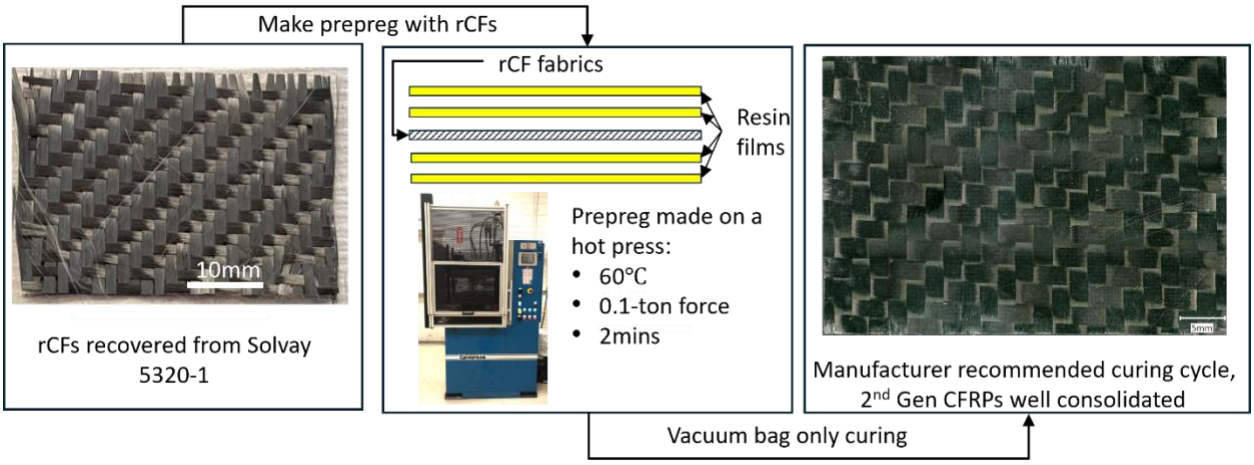

Figure S8. Process to remanufacture recovered CFs into 2nd Gen CFRPs.

b. Polished cross-section of 2nd Gen 5320-1 CFRP

Strips were cut from 2nd generation 5320-1, and its reference using a diamond saw. Strips were mounted with transparent resin (CitoPress-1, Struers) for cross-section polishing. Mounted samples were then polished using silicon carbide papers and aluminum oxide slurry. Polished cross-sections were imaged using a light microscope (X200, VHX5000, Kenyence), as shown in Figure S9.

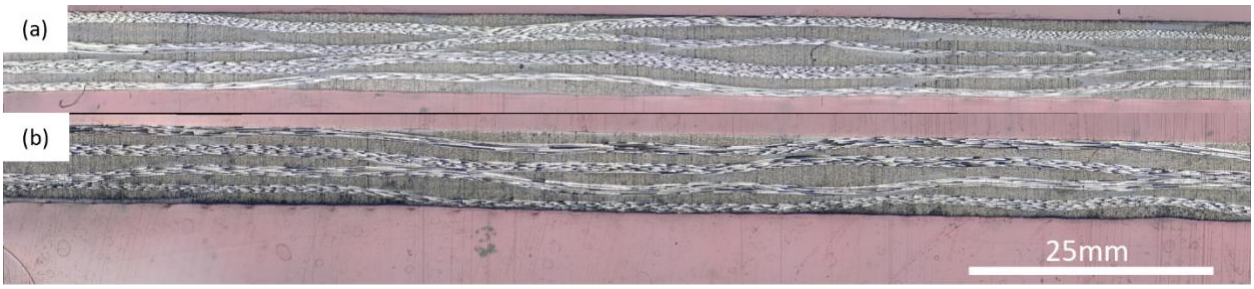

Figure S9. Cross section of reference 5320-1 CFRP (a) and 2nd Gen 5320-1 CFRP (b) at 200X.

c. Short beam shear strength measurement of 2nd 5320-1 gen CFRPs

Short beam shear strength (SBS) samples of reference and 2nd Gen CFRPs were manufactured using 10 layers of fresh or recycled CF fabrics following the procedure described in Section S3 part a. SBS samples (13.7 x 0.46 x 0.23 mm) were cut from fully cured 10-layers 5320-1 reference and 2nd generation CFRP panels on a water jet cutter.

SBS was measured following ASTM D 2344 standard on an INSTRON 5544 load frame equipped with a 2 kN load cell. The speed of crosshead movement was set as 1.0 mm/min. Eight measurements were taken on reference 10-layer 5320-1 CFRP and 8 measurements were taken on 10-layer 2nd generation 5320 CFRPs.

Table S7. SBS measurements of 10-layers ref 5320-1 and 10-layers 2nd Gen 5320-1 CFRPs.

Sample	SBS strength (Mpa)
Ref 5320-1 CFRP	72.67±5.41
2nd Gen 5320-1 CFRP	55.43±3.16
Retention (%)	76.28%

5. **Recycled carbon fiber characterizations**

a. SEM

SEM images were taken on a Helios G4 FIB/SEM (Thermo Scientific). The acceleration voltage and working distance were set as 15 Kv and around 5.5 mm respectively.

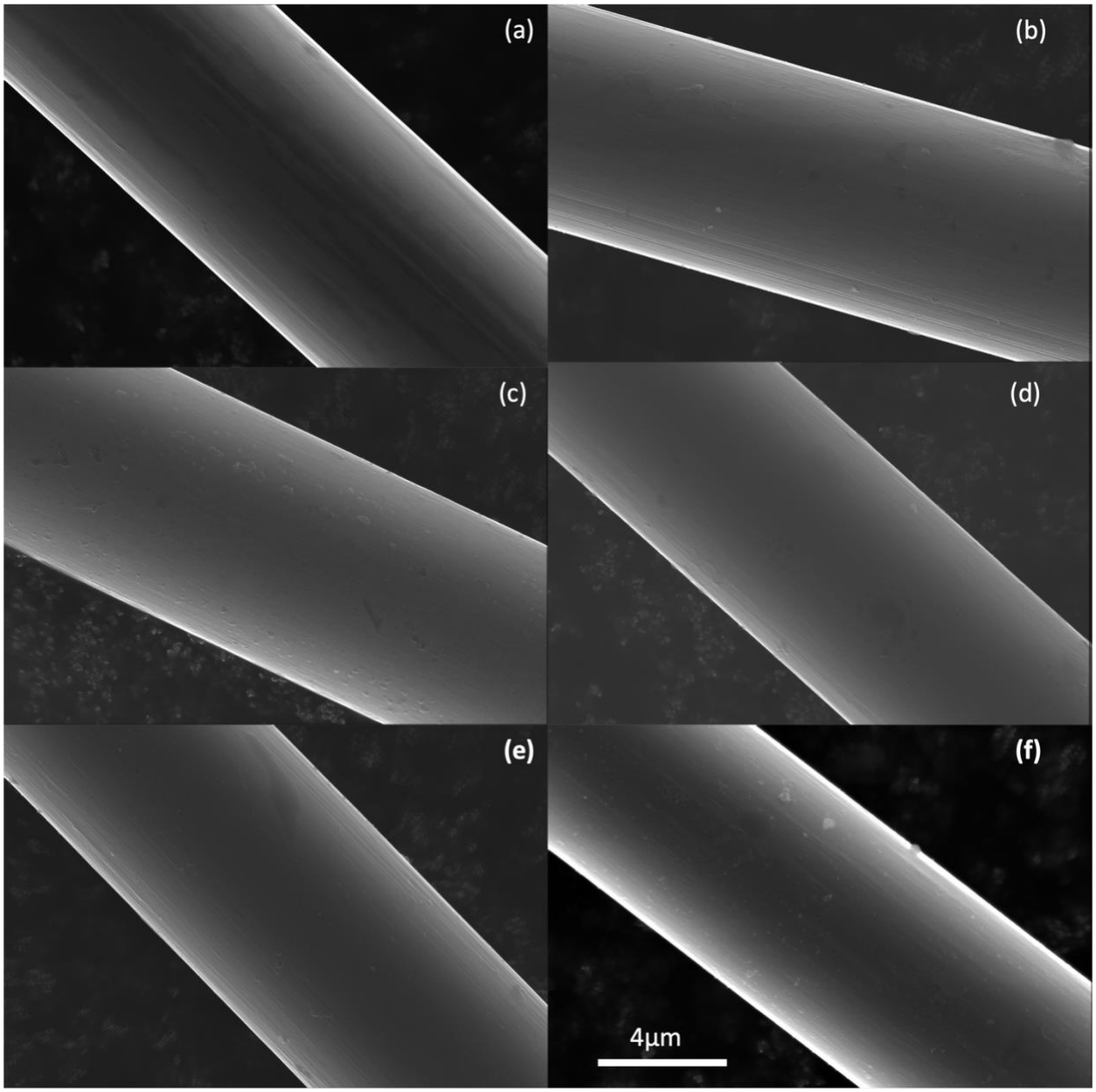

Figure S10. SEM images of fresh CF (a), recycled CFs from Bi/DDS CFRPs at 190 ℃ (b), 200 ℃ (c), 220 ℃ (d), 240 ℃ (e) and 5320-1 CFRP (f) at 2,5000 X.

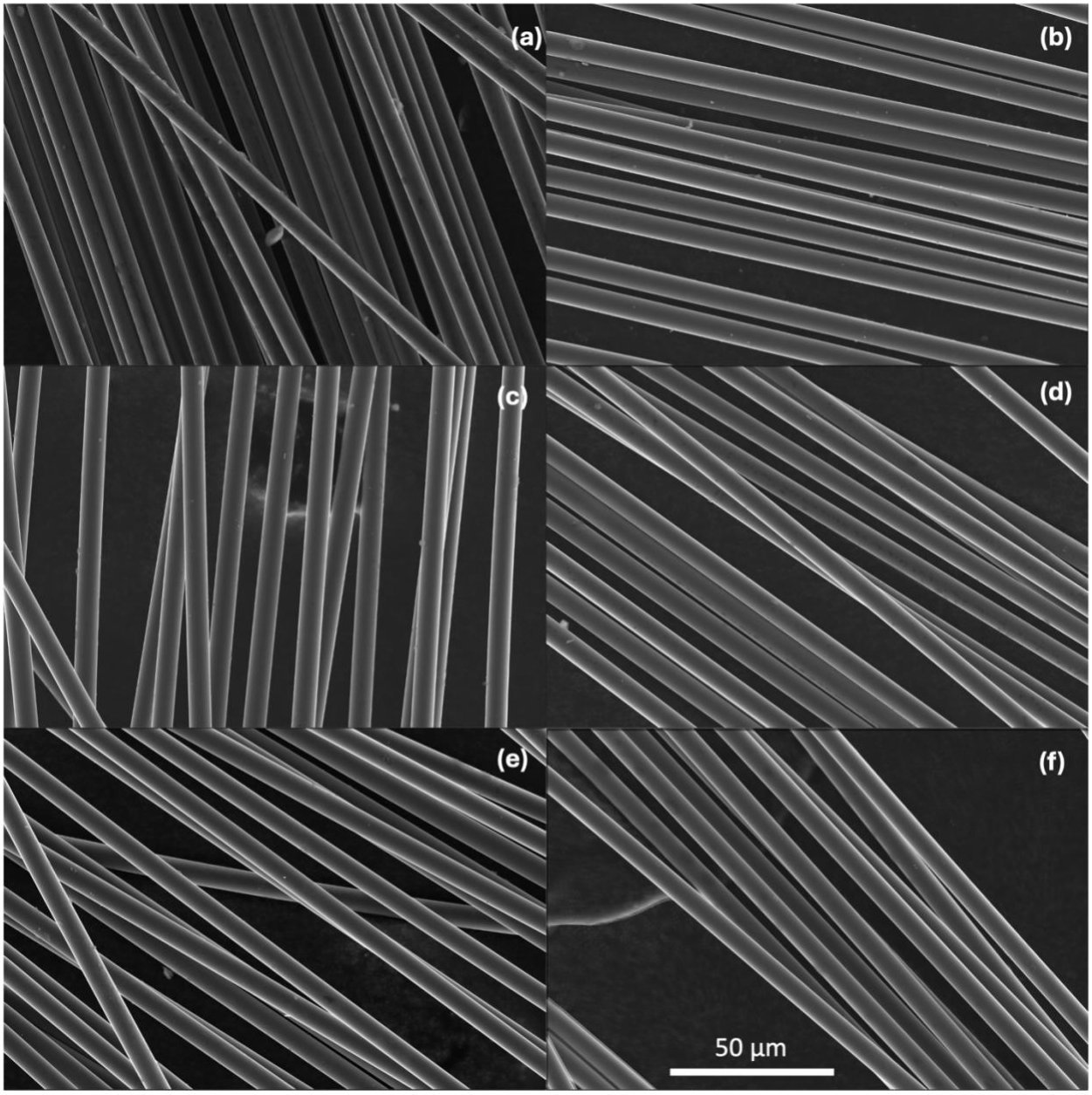

Figure S11. SEM images of fresh CF(a), recycled CFs from Bi/DDS CFRPs at 190 ℃ (b), 200℃ (c), 220℃ (d), 240℃ (e) and 5320-1 CFRP (f) at 2500 X.

b. XPS

X-ray photoelectron spectroscopy (XPS, Kratos Axis Ultra DLD) was used to analyze elements and functional groups on CF surface. A survey scan (0-1200 ev) was first acquired on each sample, followed by a high-resolution C1s scan. X-ray source was mono aluminum, and the incident angle was 90°. Curve-fitting of the C1s spectra was performed in CasaXPS software using Shirley baseline and Gaussian-Lorentzian functions, as shown in Figure S12-S13.

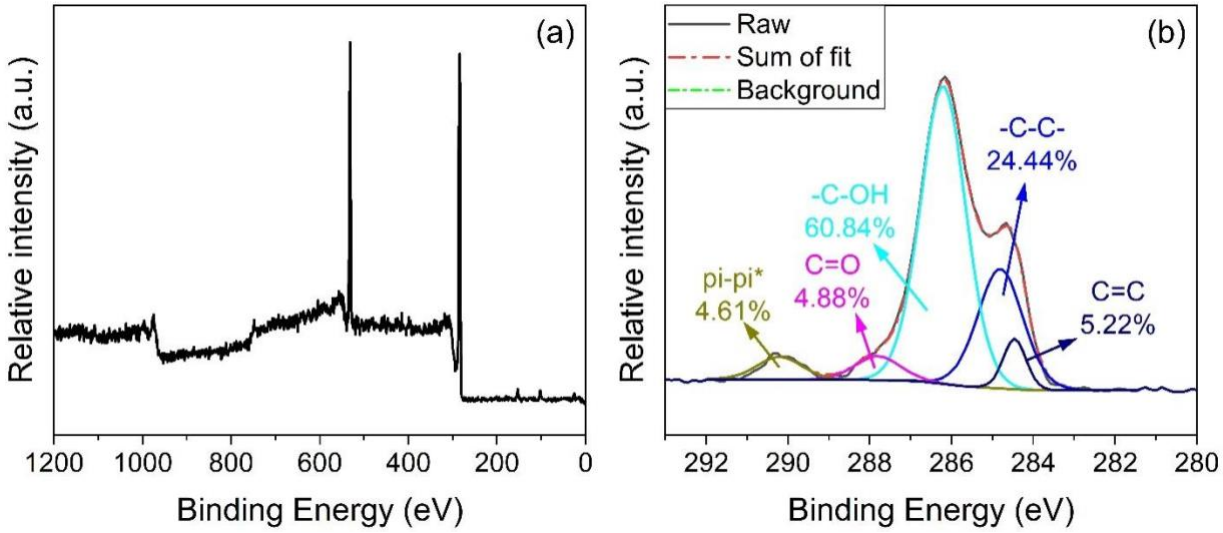

Figure S 12. XPS survey (a) and C1s high-resolution spectra (b) of fresh CF

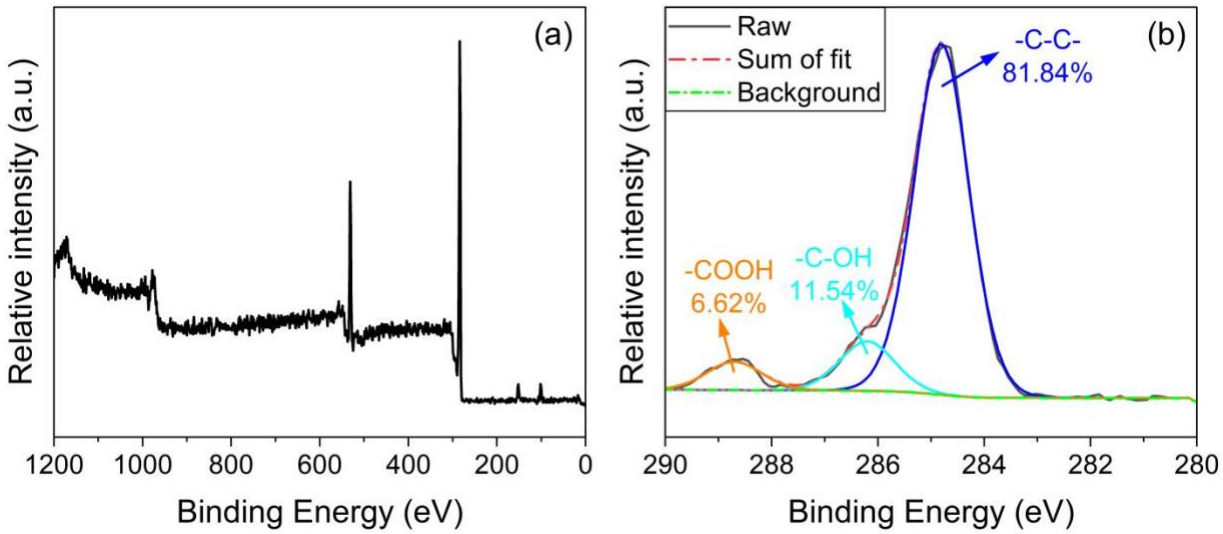

Figure S 13. XPS survey (a) and C1s high-resolution spectra (b) of CFs recovered from a 220 ℃ reaction

XPS survey spectra show four peaks assigned to C, O, N and Si. The detailed element compositions of fresh and recycled CFs are summarized in Table S6. The results show the content ratio of O/C decreased after recycling at 220 ℃ for 30 minutes, indicating the recycled CFs were not oxidized during the recycling.[9]

Table S8. XPS analysis summary of fresh CFs and recycled CFs recovered from 220 ℃.

	Surface element (%)					C1s Components (%)					
Sample	C	N	Si	O	O/C	C-C	C-OH	C=O	O-C=O	C=C	π-π*
Fresh CF*	78.86	1.25	3.35	16.55	20.99	24.44	60.84	4.88	N/A	5.22	4.61
rCF-220	82.19	0.73	4.13	12.95	15.76	81.84	11.54	N/A	6.62	N/A	N/A

*: with sizing

The C1s high-resolution spectra can be curve-fitted into five peaks: C-C (284.8ev), C-OH (286.2 ev), C=O (287.8 ev), O-C=O (288.8 ev) and π-π* satellite (290.2ev).[12] After recycling, C-O concentration greatly decreased. This indicates the sizing agents of the CFs were removed during hydroxide degradation.

c. Single fiber tensile tests of fresh and recycled CFs

The tensile properties of both fresh and recycled CFs were tested in accordance with the ISO 11566 standard. To prepare the samples, individual fibers were separated from tows and mounted on paper strips measuring 81.3 x 25.4 mm, with a 25.4 x 12.7 mm window in the center. Fibers were mount across the center window. Both ends of fiber were affixed using double side tape and epoxy adhesive (Henkel E-20HP) to secure the fibers in place.

Once the epoxy adhesive had cured, the mounted samples were examined using a light microscope (Keyence VHX-5000) using a 1500X lens to measure fiber diameter. The reference length of pixel is calibrated using reference scale (Keyence OP-87426). The diameter of each sample was measured three times, and measured values were averaged to obtain the final measurement. The CF cross-sections were assumed to be circular, and the areas were calculated using the averaged diameters.

After mounting the sample onto the load frame, a cut was made in the center of the mounting sheet to free the fiber for testing. The samples were tested at 2mm/min crosshead speed till break. A total of 200 tests were conducted, with 40 tests performed on fresh CFs and another 160 tests on recycled CFs. The tensile strength was then calculated and plotted against strain (%) using these calculated CF cross-section areas. The slope of stress-strain curves was taken as tensile modulus. Table S9-14 and Figure S14 summarize all tensile test results.

Table S9. Single fiber tensile test summary of fresh and recycled CFs.

Samples	Diameter (μm)	Strain at Break (%)	Tensile Strength (MPa)	Modulus (Gpa)
Fresh CFs	7.47±0.13	1.49±0.30	3244.96±676.10	207.28±11.44
rCF-190	7.51±0.12	1.42±0.31	3196.92±712.37	217.23±7.47
rCF-200	7.43±0.13	1.43±0.25	3151.45±579.72	217.20±13.42
rCF-220	7.43±0.12	1.49±0.25	3179.89±535.30	215.06±13.03
rCF-240	7.41±0.06	1.40±0.30	2975.99±591.12	214.03±11.97

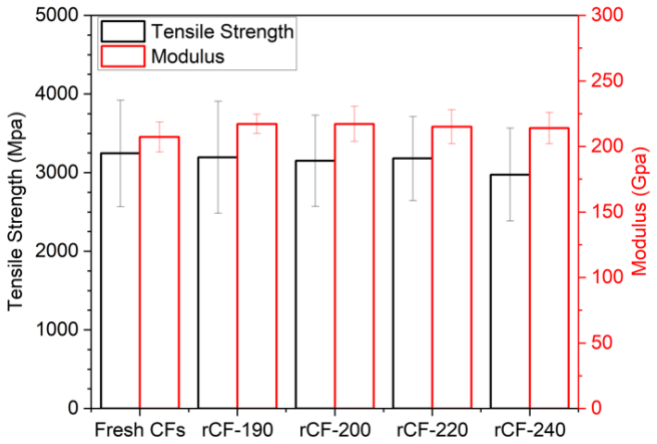

Figure S14. Single fiber tensile strength study of fresh and recycled CFs.

Table S10. Single fiber tensile strength test summary of fresh CFs.

Test#	Diameter (μm)	Strain at break (%)	Force at break(N)	Strength (Mpa)	Modulus (Gpa)
1	7.44	1.55	0.1474	3391.05	214.67
2	7.52	1.80	0.1856	4179.80	217.67
3	7.50	1.78	0.1732	3918.05	207.57
4	7.53	1.58	0.1560	3507.47	208.47
5	7.22	1.66	0.1393	3404.38	193.65
6	7.48	1.12	0.1092	2484.29	206.74
7	7.63	1.17	0.1186	2594.73	212.20
8	7.45	1.90	0.1773	4069.13	209.42
9	7.50	1.21	0.1188	2687.83	213.47
10	7.68	1.22	0.1255	2707.95	210.64
11	7.51	1.56	0.1550	3500.47	217.59
12	7.61	1.52	0.1487	3271.82	208.97
13	7.39	1.56	0.1614	3765.06	211.09
14	7.46	0.80	0.0760	1738.11	199.79
15	7.36	0.81	0.0989	2328.14	202.64
16	7.57	1.48	0.1450	3224.23	211.45
17	7.64	1.69	0.1650	3598.33	208.01
18	7.44	1.66	0.1450	3336.05	192.33
19	7.46	1.49	0.1378	3151.25	203.84
20	7.49	1.05	0.0959	2176.95	197.60
21	7.68	1.58	0.1534	3310.00	203.66
22	7.49	1.54	0.1475	3345.22	211.79
23	7.56	1.59	0.1650	3674.86	224.13
24	7.03	1.83	0.1466	3777.51	200.82
25	7.48	1.03	0.0985	2239.98	207.54
26	7.56	2.01	0.2002	4465.49	219.32
27	7.43	1.28	0.1064	2455.93	187.05
28	7.43	1.38	0.1293	2983.21	209.32
29	7.47	1.61	0.1509	3444.00	208.93
30	7.39	1.31	0.1068	2492.16	184.99
31	7.58	1.94	0.1801	3997.02	198.44
32	7.47	1.45	0.1306	2981.25	197.87
33	7.07	1.36	0.1433	3652.06	232.83
34	7.57	0.95	0.0779	1730.63	177.73
35	7.41	1.88	0.1869	4336.84	228.31
36	7.48	1.84	0.1691	3847.34	201.90
37	7.50	1.38	0.1388	3140.59	201.90
38	7.35	1.60	0.1627	3837.28	217.49
39	7.33	1.71	0.1672	3963.75	229.31
40	7.53	1.52	0.1375	3088.06	199.87
Average	7.47	1.49	0.1420	3244.96	207.28
STDV.P	0.13	0.30	0.0294	676.10	11.44

Table S11. Single fiber tensile strength test summary of recovered CFs at 190 ℃.

Test#	Diameter (μm)	Strain at break (%)	Force at break(N)	Strength (Mpa)	Modulus (Gpa)
1	7.65	1.31	0.1323	2881.91	218.49
2	7.54	1.16	0.1091	2445.07	217.92
3	7.48	1.16	0.1721	3919.08	215.52
4	7.48	1.12	0.1088	2474.96	219.49
5	7.66	1.12	0.1882	4090.37	220.76
6	7.50	1.73	0.1695	3839.09	220.07
7	7.48	1.52	0.1449	3299.10	215.66
8	7.45	1.76	0.1695	3891.03	224.20
9	7.71	1.76	0.1798	3853.11	221.28
10	7.51	1.49	0.1392	3143.60	211.42
11	7.31	1.00	0.0863	2057.10	203.30
12	7.44	0.70	0.0674	1552.97	217.50
13	7.45	1.49	0.1504	3452.65	211.42
14	7.39	1.70	0.1494	3484.21	205.02
15	7.66	1.49	0.1494	3240.97	217.54
16	7.39	1.40	0.1297	3026.32	217.48
17	7.41	1.60	0.1406	3264.20	198.92
18	7.82	1.54	0.1563	3256.35	211.33
19	7.45	1.48	0.1484	3404.91	228.02
20	7.59	1.85	0.1832	4050.21	221.15
21	7.37	1.15	0.1070	2508.75	214.93
22	7.51	0.99	0.0992	2241.49	222.93
23	7.53	1.61	0.1628	3656.91	228.73
24	7.52	1.77	0.1794	4038.13	229.61
25	7.41	0.86	0.0814	1886.11	217.62
26	7.72	1.28	0.1316	2810.24	216.45
27	7.74	1.50	0.1598	3395.51	223.96
28	7.41	1.74	0.1552	3600.46	205.63
29	7.45	1.71	0.1617	3712.23	215.59
30	7.43	1.87	0.1866	4304.98	224.97
31	7.37	1.02	0.0948	2224.03	214.54
32	7.51	1.38	0.1300	2932.52	211.82
33	7.50	1.35	0.1266	2869.64	211.84
34	7.53	1.28	0.1317	2957.97	230.13
35	7.27	1.73	0.1667	4018.85	210.14
36	7.57	1.90	0.1847	4109.27	225.14
37	7.55	1.61	0.1649	3688.20	225.53
38	7.38	0.92	0.0813	1900.30	205.76
39	7.65	1.57	0.16	3483.21	224.17
40	7.59	1.23	0.12	2658.76	213.40
Avg	7.51	1.42	0.1416	3196.92	217.23
STDV	0.12	0.31	0.0325	712.37	7.47

Table S12. Single fiber tensile strength test summary of recovered CFs at 200 ℃.

Test#	Diameter (μm)	Strain at break (%)	Force at break(N)	Strength (Mpa)	Modulus (Gpa)
1	7.37	1.13	0.1112	2608.89	225.29
2	7.38	1.13	0.1345	3142.56	219.66
3	7.21	1.36	0.1161	2844.33	209.79
4	7.21	1.48	0.1341	3287.97	225.88
5	7.33	0.85	0.0691	1636.84	188.32
6	7.50	1.54	0.1375	3110.72	207.56
7	7.55	1.20	0.1094	2443.74	202.36
8	7.51	1.36	0.1303	2943.26	215.67
9	7.31	1.62	0.1464	3489.85	215.64
10	7.43	1.73	0.1687	3892.16	224.19
11	7.43	1.71	0.1554	3585.95	217.15
12	7.53	1.37	0.1314	2949.74	214.76
13	7.44	1.59	0.1453	3341.57	216.98
14	7.41	1.37	0.1309	3037.39	222.33
15	7.45	1.53	0.1532	3516.91	230.97
16	7.23	1.85	0.1465	3569.95	200.63
17	7.47	0.95	0.0938	2142.83	224.07
18	7.50	1.48	0.1485	3363.06	227.15
19	7.54	1.16	0.1292	2895.23	247.07
20	7.45	1.62	0.1621	3720.50	234.63
21	7.21	1.23	0.1497	3667.22	237.26
22	7.25	1.23	0.1154	2796.55	227.63
23	7.41	1.47	0.1428	3310.49	235.96
24	7.33	1.67	0.1601	3794.94	228.83
25	7.41	1.54	0.1499	3476.80	198.12
26	7.29	1.67	0.1442	3457.49	208.85
27	7.49	1.46	0.1414	3208.19	226.51
28	7.54	1.77	0.1827	4091.07	239.54
29	7.45	1.69	0.1540	3533.44	207.36
30	7.48	1.66	0.1550	3525.01	214.80
31	7.13	1.66	0.1675	4197.76	225.18
32	7.53	1.60	0.1505	3381.25	211.55
33	7.46	1.57	0.1495	3425.17	218.73
34	7.43	1.38	0.1152	2654.77	201.83
35	7.70	1.83	0.1701	3651.76	203.76
36	7.71	1.03	0.0978	2098.09	203.76
37	7.71	1.33	0.1407	3013.23	222.70
38	7.43	1.41	0.1346	3105.05	217.67
39	7.37	0.93	0.0782	1832.84	190.07
40	7.51	1.15	0.1024	2313.54	197.67
Average	7.43	1.43	0.1364	3151.45	217.20
STDV.P	0.13	0.25	0.0247	579.72	13.42

Table S13. Single fiber tensile strength test summary of recovered CFs at 220 ℃.

Test#	Diameter (μm)	Strain at break (%)	Force at break(N)	Strength (Mpa)	Modulus (Gpa)
1	7.45	1.63	0.1481	3395.90	217.22
2	7.47	1.34	0.1334	3044.49	226.74
3	7.45	1.26	0.1266	2902.88	225.41
4	7.38	1.32	0.1347	3147.46	236.28
5	7.41	1.39	0.1378	3193.20	226.46
6	7.41	1.38	0.1347	3124.39	225.27
7	7.41	1.30	0.1139	2641.36	200.91
8	7.72	1.48	0.1493	3187.82	214.05
9	7.40	1.21	0.1147	2670.21	219.47
10	7.47	1.18	0.1151	2627.86	226.88
11	7.19	1.62	0.1517	3737.92	229.16
12	7.49	1.45	0.1416	2902.30	200.20
13	7.39	1.88	0.1651	3846.50	213.98
14	7.35	1.86	0.1789	3667.29	197.64
15	7.27	1.42	0.1187	2860.00	208.61
16	7.25	1.74	0.1582	3242.98	187.17
17	7.51	1.26	0.1270	2603.85	206.70
18	7.36	1.52	0.1593	3265.53	213.38
19	7.51	1.22	0.1249	2560.81	213.33
20	7.29	1.60	0.1613	3305.50	205.75
21	7.43	0.87	0.0811	1661.77	191.47
22	7.75	1.50	0.1505	3194.54	212.79
23	7.53	1.63	0.1709	3838.67	235.33
24	7.51	1.71	0.1735	3918.32	237.27
25	7.39	2.05	0.1894	4417.96	220.87
26	7.29	1.20	0.1069	2562.68	214.59
27	7.43	1.63	0.1628	3759.85	230.46
28	7.43	1.60	0.1382	3189.28	199.55
29	7.37	1.46	0.1308	3064.86	209.39
30	7.29	0.83	0.0735	1762.78	208.78
31	7.35	1.70	0.1355	3194.23	187.30
32	7.69	1.30	0.1317	2840.35	219.21
33	7.47	1.44	0.1420	3242.65	226.40
34	7.65	1.66	0.1683	3664.11	223.05
35	7.47	1.75	0.1533	3499.70	204.65
36	7.52	1.87	0.1617	3645.32	196.93
37	7.39	1.55	0.1456	3396.04	218.06
38	7.49	1.56	0.1487	3372.67	216.35
39	7.39	1.54	0.1499	3496.11	227.87
40	7.25	1.56	0.1464	3545.56	227.30
Avg	7.43	1.49	0.1414	3179.89	215.06
STDV	0.12	0.25	0.0238	535.30	13.03

Table S14. Single fiber tensile strength test summary of recovered CFs at 240 ℃.

Test#	diameter (μm)	Strain at break (%)	Force at break(N)	Strength (Mpa)	Modulus (Gpa)
1	7.42	1.29	0.1229	2845.96	219.30
2	7.40	0.89	0.0821	1907.48	212.23
3	7.43	1.26	0.1247	2875.64	229.90
4	7.39	1.63	0.1595	3717.39	235.51
5	7.45	1.63	0.1566	3598.17	219.68
6	7.34	1.32	0.1229	2903.80	218.50
7	7.51	1.23	0.1162	2625.24	211.52
8	7.40	0.99	0.0905	2106.74	210.43
9	7.40	0.95	0.0871	2024.16	210.34
10	7.55	1.61	0.1624	3626.09	228.14
11	7.33	1.62	0.1423	3376.93	208.04
12	7.28	1.84	0.1459	3505.93	204.24
13	7.53	2.03	0.1728	3881.81	196.02
14	7.40	1.12	0.1004	2338.65	206.77
15	7.37	1.47	0.1185	2776.18	189.30
16	7.33	1.05	0.0967	2295.03	190.14
17	7.4	1.33	0.1133	2621.98	199.15
18	7.30	0.99	0.0866	2067.07	203.58
19	7.41	1.78	0.1517	3515.63	206.67
20	7.53	1.55	0.1589	3572.46	235.02
21	7.49	1.15	0.1161	2637.23	228.65
22	7.38	1.58	0.1387	3244.10	203.17
23	7.42	1.22	0.1139	2633.26	215.86
24	7.46	1.89	0.1492	3418.98	186.09
25	7.36	1.45	0.1290	3032.94	208.17
26	7.45	1.41	0.1391	3195.23	226.69
27	7.40	1.84	0.1660	3864.45	218.58
28	7.43	1.84	0.1744	4028.46	223.70
29	7.49	1.83	0.1771	4017.90	220.78
30	7.46	1.22	0.1097	2511.99	207.06
31	7.34	1.47	0.1392	3287.21	223.78
32	7.43	1.01	0.0959	2215.63	219.64
33	7.35	1.24	0.1188	2801.38	223.71
34	7.45	1.18	0.1074	2465.72	209.92
35	7.40	1.68	0.1518	3534.75	213.14
36	7.36	1.21	0.1096	2578.36	208.39
37	7.31	1.01	0.0946	2255.69	221.15
38	7.42	1.44	0.1321	3056.28	214.32
39	7.43	1.52	0.1443	3333.49	224.50
40	7.38	1.19	0.1172	2744.17	229.50
Average	7.41	1.40	0.1284	2975.99	214.03
STDV.P	0.06	0.30	0.0263	591.20	11.97

6. Pretreated composite degradation reaction work-up procedure

The work up procedure used to isolate components from a pretreated composite degradation reaction is shown below.

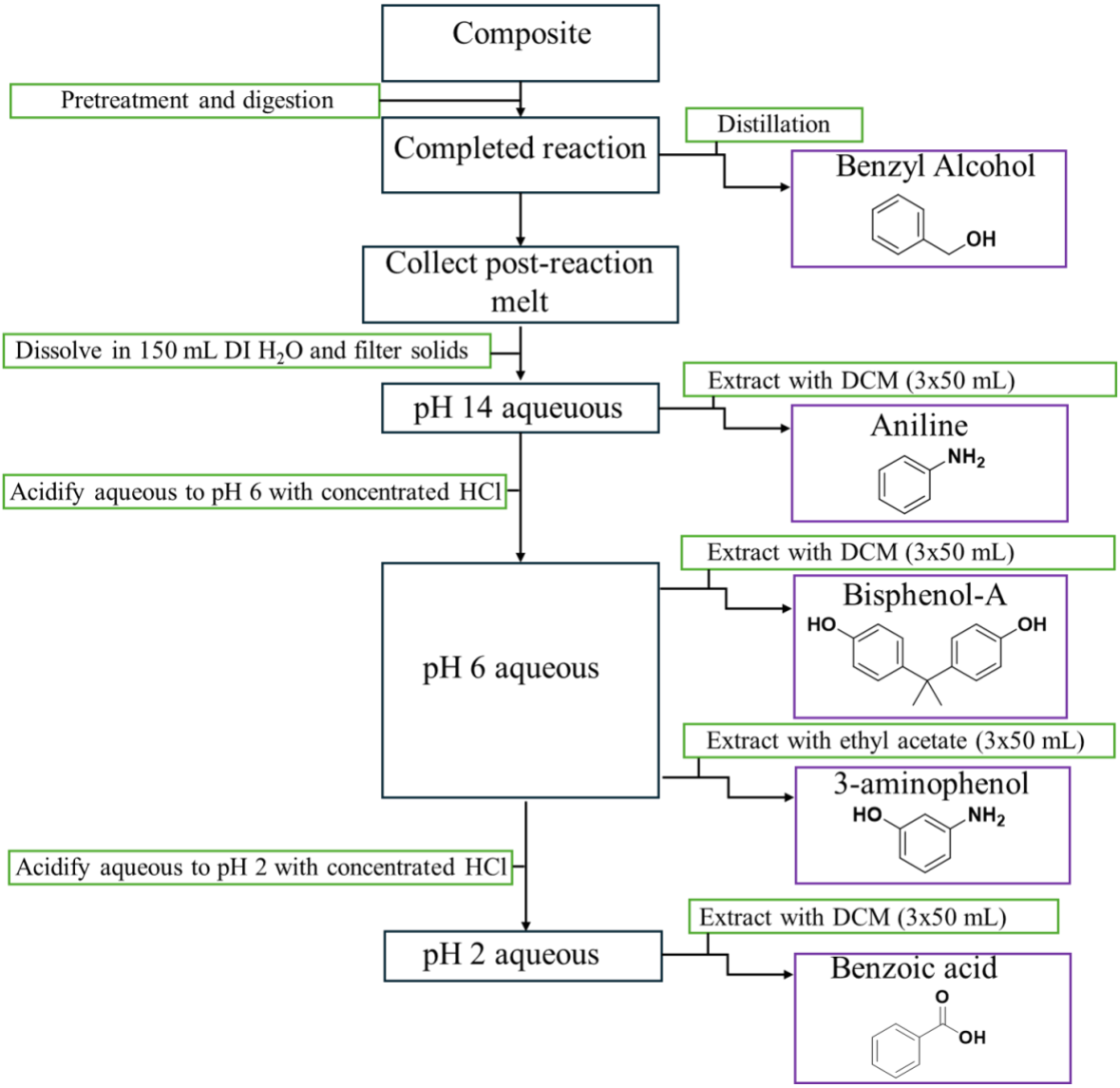

Figure S15. Work up procedure involving pH-based isolation.

After work-up the aqueous was then distilled and the leftover solid material was analyzed by NMR and showed no organic material.

a. Distillate collection

When the reaction was complete, it was allowed to cool down to 160 ˚C. Afterwards, the Hickman distillation head set up was removed and placed above a 100 mL beaker. Then it was flushed with 20 mL of dichloromethane (DCM) and combined with the collected distillate. The solution was then transferred to a 50 mL round bottom flask and the solvent was removed under reduced pressure to yield a light brown liquid. The ^{1}H and ^{13}C NMR spectra can be found in Figures S16 and S17 respectively. It comprises mostly of benzyl alcohol.

Benzyl alcohol. ^{1}H NMR (400 MHz, cdcl3) δ 7.41-7.27 (5H), 4.70 (s, 2H).

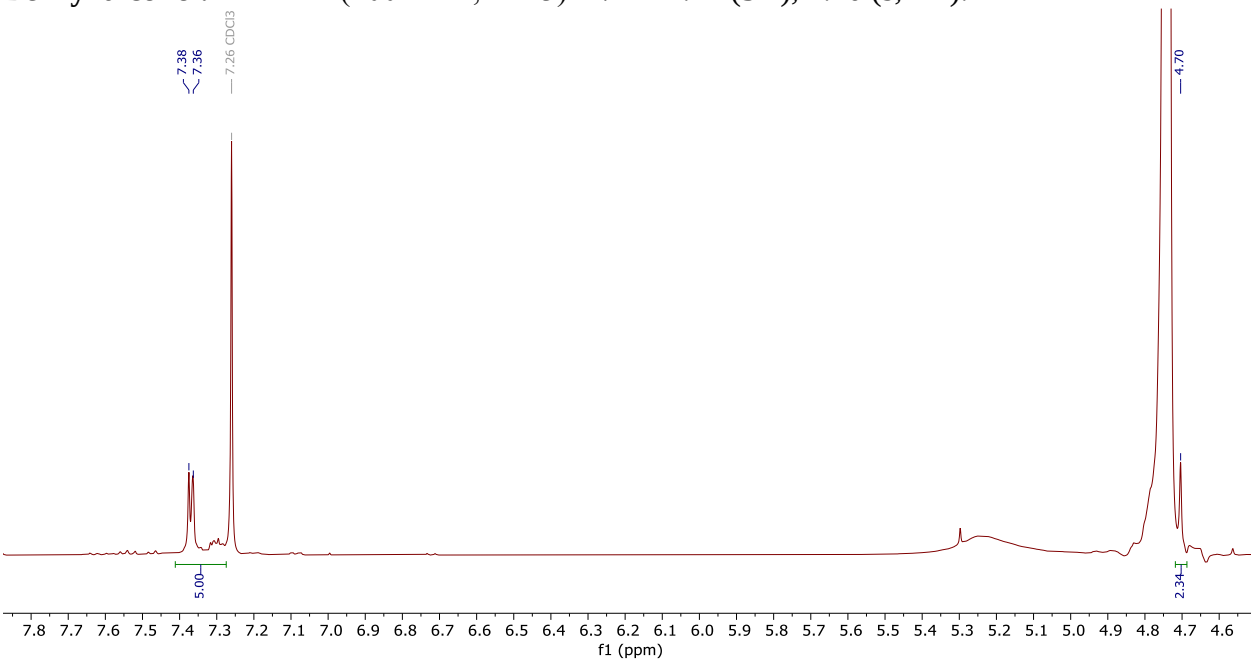

Figure S16. ^{1}H NMR of distillate in $CDCl_3$.

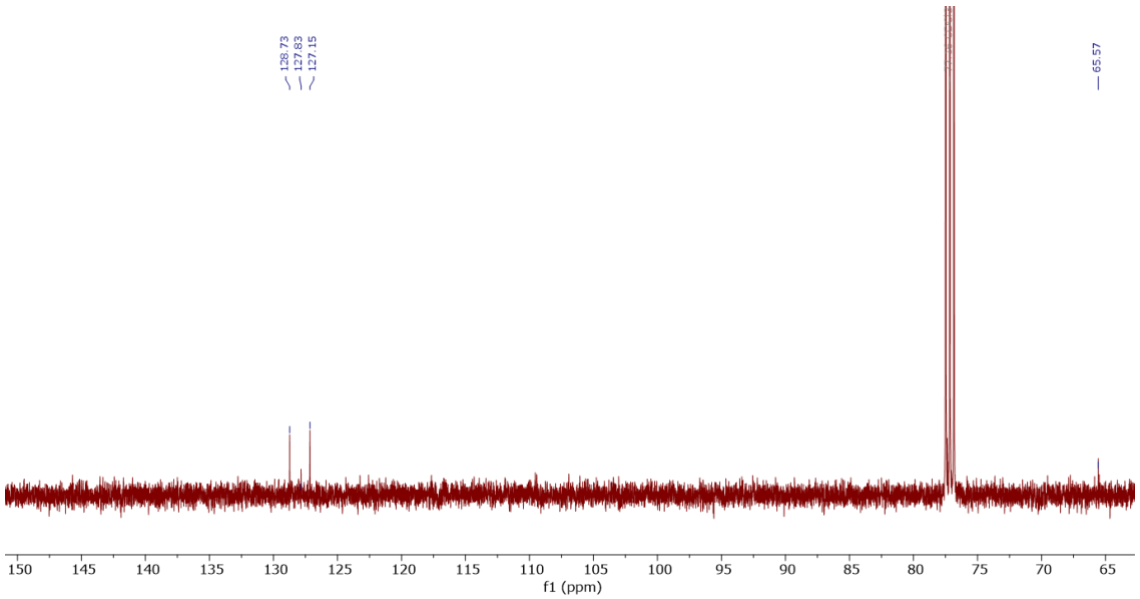

Figure S17. $^{13}C\{^{1}H\}$ NMR of distillate in $CDCl_3$.

b. Organic base extract

After the reaction was cooled down to 160 ˚C, it was scooped into a 500 mL beaker with a scoopula. The solid melt was then dissolved with H_2O (deionized, 150 mL). The mixture was solubilized and passed through a Buchner filter. The filtrate was collected, and the aqueous layer was extracted with DCM (3 x 50 mL). Afterwards, the organic layer was dried over sodium sulfate. Once dried, the solvent was removed under reduced pressure. The ^{1}H ^{13}C NMR spectra of the crude organic base extract can be found in Figures S18 and S19 respectively. The extracts show a mixture but the signals at 6.65, 6.74, and 7.18 in the HNMR resemble aniline.

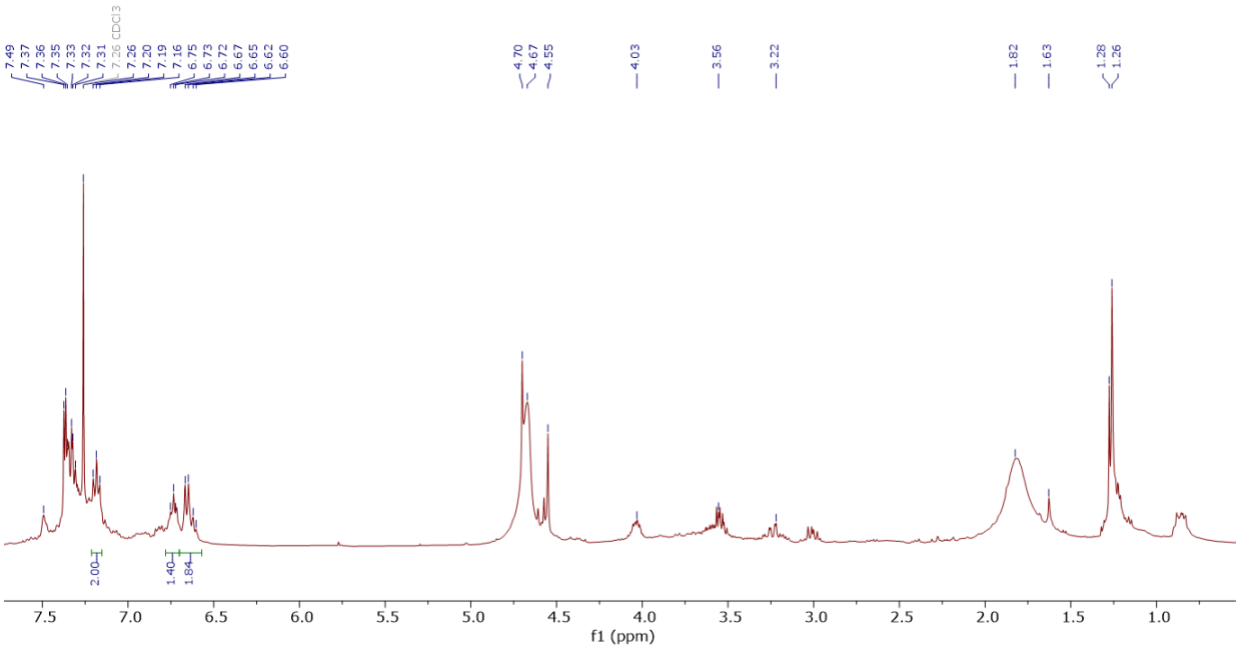

Figure S18. ^{1}H NMR of crude organic base extract in $CDCl_3$.

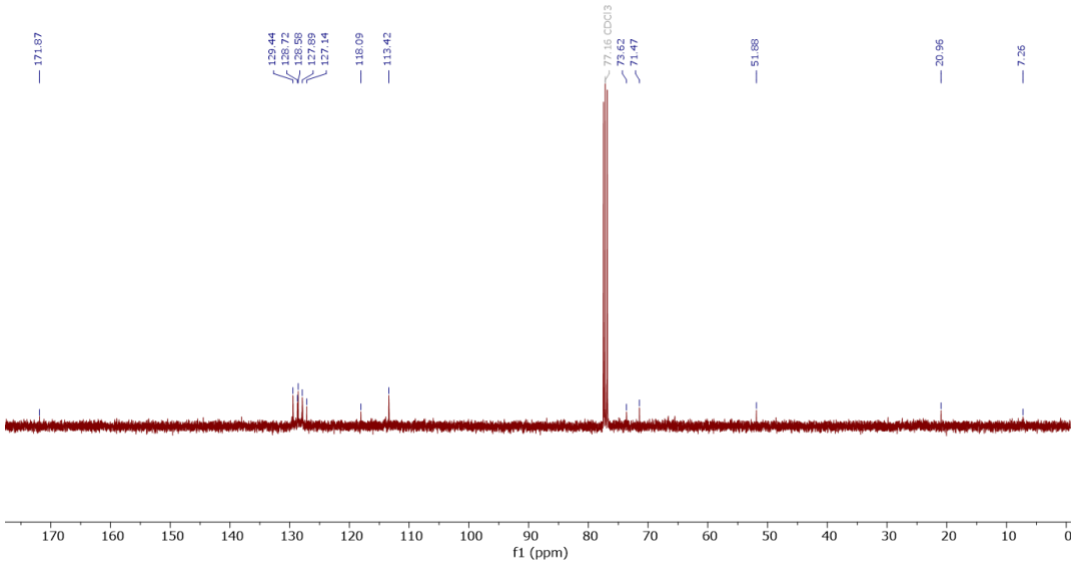

Figure S19. $^{13}C\{^{1}H\}$ NMR of crude organic base extract in $CDCl_3$.

c. Organic neutral extract from dichloromethane

The previously extracted aqueous layer was then acidified to pH 6 using concentrated hydrochloric acid (HCl). Once the solution was neutralized and cooled down, the organic material was extracted with DCM (3 x 50 mL). The organic layer was then dried over sodium sulfate and the solvent was removed under reduced pressure. The ^{1}H and ^{13}C NMR spectra of the crude organic neutral extract can be found in Figures S20 and S21 respectively. The extract is primarily bisphenol A (BPA).

Bisphenol-A: ^{1}H NMR (400 MHz, cdcl3) δ 7.09 (d, J = 7.7 Hz, 4H), 6.72 (d, J = 7.8 Hz, 4H), 1.62 (s, 6H). ^{13}C NMR (100 MHz, dmso) δ 154.88, 141.05, 127.29, 114.54, 40.91, 30.89.

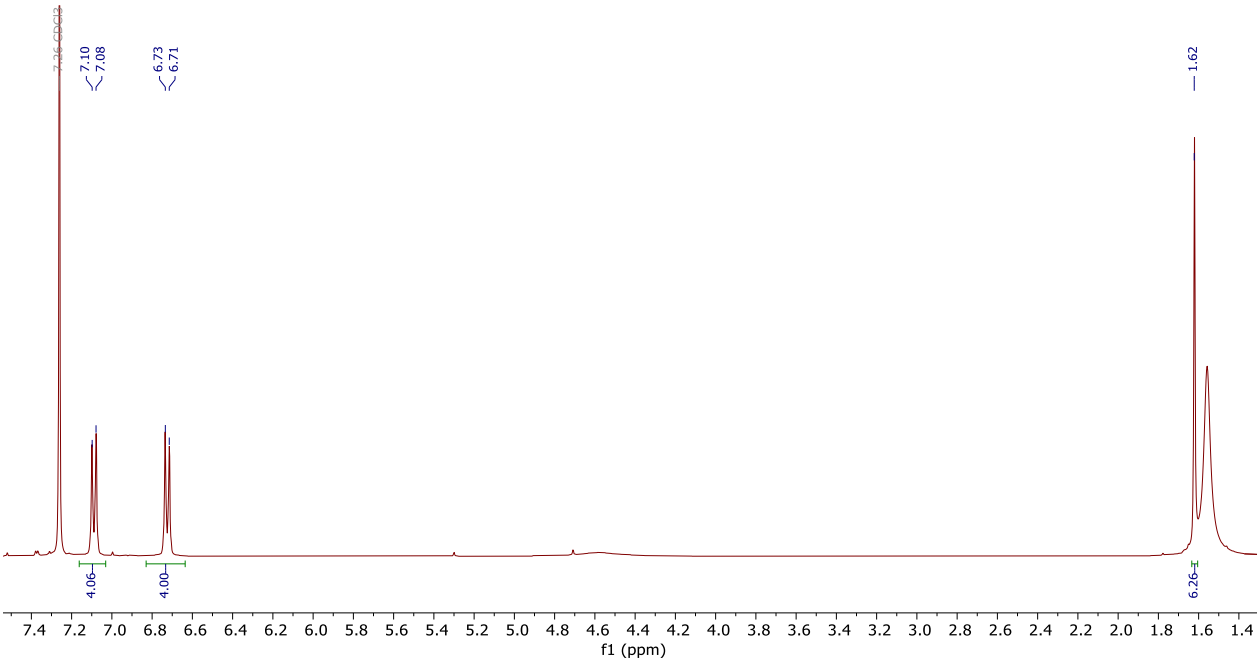

Figure S20. ^{1}H NMR of crude organic neutral extract from DCM in $CDCl_3$.

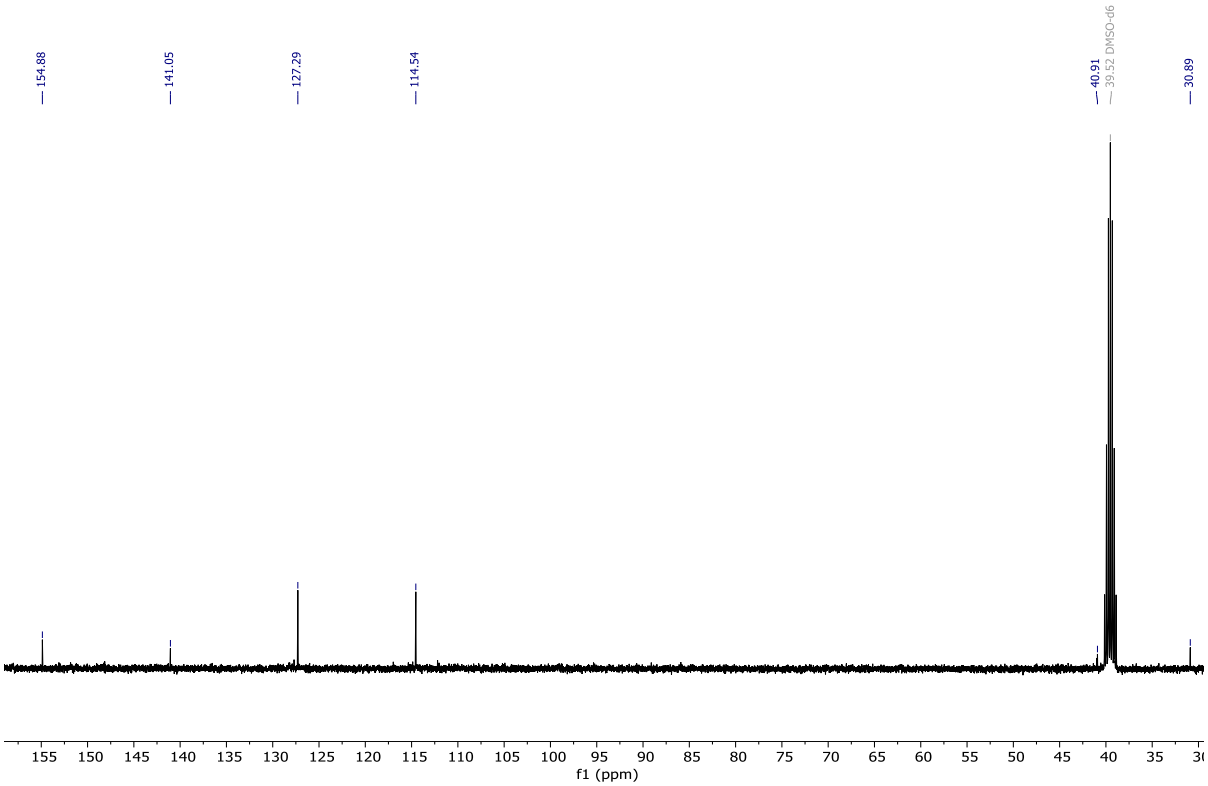

Figure S21. ^{13}C{^{1}H} NMR of crude organic neutral extract from DCM in DMSO-d_6.

d. Organic neutral from ethyl acetate

The aqueous layer was then extracted with ethyl acetate (3 x 50 mL). The organic layers were then collected, combined and dried over sodium sulfate. Once dried, the solvent was removed under reduced pressure and left behind a brown-yellow oily residue. The ^{1}H NMR spectrum of this extract can be found in Figure S22. The extract contained both BPA and 3-aminophenol.

3-aminophenol. ^{1}H NMR (400 MHz, dmso) δ 6.75 (t, J = 8.2 Hz, 1H), 6.03 – 5.87 (m, 3H).

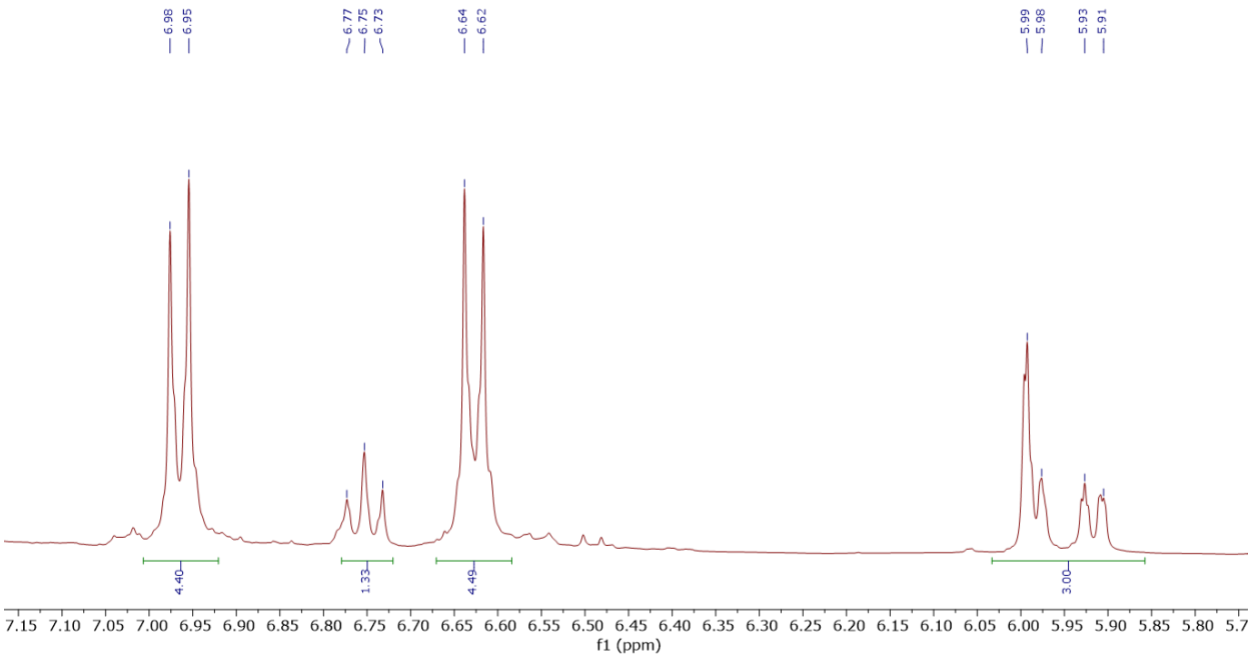

Figure S22. ^{1}H NMR of crude organic neutral extract from ethyl acetate in DMSO-d_6.

e. Organic acid extract

The previously extracted aqueous layer was then acidified to pH 2 using concentrated HCl. Once the solution was acidified, it was allowed to cool, and the organic material was extracted with DCM (3 x 50 mL). The organic layers were then combined and dried over sodium sulfate. Afterwards, the solvent was removed under reduced pressure. The ^{1}H and ^{13}C NMR spectra of the crude organic acid extract can be found in Figures S23 and S24. It contains benzoic acid.

Benzoic acid. ^{1}H NMR (400 MHz, cdcl3) δ 8.12 (d, J = 8.4 Hz, 2H), 7.62 (t, J = 7.4 Hz, 1H), 7.48 (t, J = 7.7 Hz, 2H). ^{13}C NMR (100 MHz, cdcl3) δ 170.73, 133.88, 130.35, 129.30, 128.65.

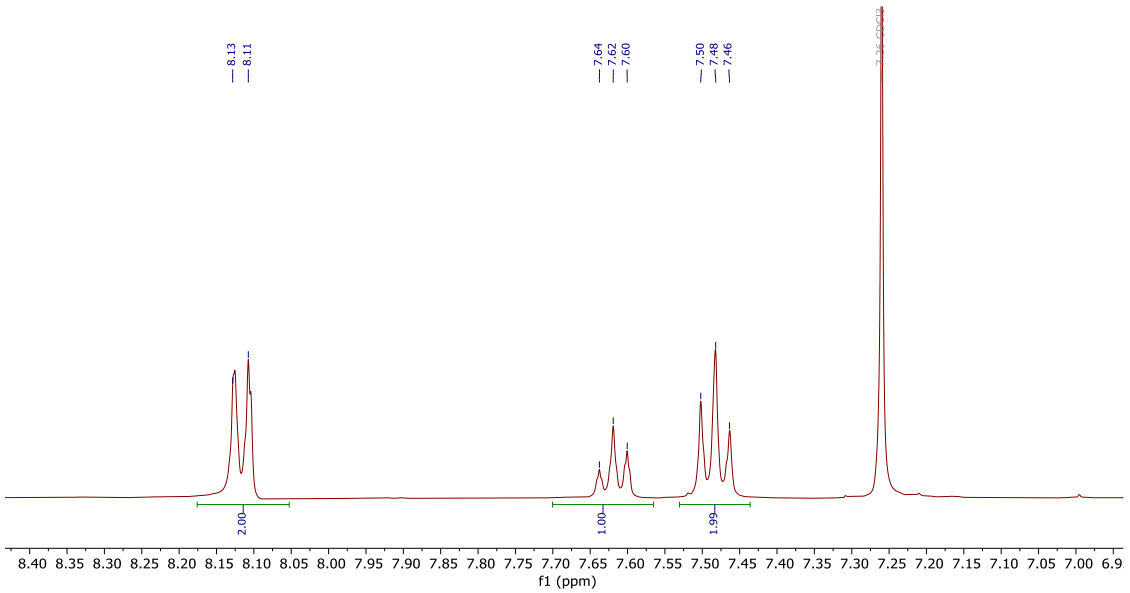

Figure S23. ^{1}H NMR of crude organic acid extract in $CDCl_3$.

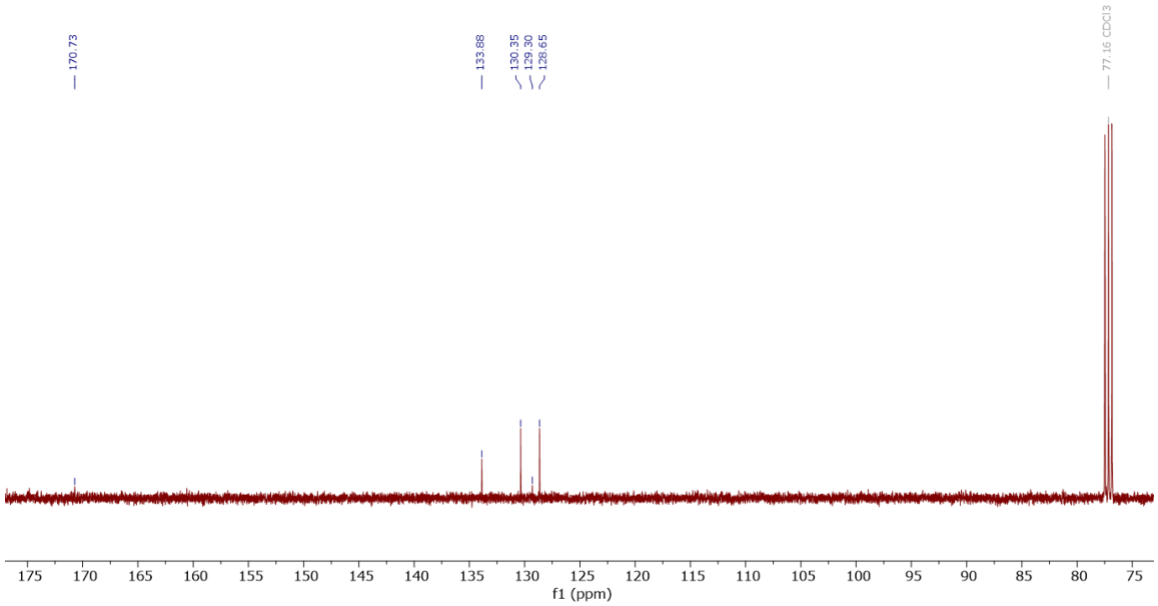

Figure S24. $^{13}C\{^{1}H\}$ NMR of crude organic acid extract in $CDCl_3$.

7. **Unpretreated composite degradation extracts**

Scheme S1. Unpretreated degradation of Bi/DDS neat resin and CFRPs.

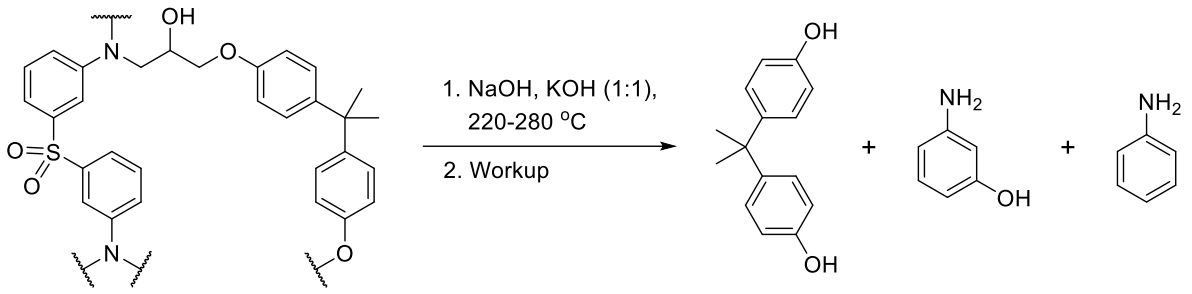

Resin degradation trials are summarized in Table S15, 20. Ground resin (d < 5 mm) or pieces of resin/carbon fiber composite (13 x 10 mm) were tested. The reaction was conducted either in a round-bottom flask (25 or 50 mL, borosilicate glass) or in a regular glass test tube (entry 3). Heat sources were either a sand bath or an alcohol burner (entries 3 and 5). The reaction temperature was measured by a thermocouple.

A source of resin, NaOH and KOH·½H_2O (1:1 molar ratio) were placed in a reactor and the degradation was conducted at 220–280 °C for 0.3–3 hours according to Table S15. Manual stirring was applied for entries 3–5.

When a distillation head was used (Table S20, entries 1, 2, and 5), a colorless emulsion was collected (ca. 1–2 mL) as a distillate. It was extracted with DCM (1 mL x 3). The extract was dried with sodium sulfate and evaporated to give a yellow oil (crude aniline). Once cooled, the reaction melt was dissolved in a minimal amount of DI water to form a clear beige-brown solution. Carbon fibers and/or unreacted resin were filtered, washed with water, and air-dried.

The basic solution was extracted with DCM (5 mL x 3). The extract was dried with sodium sulfate and evaporated to give a brown residue (unreacted oligomers).

Then, the aqueous solution was brought to pH 0–1 by adding 6 M HCl carefully at stirring (Caution: exothermic reaction and evolution of SO_2 gas). Once at 25 °C, the acidic solution was extracted with DCM (5 mL x 4). The extract was dried with sodium sulfate and evaporated to give crude BPA as yellowish crystalline solid.

The resulting aqueous solution was filtered (to remove $SiO_2 \cdot nH_2O$) and brought to pH 7–8 by adding solid sodium bicarbonate in small portions at stirring. The neutral solution was extracted with ethyl acetate (5 mL x 4). The extract was dried with sodium sulfate and evaporated to give a yellow oil (mostly 3-aminophenol). All the isolated materials were characterized by ^1H and ^{13}C NMR spectroscopy (Figures S25-30).

Table S15. Summary of reaction conditions of unpretreated Bi/DDS neat resin and CFRP.

Entry	Substrate	M_I (g)	NaOH-KOH mixture (g)	Temperature (^oC)	Time(hr)
1	Bi/DDS neat resin	2.00	10	220-240	2
2	Bi/DDS neat resin	2.00	20	230-250	3
3	Bi/DDS neat resin	0.50	5	250-280	0.5
4	Bi/DDS CFRP	3.00	20	230-250	3
5	Bi/DDS CFRP	2.00	9.6	>270	0.3

Aniline. ^{1}H NMR (400 MHz, $CDCl_3$): δ 7.17 (t, *J* = 7.0 Hz, 2H, *m*-CH), 6.78 (t, *J* = 7.3 Hz, 1H, *p*-CH), 6.70 (d, *J* = 7.7 Hz, 2H, *o*-CH), 3.65 (br s, 2H, NH_2). ^{13}C{^{1}H} NMR (151 MHz, $CDCl_3$): δ 146.46, 129.39, 118.66, 115.22.

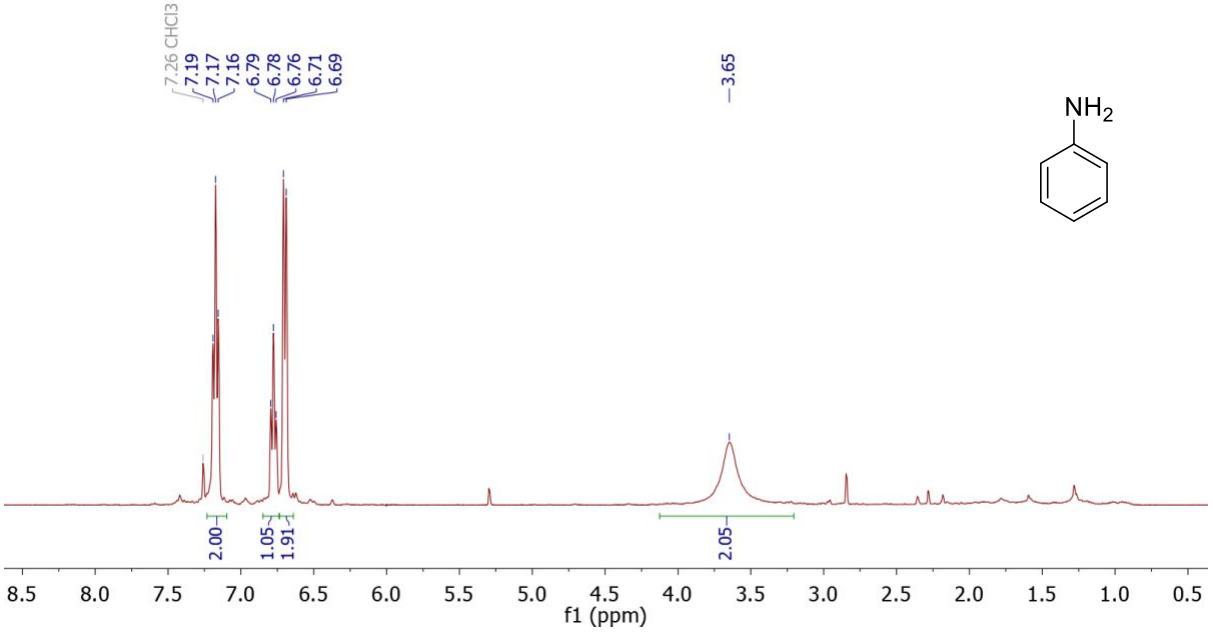

Figure S25. ^{1}H NMR spectrum of the crude aniline in $CDCl_3$.

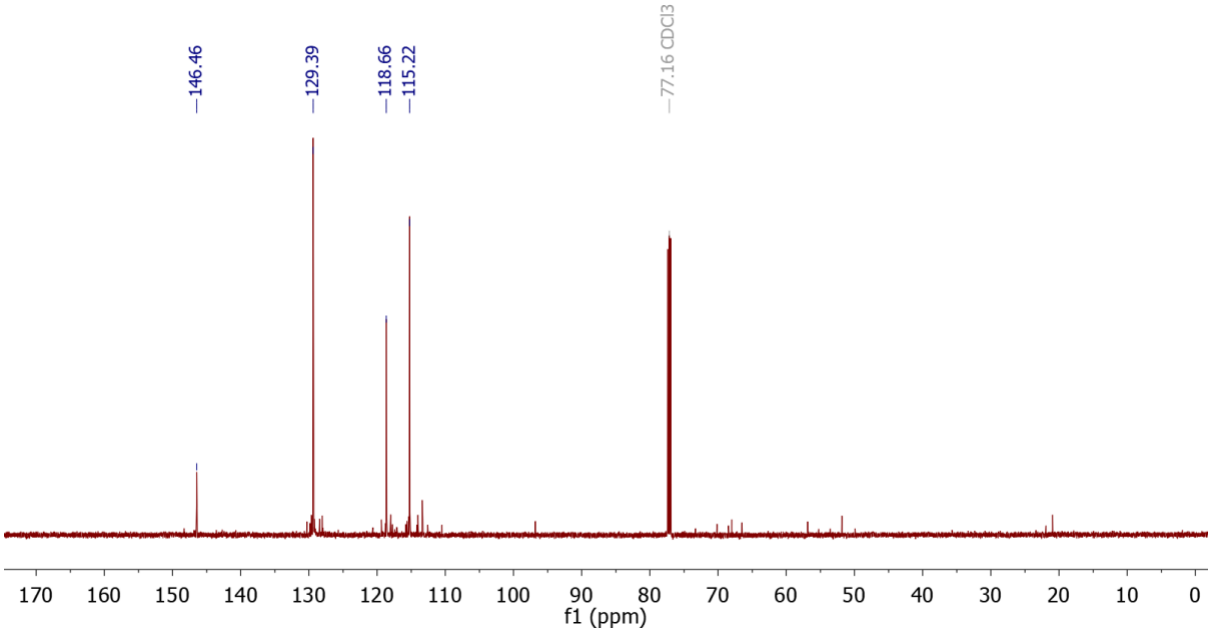

Figure S26. ^{13}C{^{1}H} NMR spectrum of the crude aniline in $CDCl_3$.

3-Aminophenol. ^{1}H NMR (600 MHz, CD_3OD): δ 6.91 (t, *J* = 7.9 Hz, 1H, CH), 6.24 (d, *J* = 7.9 Hz, 1H, CH), 6.22 (s, 1H, CH), 6.17 (d, *J* = 8.0 Hz, 1H, CH). ^{13}C{^{1}H} NMR (151 MHz, CD_3OD): δ 159.20, 149.60, 130.81, 108.62, 106.72, 103.85.

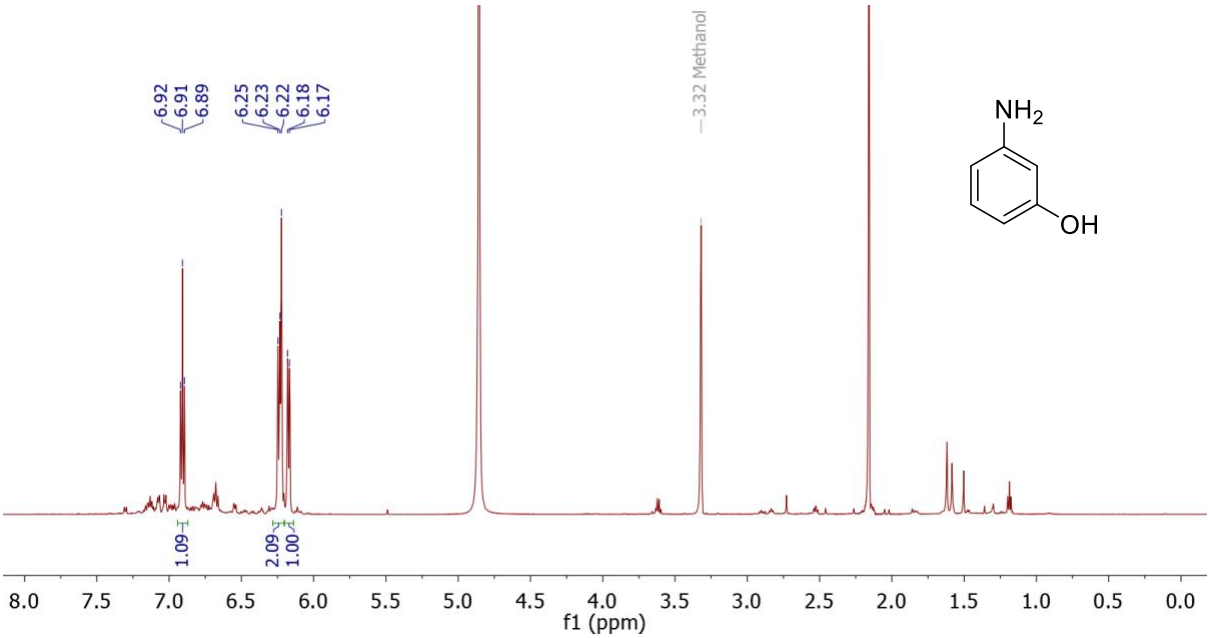

Figure S27. ^{1}H NMR spectrum of the crude 3-aminophenol in CD_3OD.

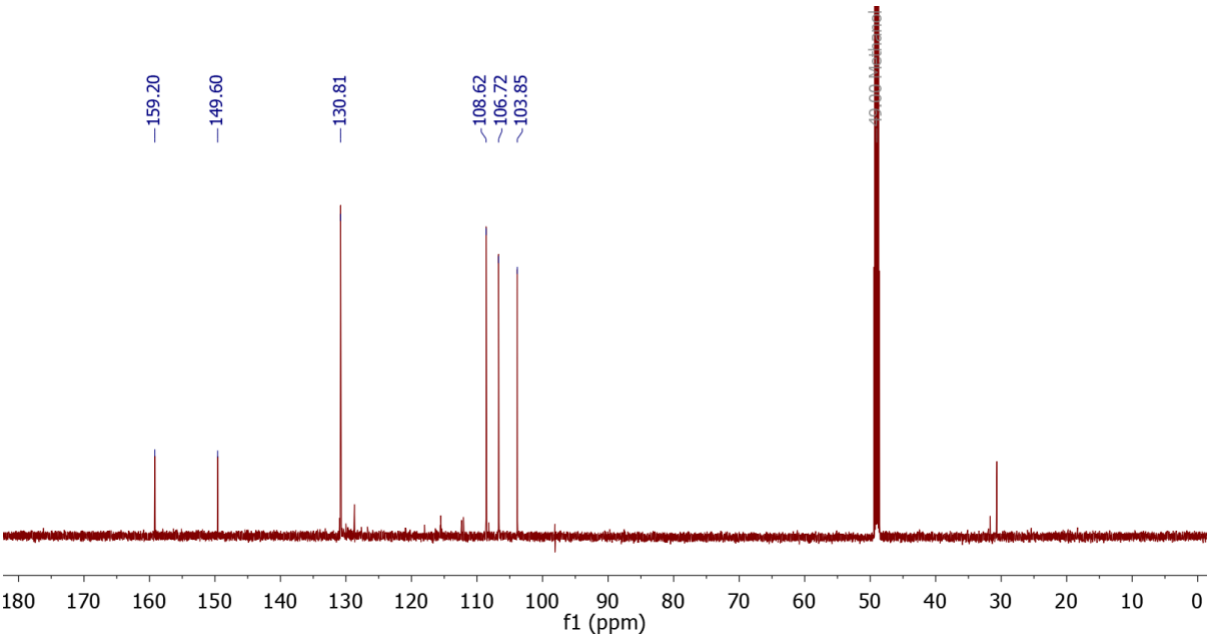

Figure S28. ^{13}C{^{1}H} NMR spectrum of the crude 3-aminophenol in CD_3OD.

2,2-Bis(4-hydroxyphenyl)propane (bisphenol A, BPA). ^{1}H NMR (400 MHz, $CDCl_3$): δ 7.09 (d, *J* = 6.8 Hz, 4H, CH), 6.73 (d, *J* = 7.1 Hz, 4H, CH), 4.81 (s, 2H, OH), 1.62 (s, 6H, $2CH_3$). $^{13}C\{^{1}H\}$ NMR (101 MHz, CD_3OD): δ 155.73, 143.43, 128.67, 115.48, 42.39, 31.63. The peaks of non-quaternary carbon atoms appear as multiplets, probably, due to a rapid acid-catalyzed H/D exchange with CD_3OD.

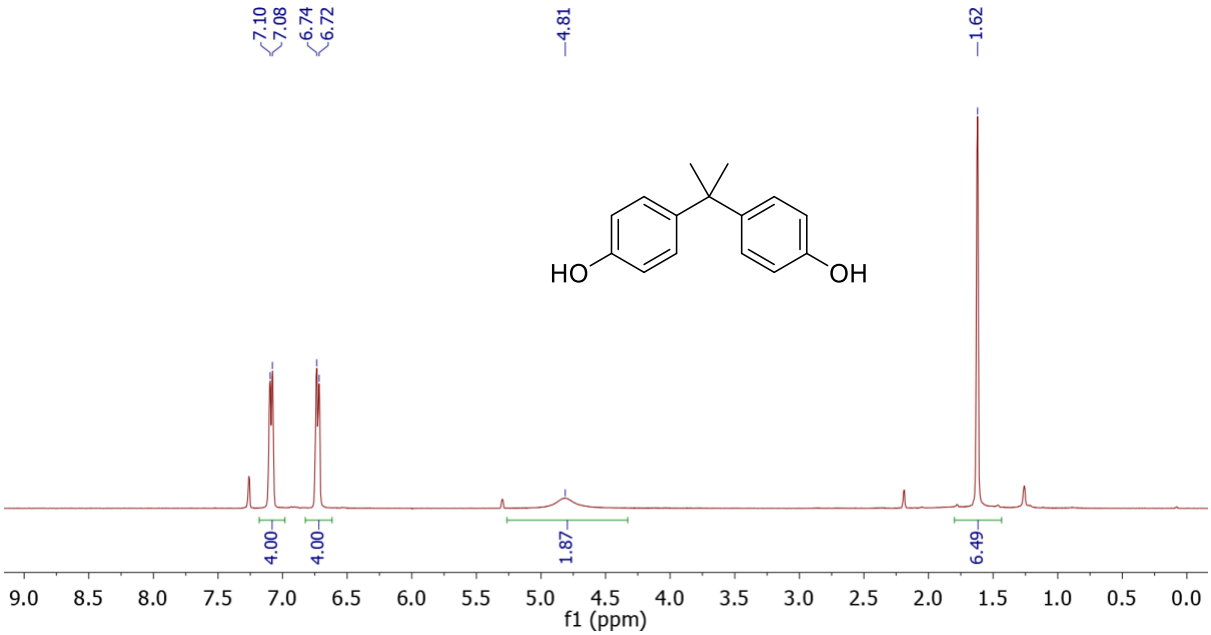

Figure S29. ^{1}H NMR spectrum of the crude 2,2-bis(4-hydroxyphenyl)propane in $CDCl_3$.

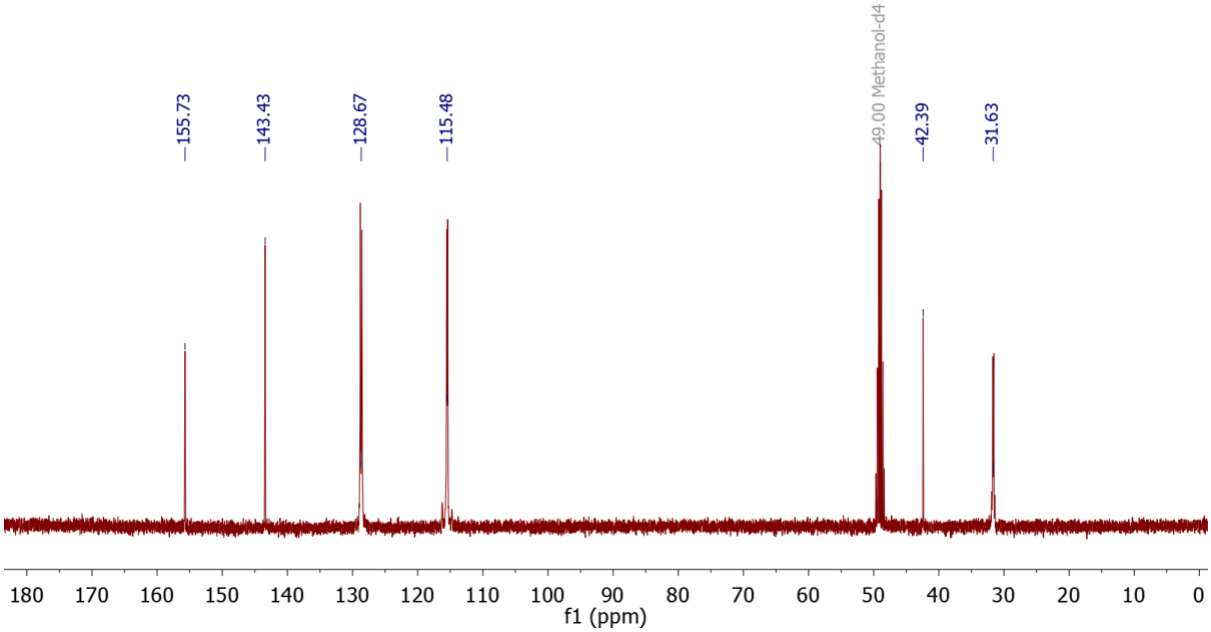

Figure S30. $^{13}C\{^{1}H\}$ NMR spectrum of the crude 2,2-bis(4-hydroxyphenyl)propane in CD_3OD.

8. Ion exchange chromatography

In addition to the pH-based separation strategy, we also offer a more sustainable separation strategy by using ion exchange resins. This technique requires less water, uses no organic solvent, and enables the recovery of hydroxide (91 mol%). The experiment went as described:

A CFRP composite (560 mg) is digested by NaOH (5.99 g, 0.1497 mol) and KOH×0.5H_2O (9.00 g, 0.1384 mol) in a steel crucible at 260 °C within 2 h. The cooled melt is dissolved in water (50 mL) and the brown solution is filtered through a PTFE filter (0.45 μm). CFs are recovered (309 mg).

A glass column (230×20 mm) is then filled with an anion-exchange resin (Amberlite, IRN-78), which is then prepared for the experiment by washing with aqueous NaOH (0.9 M) and DI water until pH 9.0–9.5. The resin is charged with the aqueous degradation solution. Then, pure OH^- is eluted by DI water. The collected fractions are listed in Table S17. Fractions 1–3 are combined (V_F = 136 mL) and OH^- is quantified by the acid-base titration. A sample of the hydroxide solution (V_S = 1.00 mL) is titrated with standard HCl (c_{HCl} = 0.1753 M) in the presence of phenolphthalein indicator. Fractions 1–3 contain 0.263 mol of hydroxide (c_{OH} = 1.928 M), which corresponds to 91% hydroxide recovery. The recovered solution shows no presence of organic compounds as suggested by ^{1}H NMR after the HCl/CH_2Cl_2 extraction (Figure S31).

BPA^{2-} is not eluted by aqueous OH^-, so it was eluted as H_2BPA using HCl (6 M, 20 mL) in aqueous ethanol (1:1 v/v). The collected fractions are listed in Table S17. Fractions 5–8 are combined and evaporated under reduced pressure. A red oily residue is dried in a desiccator over KOH resulting in 100 mg of recovered organic material.

These collected fractions (5-8) were then analyzed by NMR and these spectra are shown in Figure S32. 1H ^{NMR} of crude combined fractions 5-8. Upon assignment, we observe that BPA is the major component in this mixture, however we do notice a number of impurities that are plasticizers from the plastic ethanol bottle we used to elute these fractions.

The crude mixture was then dissolved in 2 mL of DI H_2O in a vial and heated to 90˚C using an oil bath for 5 minutes. Afterwards, 2 mL of toluene was added, and a second phase was observed. The mixture was then placed back over the heat for another 5 minutes with agitation. After 5 minutes have elapsed, the water layer was transferred to a 50 mL round bottom flask and another 2 mL of water was added back into the vial. Then it was heated again for another 5 minutes and when that time had elapsed, the water layer was combined with the previously extracted aqueous solution in the round bottom flask. Finally, the water was removed by rotary evaporation until the volume was 1 mL. At this point, the flask was allowed to cool to room temp and then the excess water was removed by pipette. The residue was then dissolved in deuterated chloroform and revealed BPA was purified as shown by NMR (Figure S38).

Table S16. Fraction of recovered hydroxide.

$Resin–NR_3^+OH^- + BPA^{2-} \leftrightarrow Resin–NR_3^+BPA^{2-} + OH^-$

Fraction #	Color	Volume, mL	pH	$[OH^-]$, M	$n(OH^-)$, mol
1	brown	53	–		
2	light brown	35	–	1.928	0.263
3	pale yellow	42	13.39		
4	–	36	11.77	5.89×10^{-3}	
5	–	44	10.64	4.37×10^{-4}	2.34×10^{-4}
6	–	68	9.59	3.89×10^{-5}	
7	–	22	9.36	2.29×10^{-5}	

Table S17. Fractions of recovered organics acids.

$Resin–NR_3^+BPA^{2-} + 2H^+ + Cl^- \leftrightarrow Resin–NR_3^+Cl^- + H_2BPA$

Fraction #	Color	Volume, mL	pH
1	–	35	
2	–	50	8–9
3	–	50	
4	–	20	
5	orange	50	
6	pale yellow	50	1–3
7	pale brown	40	
8	pale yellow	45	

Table S18. Summary of anionic exchange chromatography experiments

CFRP (mg)	Recovered CFs (mg)	Isolated crude BPA (mg)	Crude BPA yield (%)	Initial hydroxide (g)	Recovered hydroxide (mol)	Hydroxide recovery yield (mol %)
560	309	100	81.2	5.99 g NaOH + 9.00 g $KOH\times0.5H_2O$	0.263 mol	91

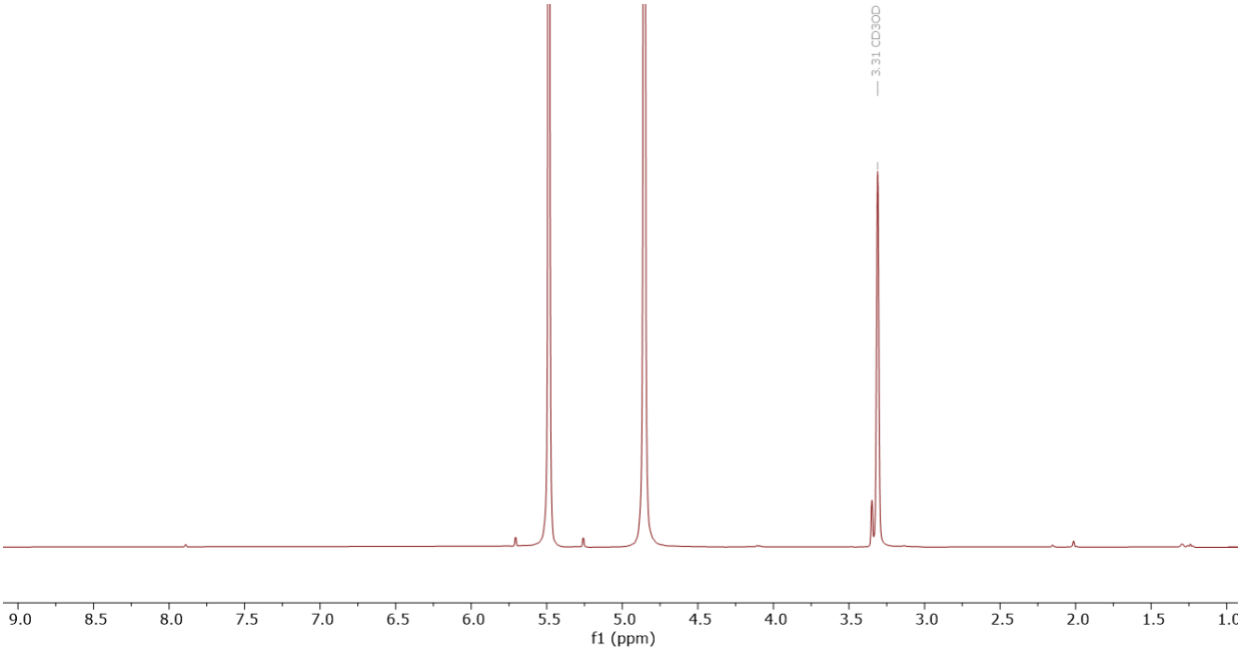

Figure S31. Extract from combined fractions 1-3 reveal no organic molecules in CD_3OD.

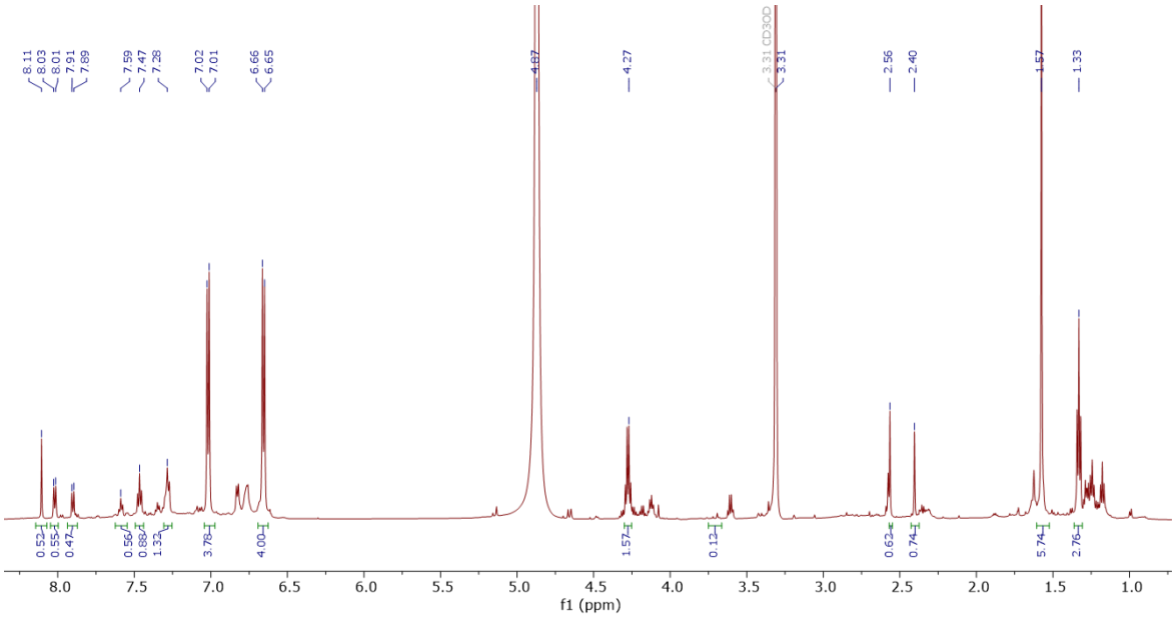

Figure S32. ^1H NMR of crude combined fractions 5-8 in CD_3OD.

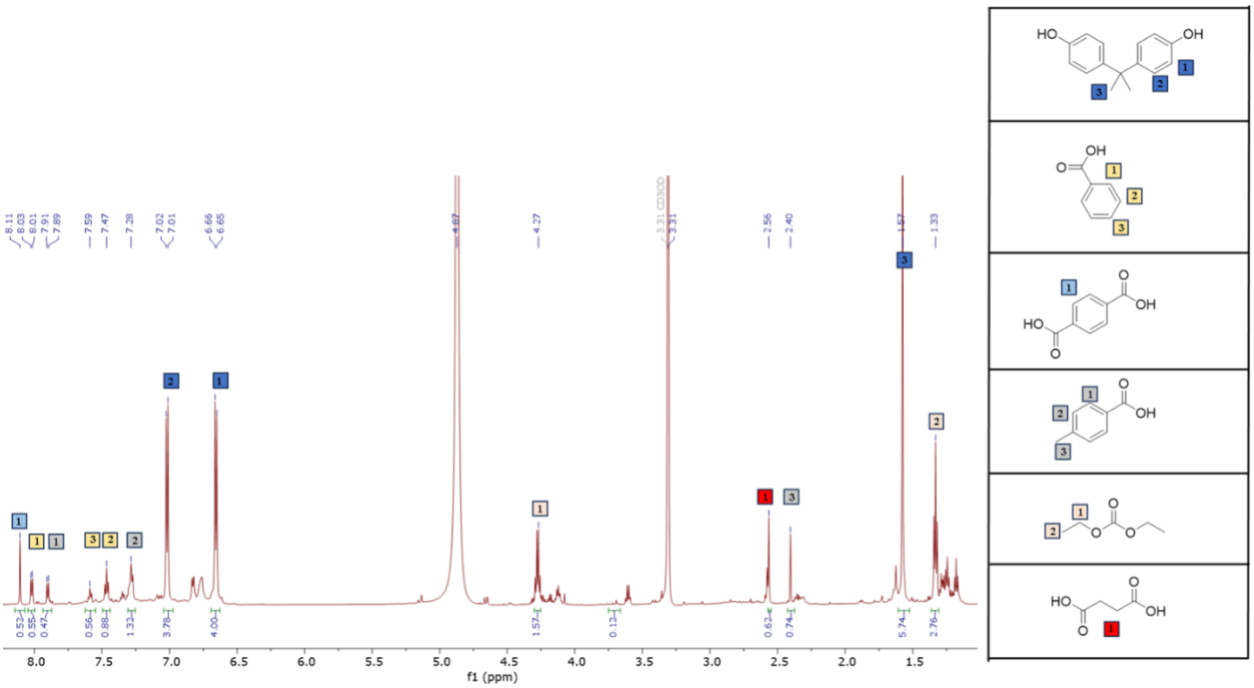

Figure S33. Annotated ^{1}H NMR of crude combined fractions 5-8 in CD_3OD.

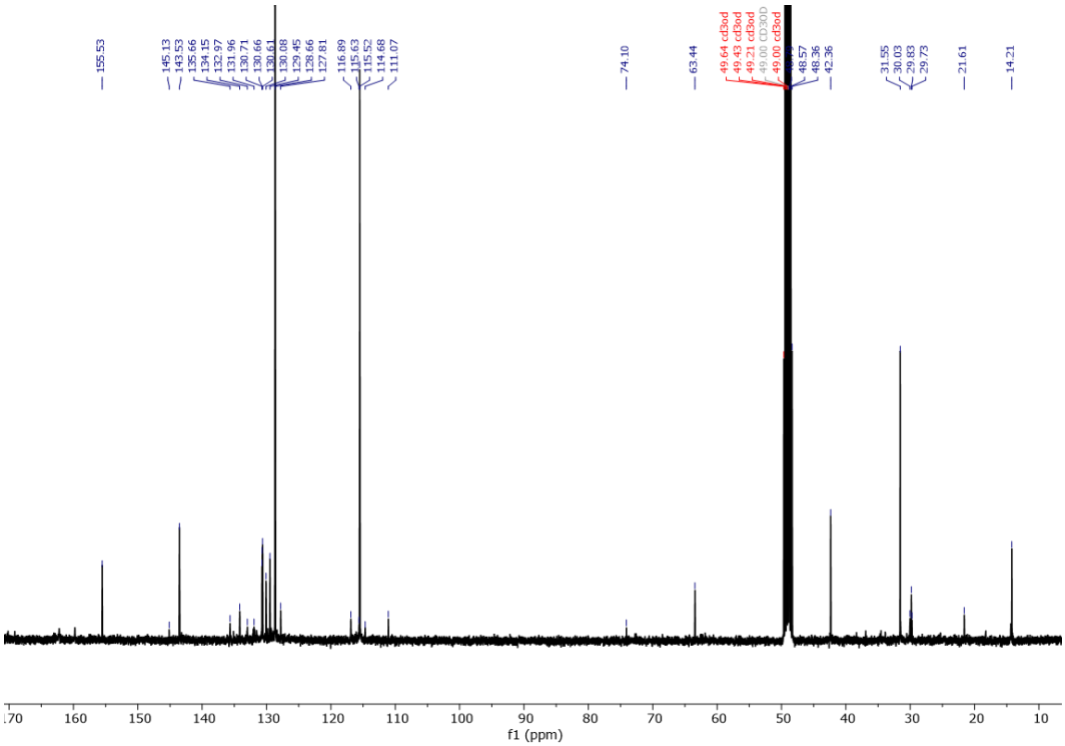

Figure S34. $^{13}C\{^{1}H\}$ NMR of crude fractions 5-8 in CD_3OD.

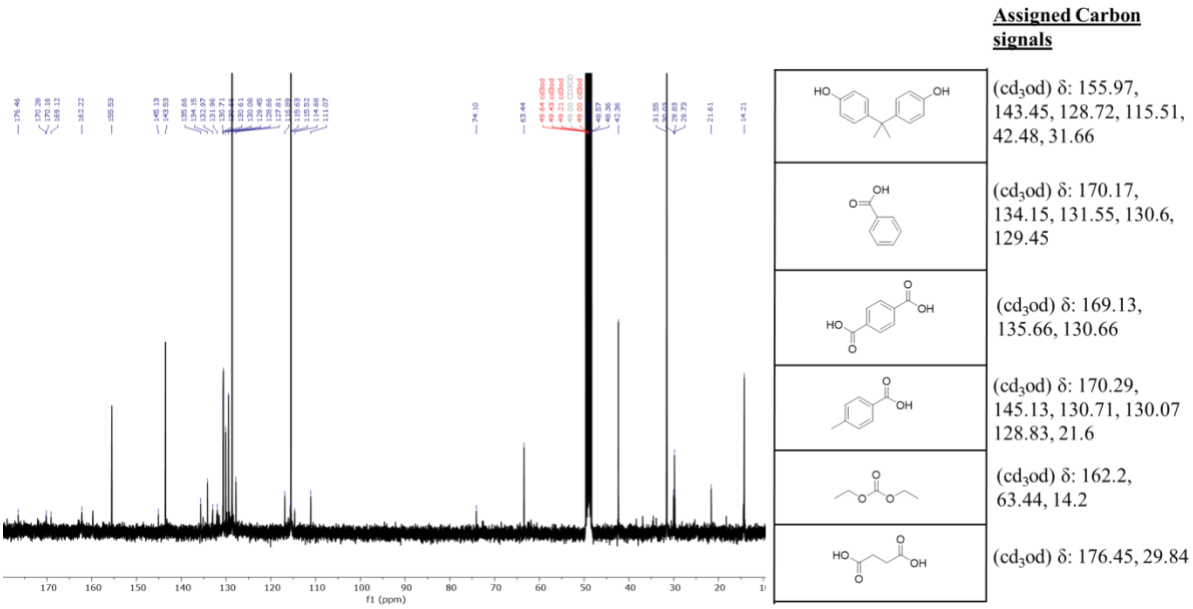

Figure S35. Annotated $^{13}C\{^{1}H\}$ NMR of crude fractions 5-8 in CD_3OD.

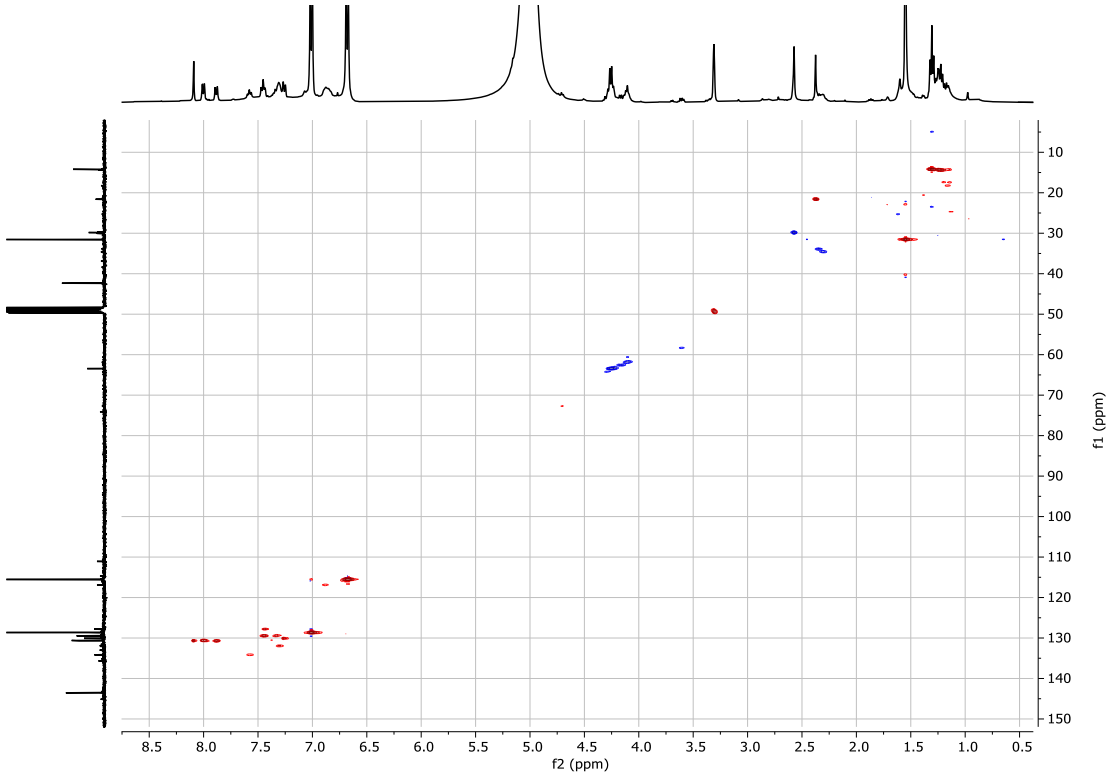

Figure S36. HSQC of crude fractions 5-8 in CD_3OD.

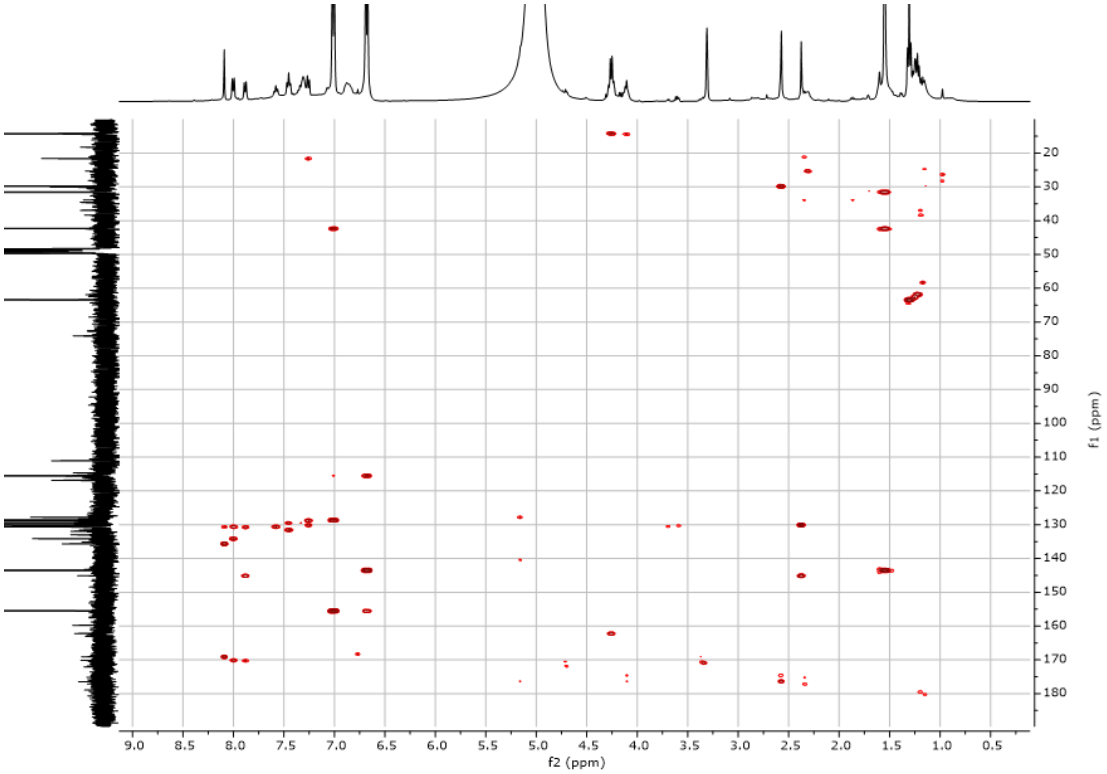

Figure S37. HMBC of crude fraction 5-8 in CD_3OD.

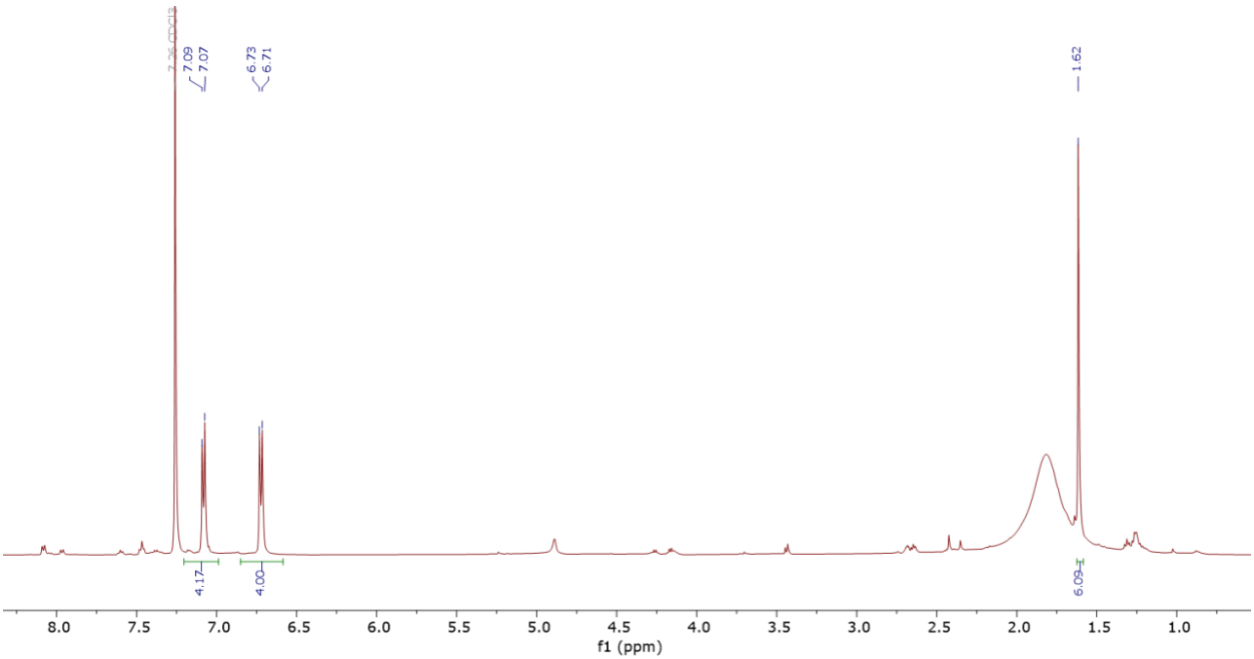

Figure S38. ^1H NMR of purified BPA from fractions 5-8 in $CDCl_3$.

9. **Bi/MDEA neat resin degradation component**

After digestion and cooling, the reaction melt was dissolved using 15 mL DI water, forming a beige-brown basic solution. The stainless-steel lid and Hickman distillation apparatus were washed with 10 mL of DI water and dichloromethane (DCM). The wash solutions (DI water and DCM) were combined with the basic solution

a. Organic base extract from dichloromethane

The basic solution was extracted with DCM (15 mL x 3). The organic layer was washed using 1M NaOH aqueous solution (5 mL x 3), dried over sodium sulfate, and evaporated to give a black residue (recovered M-DEA). Isolated materials were characterized by ^{1}H, ^{13}C NMR, and MALDI spectroscopy (Figure S39-S43).

Recovered 4,4'-Methylenebis(2,6-diethylaniline) (MDEA). ^{1}H NMR (400 MHz, dmso) δ 6.63 (s, 4H), 4.28 (s), 3.55 (s, 2H), 2.49 – 2.32 (q, 10H), 1.08 (t, J = 7.5, 1.8 Hz, 15H). ^{13}C{^{1}H} NMR (151 MHz, dmso) δ 140.46, 129.79, 126.60, 125.92, 40.33, 23.84, 13.42.

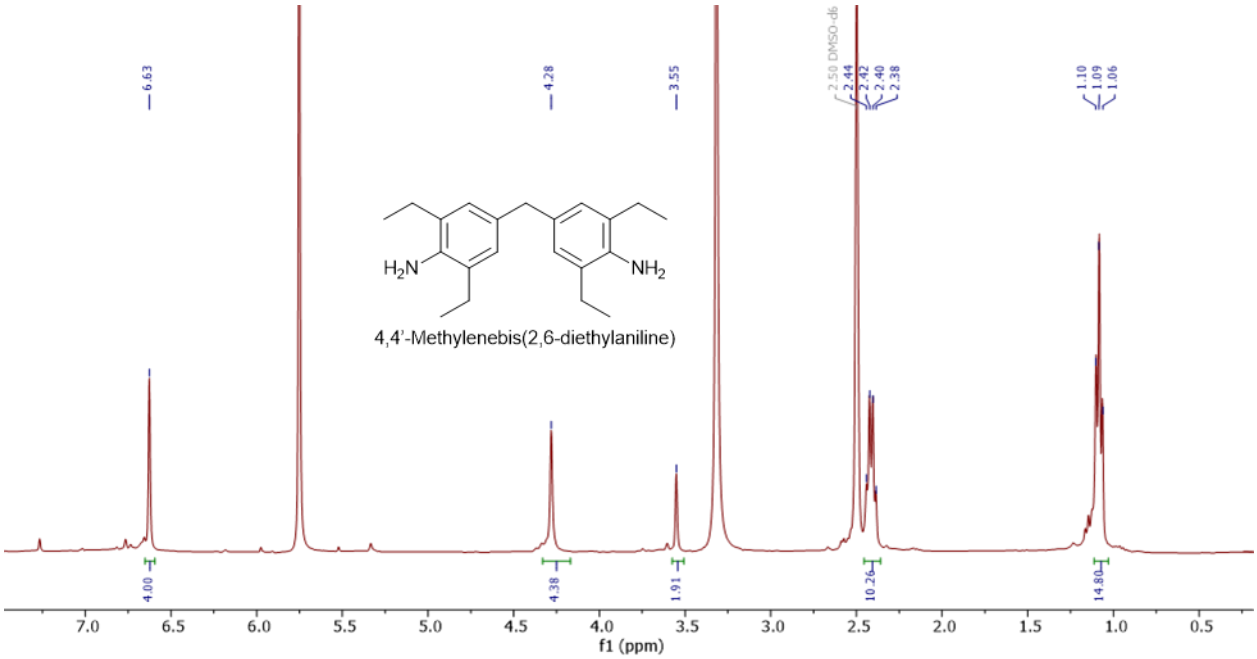

Figure S39. ^{1}H NMR of recovered MDEA in DMSO-d_6.

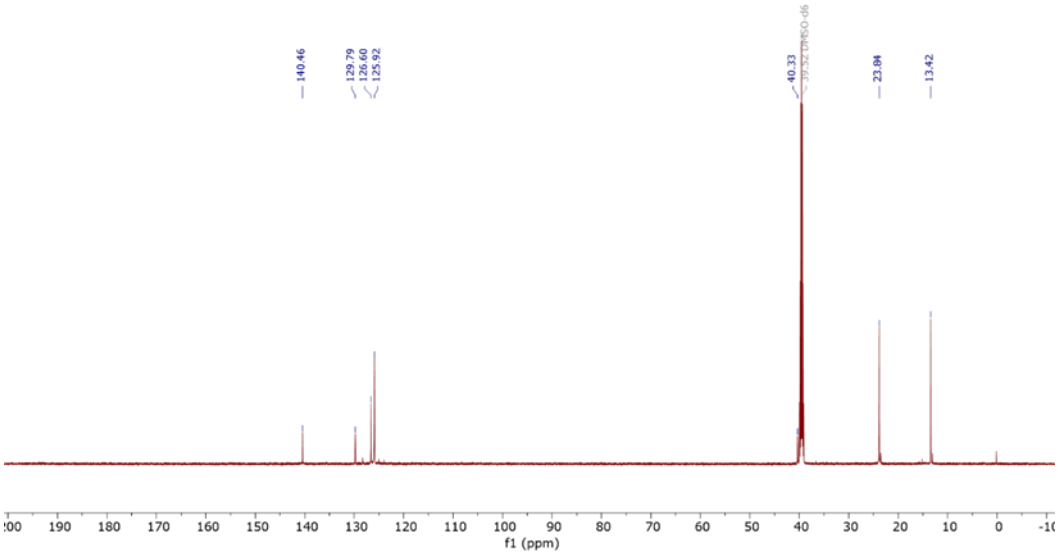

Figure S40. ^{13}C{^{1}H} NMR of recovered MDEA in DMSO-d_6.

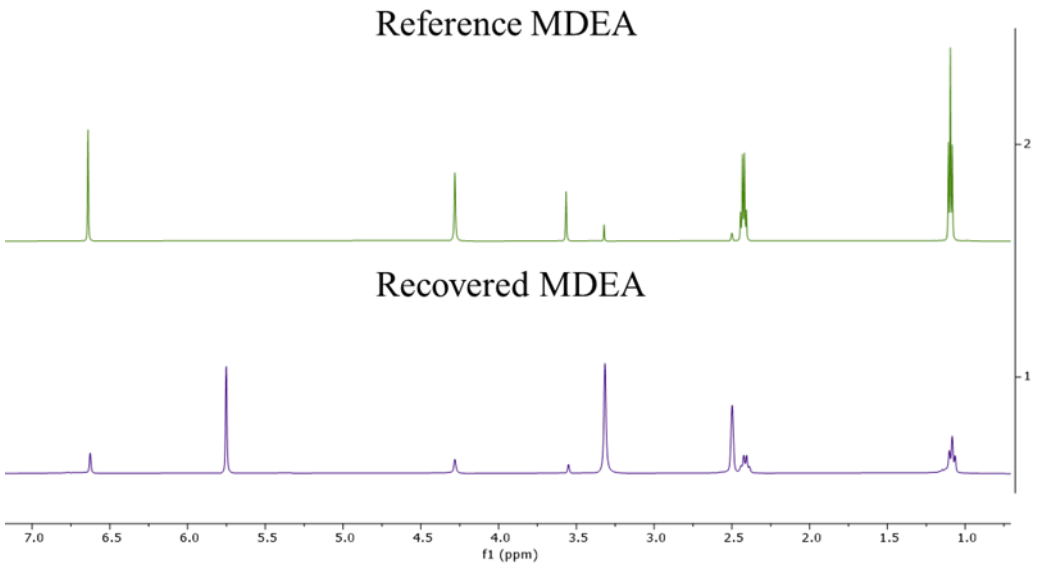

Figure S41. Stacked ^{1}H NMR of recovered MDEA and reference MDEA in DMSO-d_6.

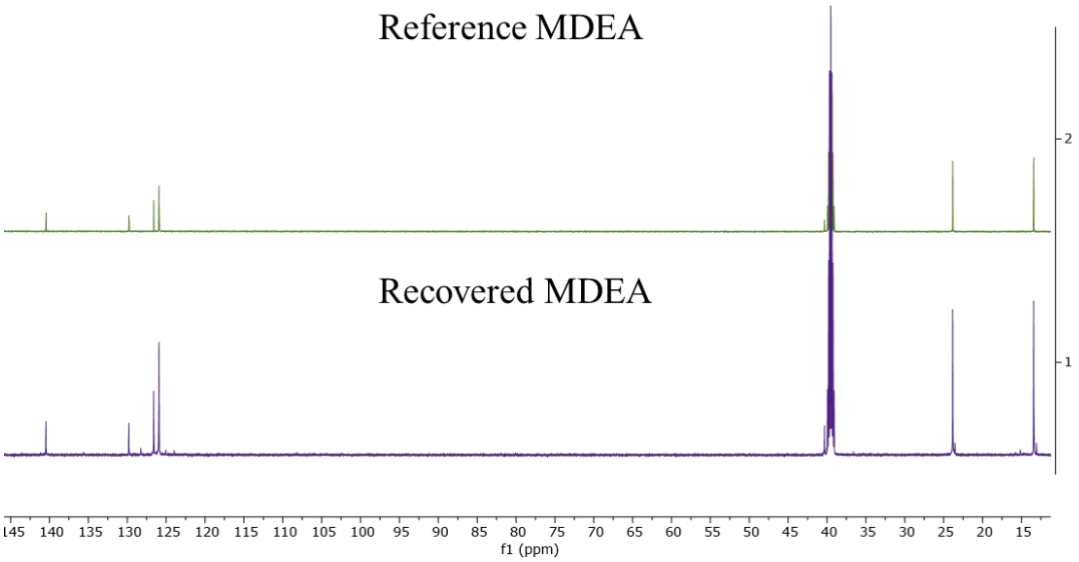

Figure S42. Stacked ^{13}C{^{1}H} NMR of recovered MDEA and reference MDEA in DMSO-d_6.

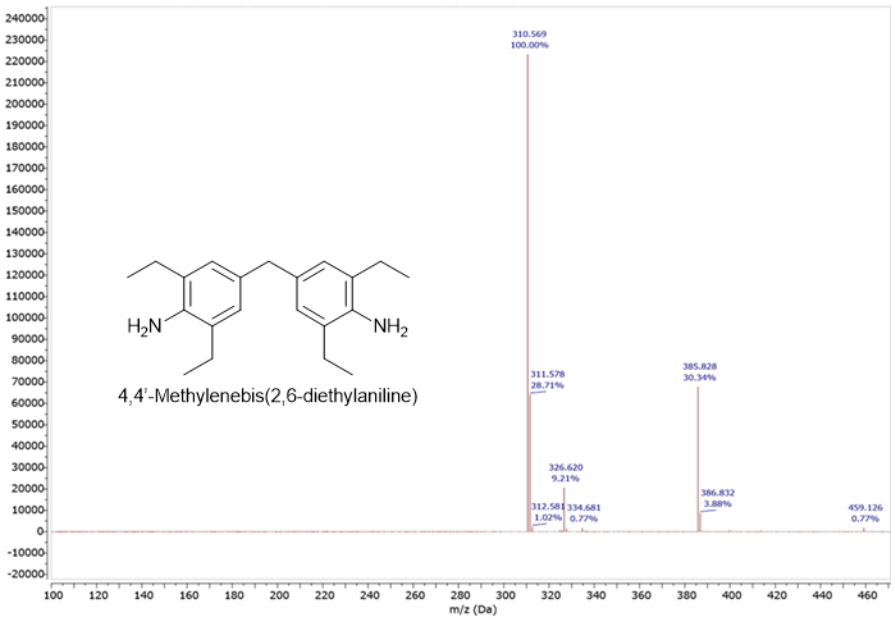

Figure S43. MALDI data of recovered MDEA, anthracene matrix.

b. Organic neutral extract from dichloromethane

Next, the aqueous phase was brought to pH 6 by adding concentrated HCl. After cooling, the neutral solution was extracted with DCM (15 mL x 3). The organic layer was cleaned using DI water (5 mL x 3), dried over sodium sulfate, and evaporated to give a yellowish solid (recovered BPA). Isolated materials were characterized by ^{1}H NMR spectroscopy (Figure S44). A summary of the degradation component isolation is provided in Table S22.

Recovered bisphenol-A (BPA). ^{1}H NMR (400 MHz, cdcl3) δ 7.15 – 7.04 (m, 4H), 6.79 – 6.64 (m,4H), 1.62 (s, 6H).

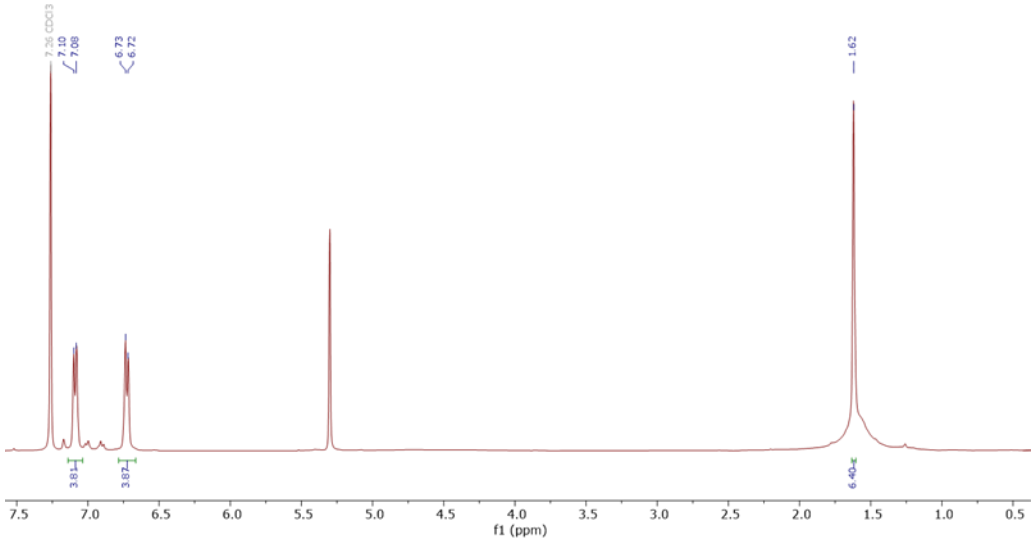

Figure S44. ^{1}H NMR of recovered BPA from the MDEA-cured polymer degradation reaction in $CDCl_3$.

10. **Reaction yields of degradation components**

a. Determination of unit polymer

To determine the moles of BPA recovered we first had to determine the number of moles of BPA in a given mass of polymer. Based on the formulation of the resin (SI section 1a), it is comprised of 2 molar equivalents of the epoxy monomer DGEBA and 1 molar equivalent of the curing agent 3,3'-DDS. Therefore, we can define the smallest unit of the polymer as (1 eq. 3,3'-DDS + 2 eq. DGEBA). The molecular weight of the Bi/DDS unit polymer is 928 g/mol ($C_{54}H_{60}N_2O_{10}S$). With the same amine to epoxy mixing ratio, we assume that Bi/MDEA formulation has the same molar ratio between epoxy monomer DGEBA and curing agent MDEA. The molecular weight of the Bi/MDEA unit polymer is 990 g/mol ($C_{63}H_{78}N_2O_8$).

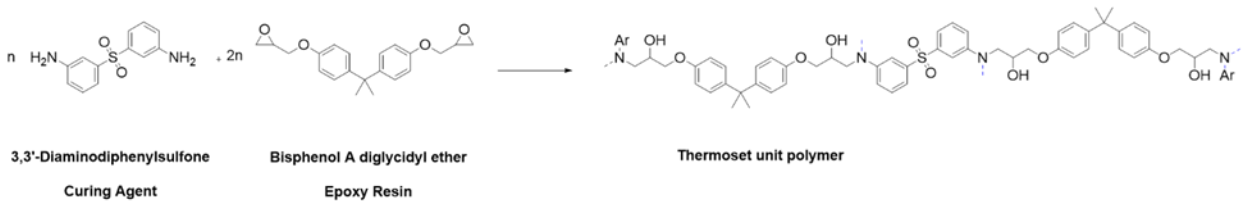

Figure S45. Portrayal of the thermoset unit polymer ($C_{54}H_{60}N_2O_{10}S$). The unit polymer has a molecular weight of 928 g/mol.

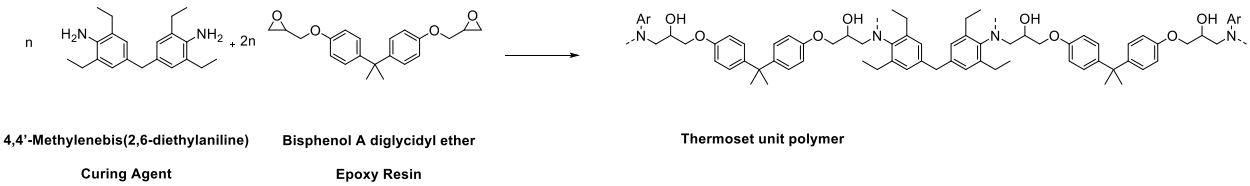

Figure S46. Portrayal of the thermoset unit polymer ($C_{63}H_{78}N_2O_8$). The unit polymer has a molecular weight of 990 g/mol.

b. Verification of proposed unit polymer using CHNS elemental analysis

To further verify that the proposed unit polymer is the smallest representative unit of this thermoset system we did an experiment by analyzing the polymer in the CHNS elemental analyzer (Flash 2000 Elemental Analyzer (CHNS)) and comparing its elemental percentages to the proposed unit polymer. The results are shown in Table S19.

The elemental percentages of the resin nearly match the elemental percentages of the proposed unit polymer. Therefore, the proposed unit polymer is an appropriate chemical formula to use to represent the polymer.

Table S19. CHNS elemental analysis results of the resin polymer. The elemental percentages are compared against the elemental percentages of the proposed unit polymer.

	C (%)	H (%)	N (%)	S (%)
$C_{54}H_{60}N_2O_{10}S$	69.81	6.57	3.02	3.45
Bi/DDS matrix	70.86	6.63	2.89	2.56

c. Reaction yields of degradation components from Bi/DDS sample digestion

Mass of degraded matrix of CFRP digestion:

$$Mass\ of\ degraded\ matrix\ of\ CFRP\ digestions = \text{Mass of CFRP} - \text{Mass of recovered CFs}$$

Moles of DGEBA in degraded matrix:

$$Mol\ of\ DGEBA\ in\ degraded\ matrix = \frac{Mass\ of\ degraded\ matrix}{(Polymer\ Unit\ MW)} \cdot 2$$

Moles of 3,3'-DDS in degraded matrix:

$$Mol\ of\ 3{,}3'DDS\ in\ degraded\ matrix = \frac{Mass\ of\ degraded\ matrix}{(Polymer\ Unit\ MW)}$$

Yield of BPA:

$$BPA\ Yield = \frac{Mol\ of\ recovered\ BPA}{Mol\ of\ DGEBA\ in\ degraded\ matrix} \cdot 100\%$$

Yield of aniline or 3-aminophenol:

$$Aniline\ or\ 3\ aminophenol\ Yield = \frac{Mol\ of\ recovered\ aniline\ or\ 3\ aminophenol}{(Mol\ of\ 3{,}3'DDS\ in\ degraded\ matrix) \cdot 2} \cdot 100\%$$

The following tables display the yield of isolated BPA from pre-treated and unpretreated Bi/DDS sample digestion experiments:

Table S20. BPA yield summary for pre-treated Bi/DDS CFRP digestion.

Temperature (˚C)	Composite initial mass (g)	Recovered CFs (g)	Isolated BPA (g)	BPA yield (%)
220	0.5739	0.3514	0.0939	86

Table S21. Products isolation summary of unpretreated Bi/DDS neat resin and CFRP digestions.

Entry	Mass change (g,wt%)	Extracted products (mg, yield%)			
		Distillate (aniline)	Basic extract	Acid extract (BPA)	Neutral extract (C_6H_7NO)
1	1.631 (82%)	46 (14%)	27	626 (78%)	
2	1.970 (99%)	75 (19%)			
3	0.475 (95%)		15	213 (92%)	41 (<37%)
4	0.700 (23%)		13	343 (>99%)	43 (<26%)
5	0.720 (36%)	42 (29%)			

d. Reaction yields of degradation components from Bi/MDEA sample digestion

Moles of DGEBA in degraded matrix:

$$Mol\ of\ DGEBA\ =\ \frac{Mass\ of\ degraded\ matrix}{(Polymer\ Unit\ MW)} \cdot 2$$

Moles of MDEA in degraded matrix:

$$Mol\ of\ MDEA\ =\ \frac{Mass\ of\ degraded\ matrix}{(Polymer\ Unit\ MW)}$$

Yield of BPA:

$$BPA\ Yield\ =\ \frac{Mol\ of\ recovered\ BPA}{Mol\ of\ DGEBA\ in\ degraded\ matrix} \cdot 100\%$$

Yield of MDEA:

$$MDEA\ Yield\ =\ \frac{Mol\ of\ recovered\ MDEA}{Mol\ of\ MDEA\ in\ degraded\ matrix} \cdot 100\%$$

Table S22. Products isolation summary of Bi/MDEA neat resin and CFRP digestions.

Temperature (˚C)	Sample mass (g)	Isolated crude MDEA (g)	MDEA yield (%)	Isolated BPA (g)	BPA yield (%)
260	0.2018	0.0374	59	0.0501	54

11. **Model 1 synthesis and degradation reactions**

a. Synthesis of Model 1

Scheme S2. Synthesis of Model 1.

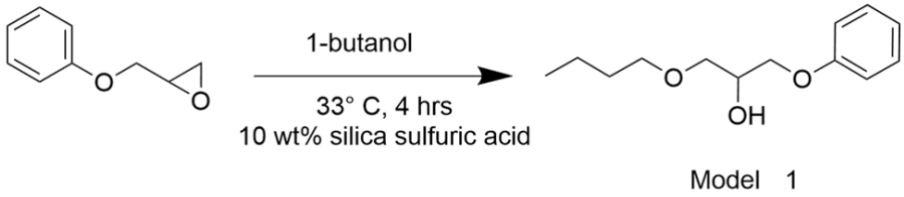

In a 100 mL round bottom flask 30 mL (24.3 g, 0.328 mol, 16.4 eq.) of 1-butanol was combined with 0.34 g silica sulfuric acid. Then 3.1 mL (3.45 g, 23 mmol) of the 2-(phenoxymethyl)oxirane was slowly added. Once all combined, the flask was placed in an oil bath and heated to 33˚C for four hours.

After four hours have passed, 50 mL of dichloromethane was added. Then the reaction mixture was transferred to a 250 mL separatory funnel and washed with DI H_2O (3 x 50 mL). The organic layer was collected, and the solvent was removed under reduced pressure. The oily liquid was then dry loaded on silica and the product was isolated by flash chromatography (15:85 Ethyl Acetate: Hexanes).

The ^{1}H and ^{13}C NMR spectra can be found in Figures S47 and S48. Literature reports of this compound exist and confirm we selectively synthesized the desired regioisomer (Yield = 63%)

^{1}H NMR (600 MHz, $CDCl_3$): δ 7.35 – 7.22 (m, 2H), 6.95 (dd, J = 25.3, 7.8 Hz, 3H), 4.30 – 4.12 (m, 1H), 4.10 – 3.98 (m, 2H), 3.66 – 3.54 (m, 2H), 3.50 (tt, J = 6.6, 3.1 Hz, 2H), 1.66 – 1.46 (m, 2H), 1.38 (h, J = 7.4 Hz, 2H), 0.92 (t, J = 7.3 Hz, 3H).

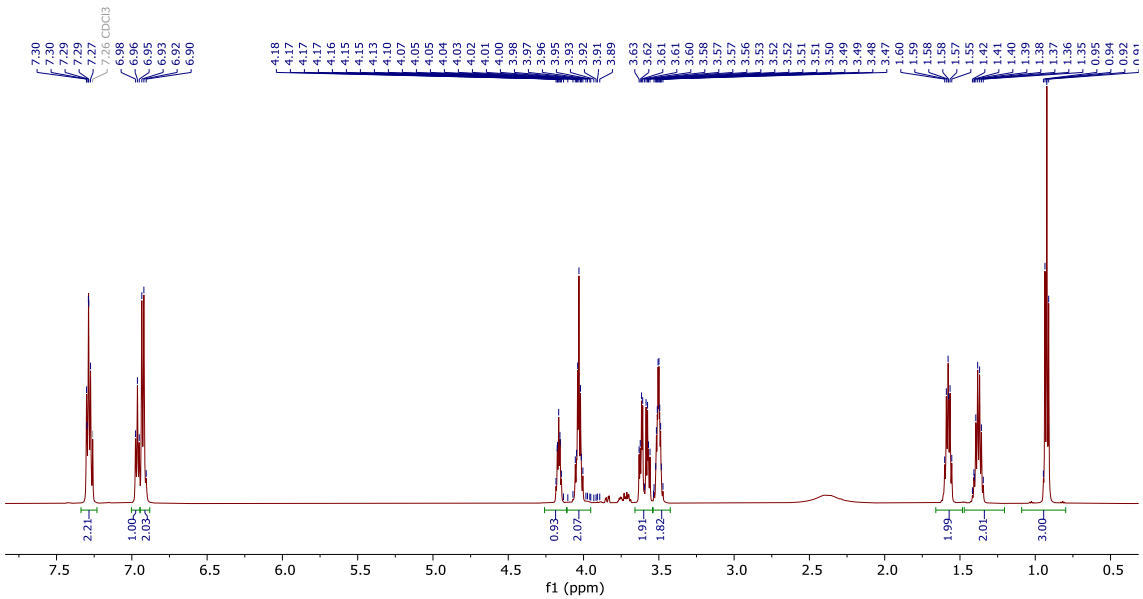

Figure S47. ^{1}HNMR of Model 1 in $CDCl_3$

^{13}C NMR (151 MHz, $CDCl_3$): δ 158.74, 129.60, 121.18, 114.70, 71.62, 71.58, 69.25, 69.09, 31.80, 19.39, 14.01.

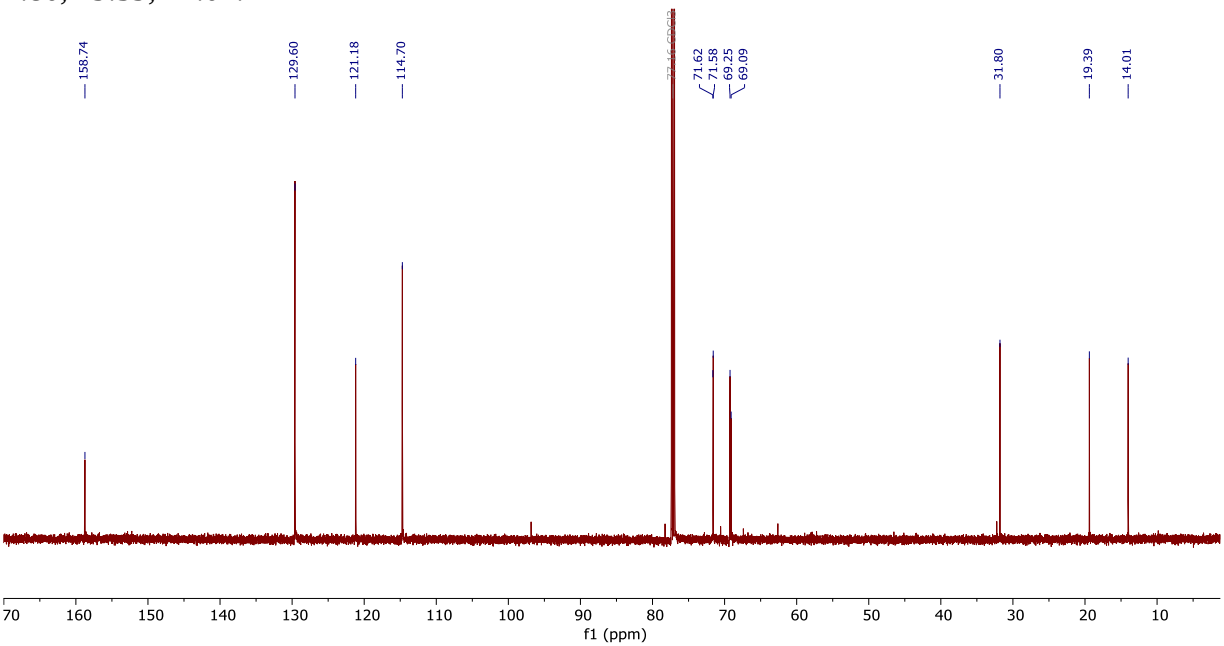

Figure S48. ^{13}C{^{1}H} NMR of isolated Model 1 in $CDCl_3$

b. Model 1 degradation reaction at 180 ˚C

Scheme S3. Degradation reaction of Model 1 at 180˚C.

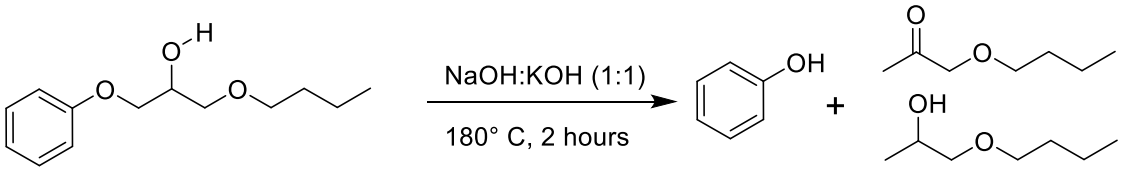

Finely ground NaOH (0.1 g, 2.5 mmol) and KOH (0.14 g, 2.5 mmol) were added to a 50 mL Schlenk flask. Model 1 (0.18 g, 0.8 mmol) was then transferred into the flask. Finally, the flask was flushed with nitrogen gas and placed in an oil bath set to 180 ˚C for two hours. After the reaction, aqueous sodium bicarbonate solution (saturated, 50 mL) was added to the Schlenk flask to dissolve the solid residue. The aqueous mixture was then transferred to a 250 mL separatory funnel. Dichloromethane (50 mL) was then added to the Schlenk flask and then transferred to the separatory funnel, extracted, and collected in a 250 mL round bottom flask. This was repeated twice. The organic layers were then combined, and the solvent was removed under reduced pressure. The ^{1}H,^{13}C, HMBC and HSQC spectra can be found in Figures S49-56 respectively.

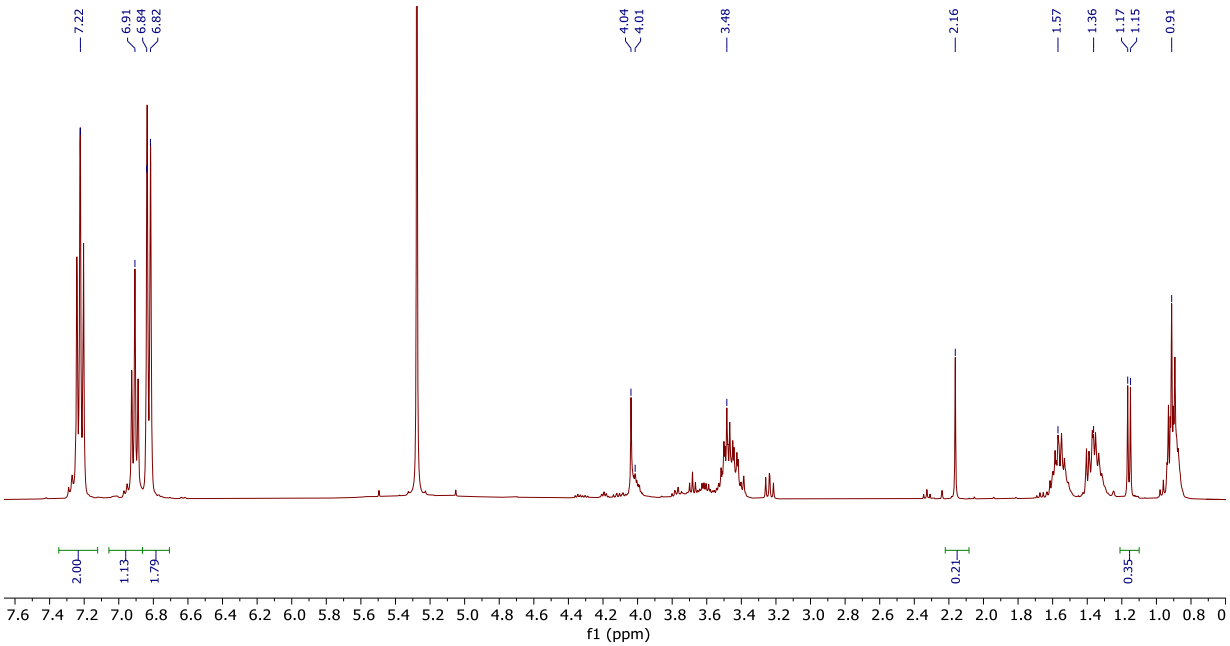

Figure S49. ^{1}HNMR of 180˚C Model 1 degradation reaction extract in $CDCl_3$.

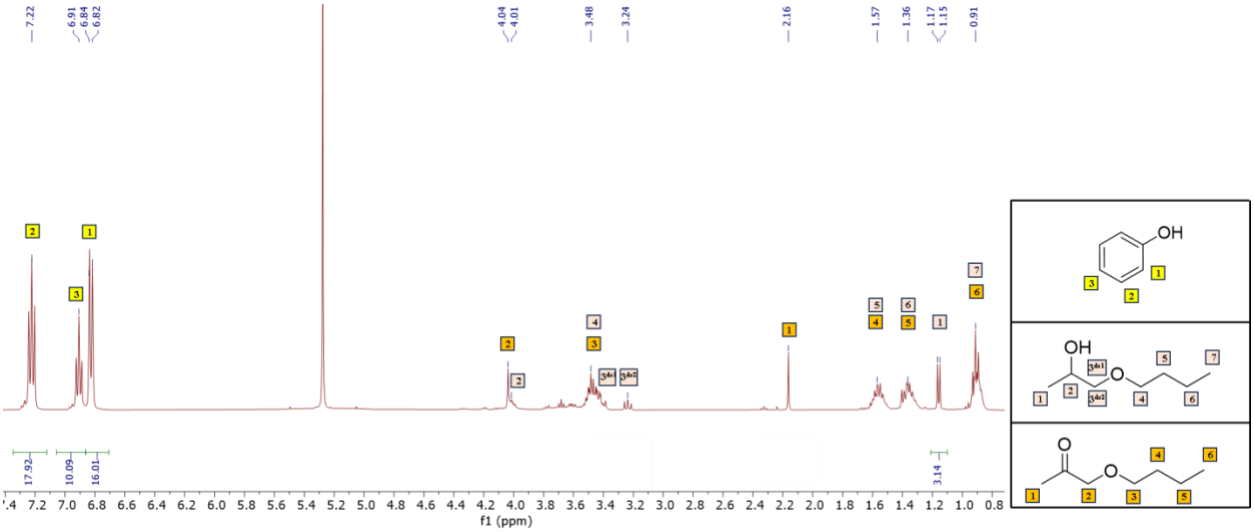

Figure S50. Annotated 1HNMR of 180˚C Model 1 degradation reaction extract in $CDCl_3$.

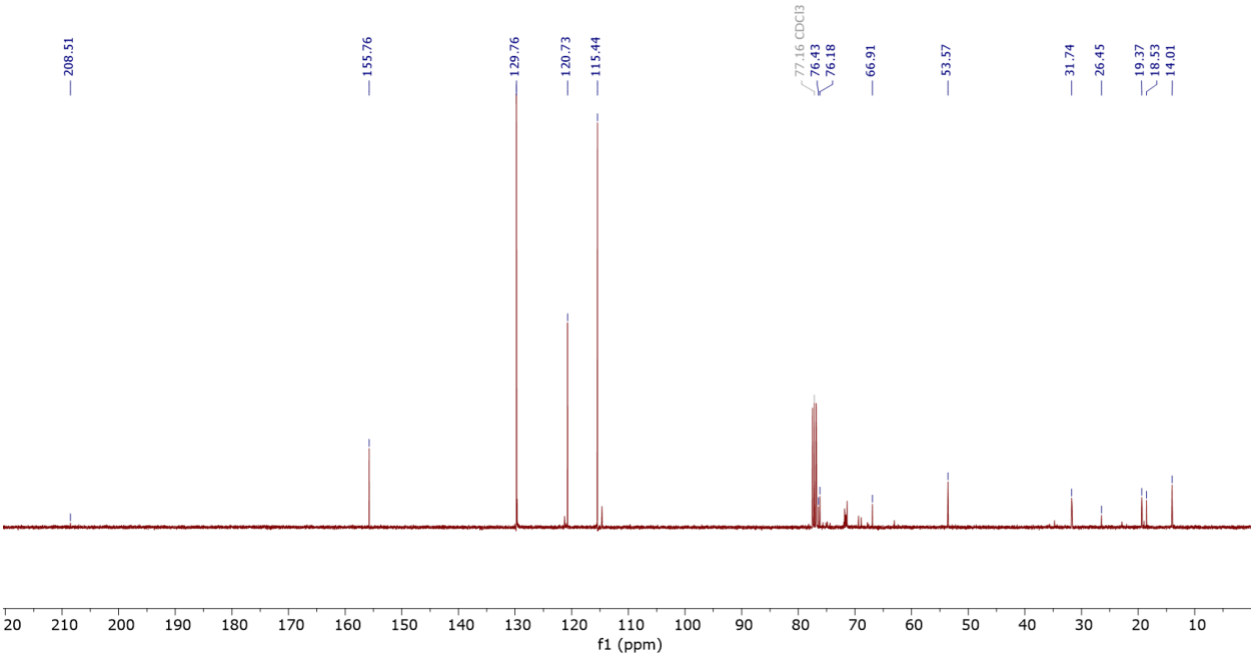

Figure S51. $^{13}C\{^{1}H\}$ NMR of Model 1 180˚C degradation reaction extract in $CDCl_3$.

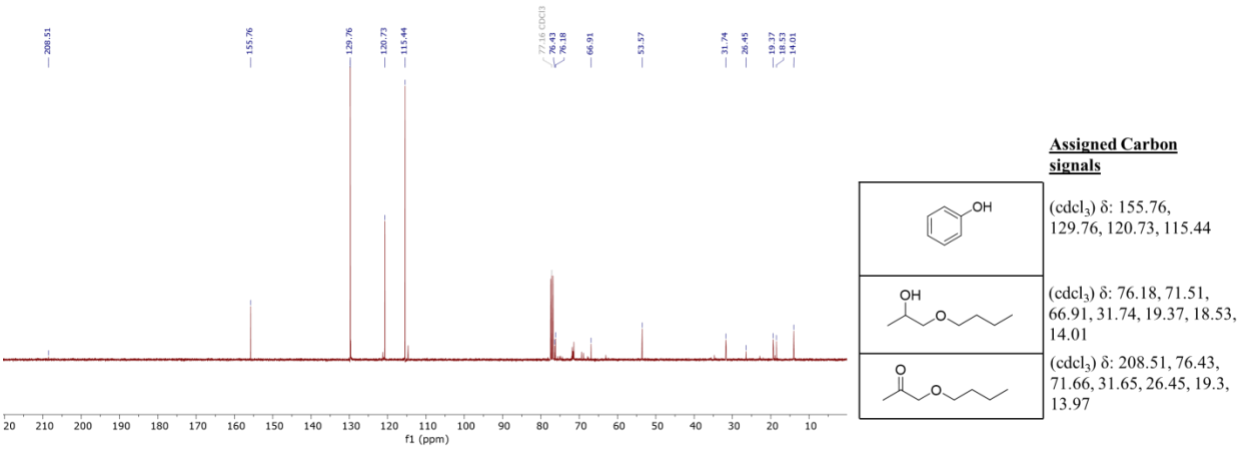

Figure S52. Annotated $^{13}C\{^{1}H\}$ NMR of Model 1 180˚C degradation reaction extract in $CDCl_3$.

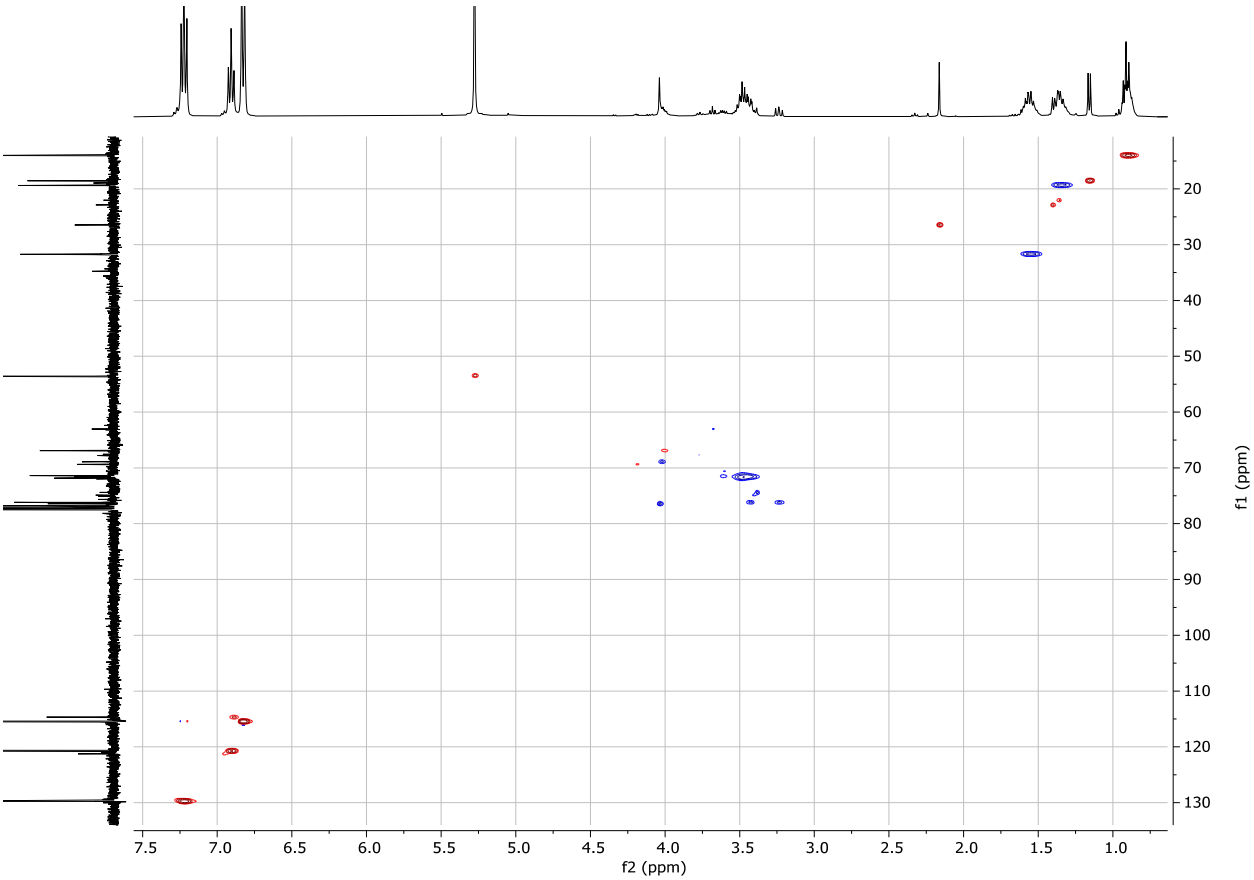

Figure S53. HSQC of Model 1 180˚C degradation reaction extract in $CDCl_3$.

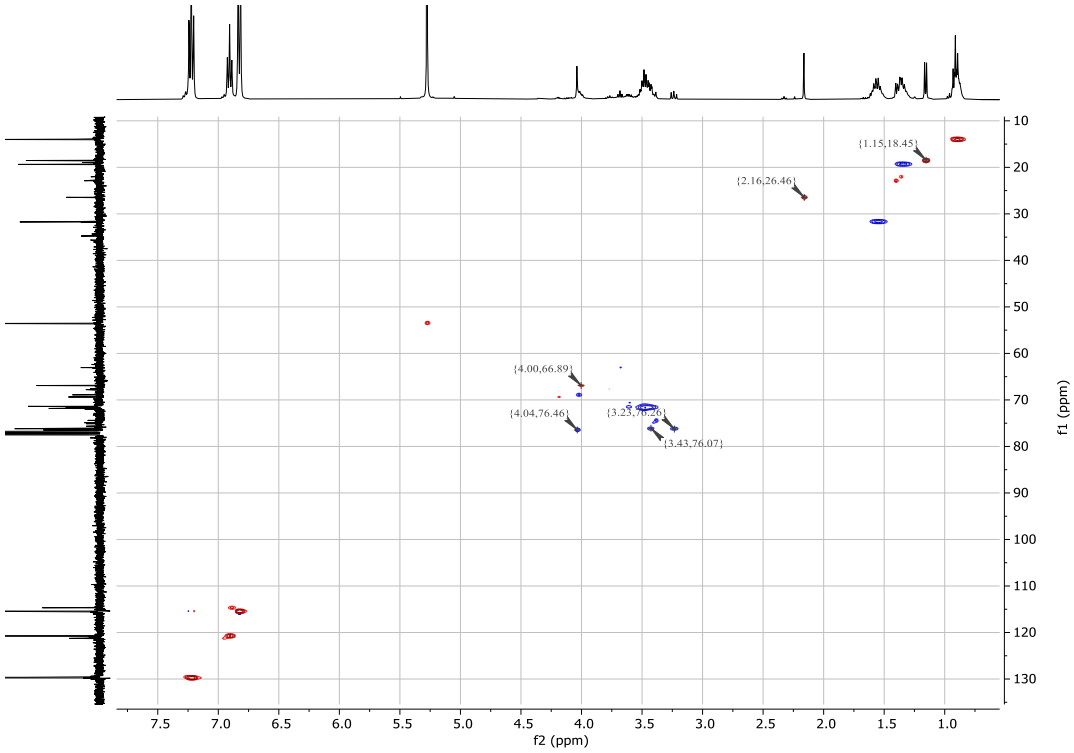

Figure S54. Annotated HSQC NMR of Model 1 180 ˚C degradation reaction extract in $CDCl_3$.

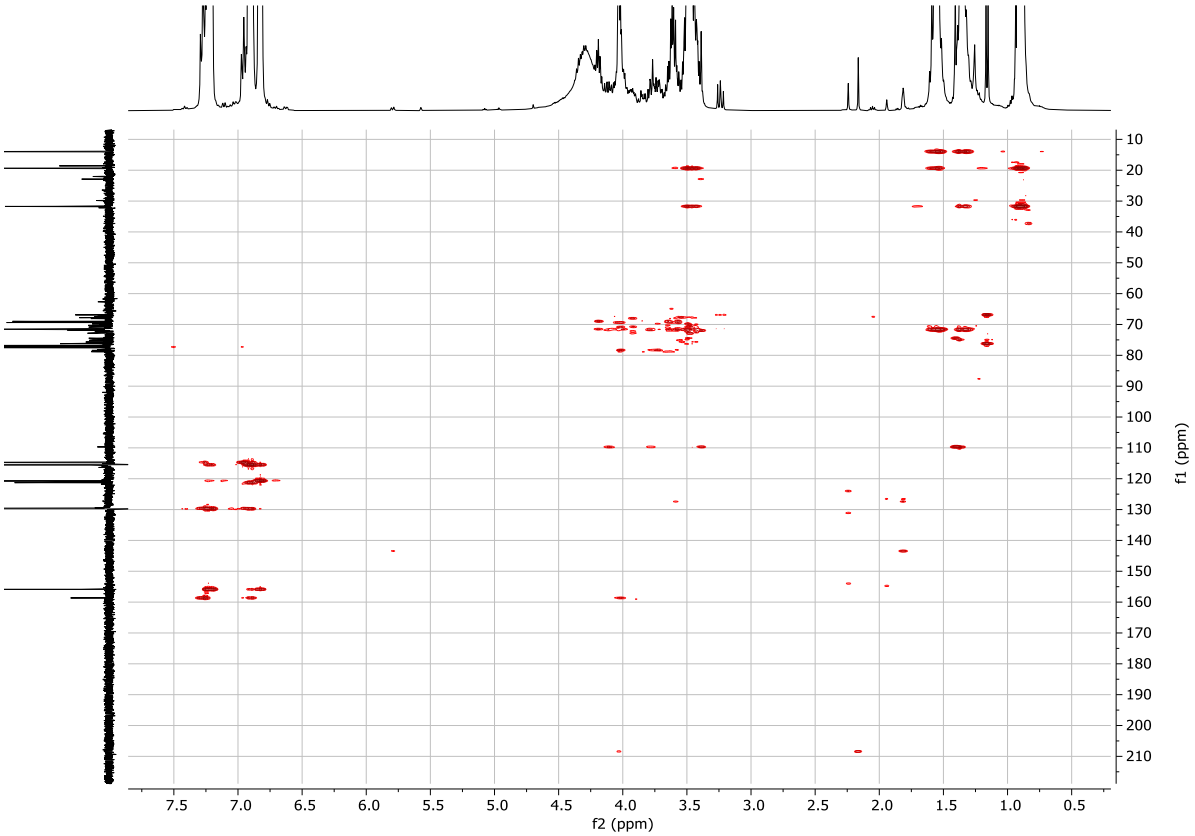

Figure S55. HMBC of Model 1 180˚C degradation reaction extract in $CDCl_3$.

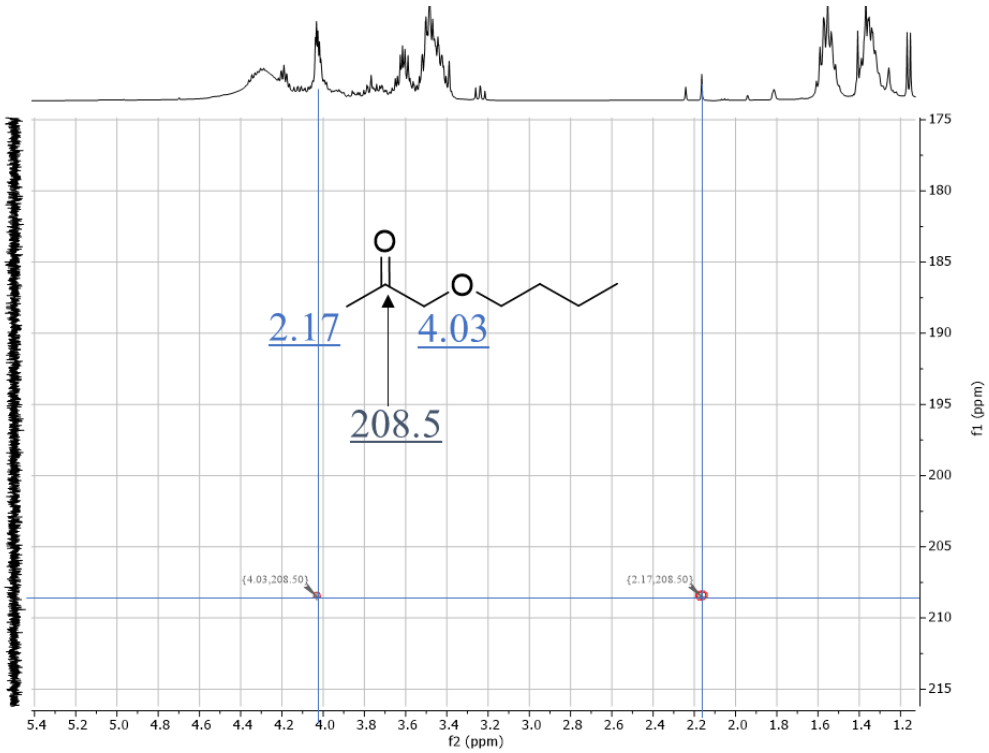

Figure S56. Annotated HMBC NMR of Model 1 180˚C degradation reaction extract in $CDCl_3$.

c. Model 1 Degradation Reaction at 150 ˚C

Scheme S4. Degradation reaction of Model 1 at 150 ˚C.

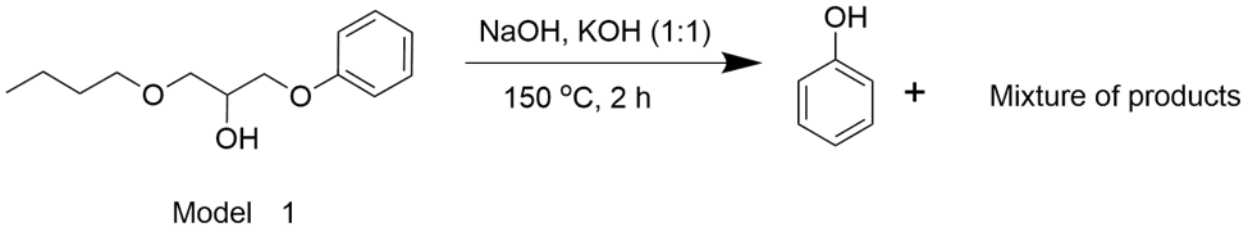

Model 1

Finely grounded NaOH (0.1 g, 2.5 mmol) and KOH (0.14 g, 2.5 mmol) were added to a 50 mL Schlenk flask. Then Model 1 (0.18 g, 0.8 mmol) was transferred into the flask. Finally, the flask was carefully flushed nitrogen gas and placed in an oil bath set to 150 ˚C for two hours. After the reaction, aqueous sodium bicarbonate (saturated, 50 mL) was added to the Schlenk flask to dissolve the solid residue. The aqueous mixture was then transferred to a 250 mL separatory funnel. Dichloromethane (50 mL) was then added to the Schlenk flask and then transferred to the separatory funnel, extracted, and collected in a 250 mL round bottom flask. This was repeated twice. The organic layers were then combined, and the solvent was removed under reduced pressure. The ^{1}H and ^{13}C NMR spectra can be found in Figures S57-58. The LC/MS data can be found in Figure S59.

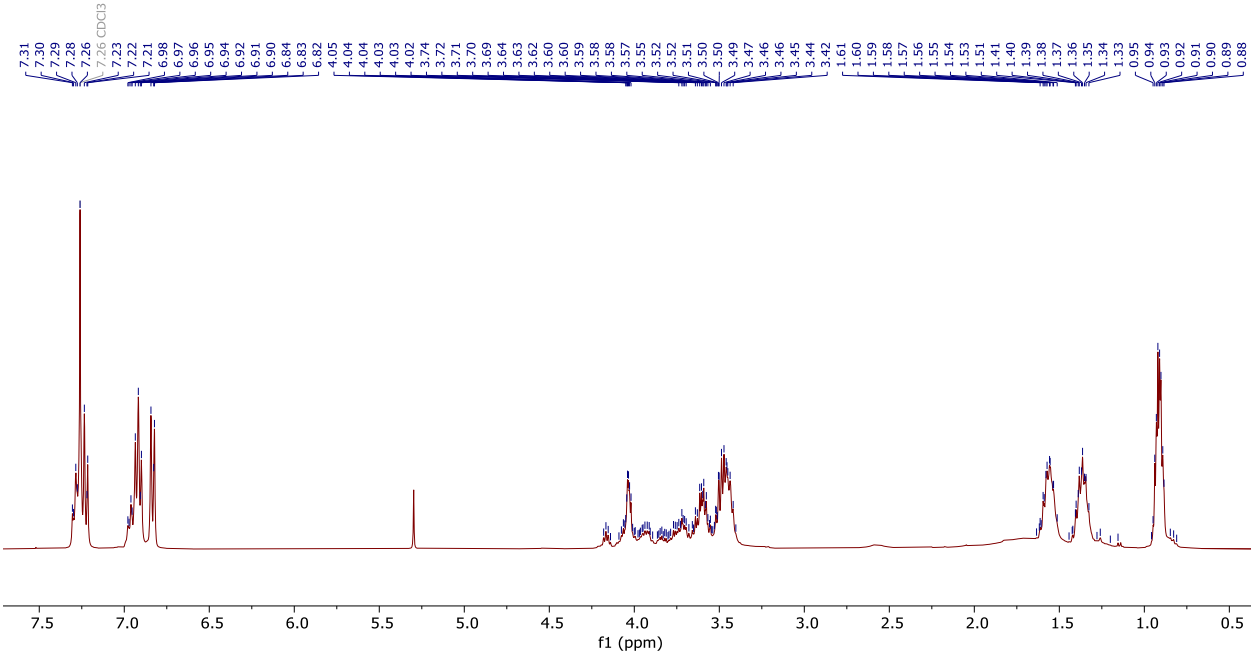

Figure S57. ^{1}HNMR of Model 1 150˚C degradation reaction extract in $CDCl_3$.

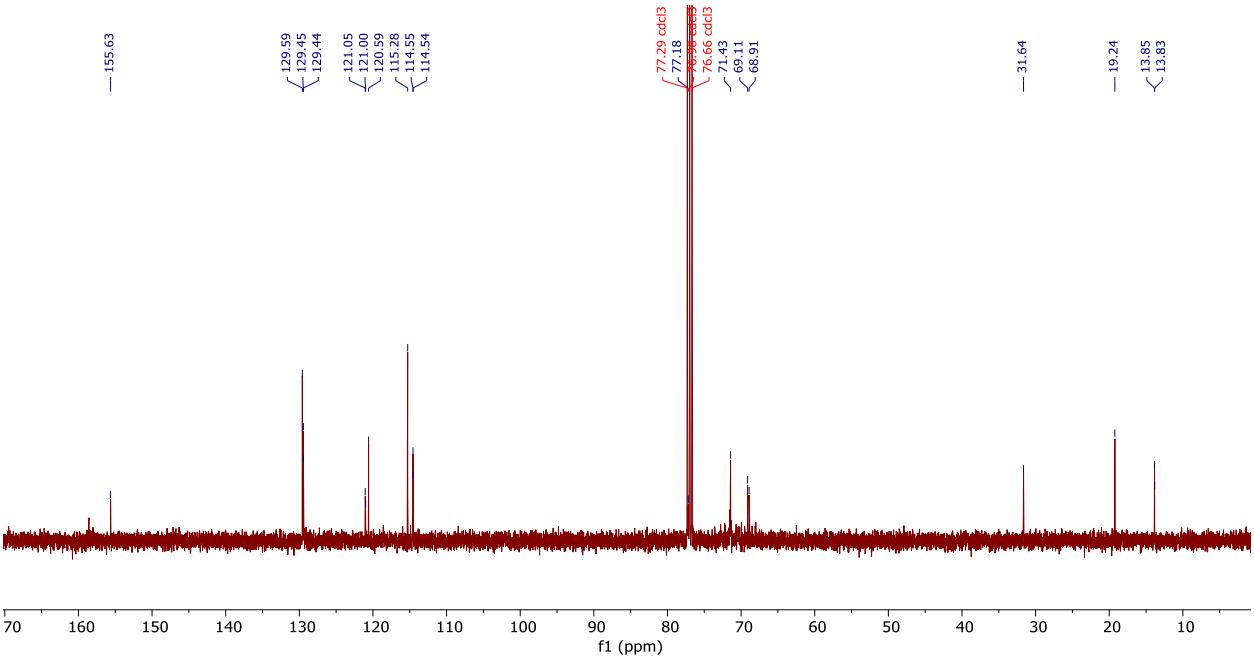

Figure S58. $^{13}C\{^{1}H\}$ of Model 1 150˚C degradation reaction extract in $CDCl_3$.

Scheme S5. Degradation of Model 1 at 150 ˚C examined on LC-QTOF.

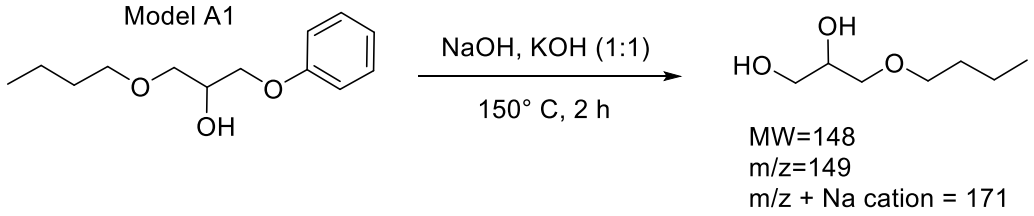

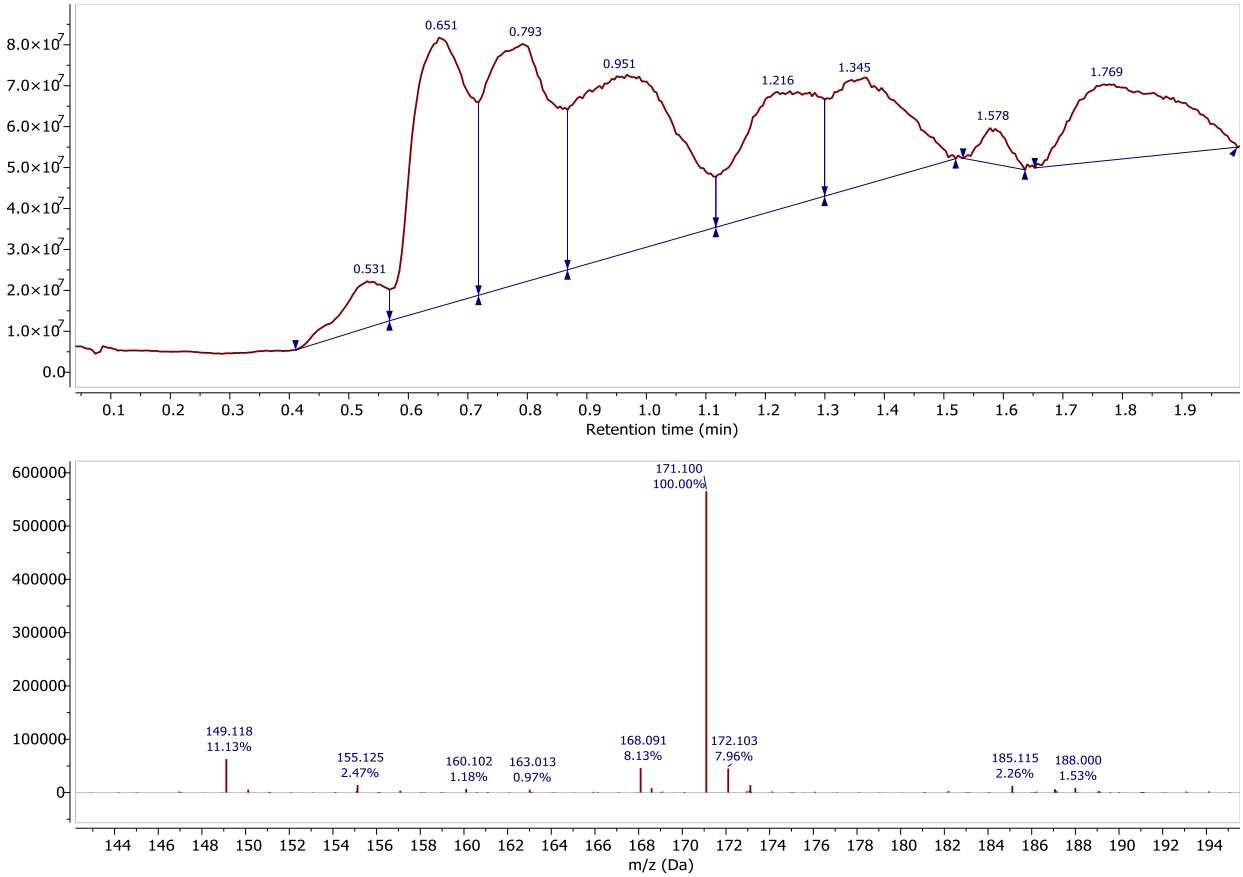

Figure S59. LC-QTOF of Model 1 150 ˚C degradation reaction extract at retention time = 0.49 min.

12. **Model 2 synthesis and degradation reactions**

a. Synthesis of Model 2

Scheme S6. Synthesis of Model 2.

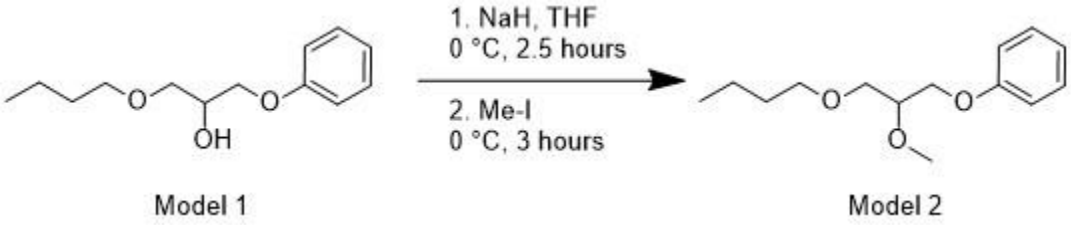

To a 250 mL round bottom flask was added tetrahydrofuran (THF, 80 mL, 71 g, 985 mmol), and the flask was placed in a 0 °C ice bath. Once cool, NaH (420 mg, 17.5 mmol, 1.56 eq.) was added to the flask to create a suspension. The ice bath was then moved over a stirrer and a magnetic stir bar was added inside the flask. Over the course of 15 minutes, Model 1 (2.5 g, 11.2 mmol, 1eq.) was added dropwise to the flask. After Model 1 was added, the vessel was flushed with nitrogen and a glass stopper was placed above the flask (without completely closing it) and the suspension was allowed to stir for 2.5 hours.

When 2.5 hours had elapsed, methyl iodide (1.88 mL, 4.29 g, 30.2 mmol, 2.7 eq.) was added into the flask and it was allowed to continue stirring for 3 hours. Thereafter, volatiles were removed under reduced pressure and the remaining contents of the flask were dissolved in H_2O (deionized, 50 mL) and transferred to a separatory funnel. Then the liquid mixture was extracted with DCM (3 x 50 mL).

The organic layers were combined, and the solvent was removed under reduced pressure. The resulting oily liquid was then dry loaded on silica and the product was isolated by flash chromatography (15:85 ethyl acetate: hexanes). The ^{1}H NMR, ^{13}C NMR, FT-IR, and LC-QTOF spectra can be found in Figures S60-63.

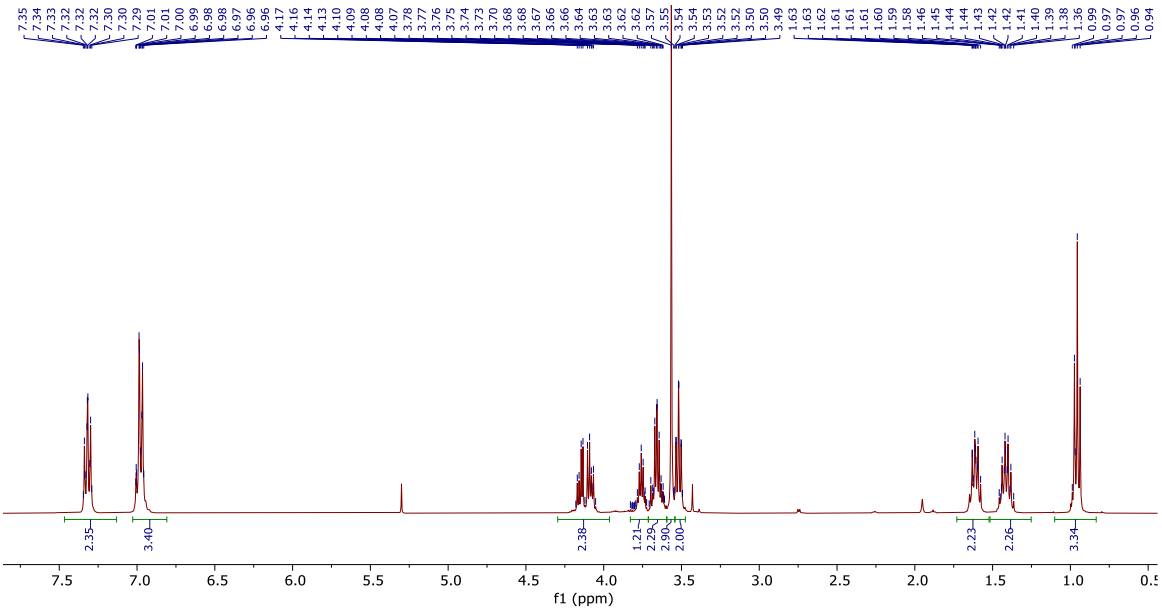

Figure S60. ^{1}HNMR of Model 2 in $CDCl_3$.

^{1}H NMR (400 MHz, cdcl3) δ 7.40 – 7.24 (m, 2H), 6.99 (td, J = 7.6, 1.4 Hz, 3H), 4.22 – 4.03 (m, 2H), 3.76 (p, J = 5.0 Hz, 1H), 3.71 – 3.60 (m, 2H), 3.57 (s, 3H), 3.52 (td, J = 6.6, 1.0 Hz, 2H), 1.73 – 1.51 (m, 2H), 1.50 – 1.32 (m, 2H), 0.96 (t, J = 7.4 Hz, 3H).

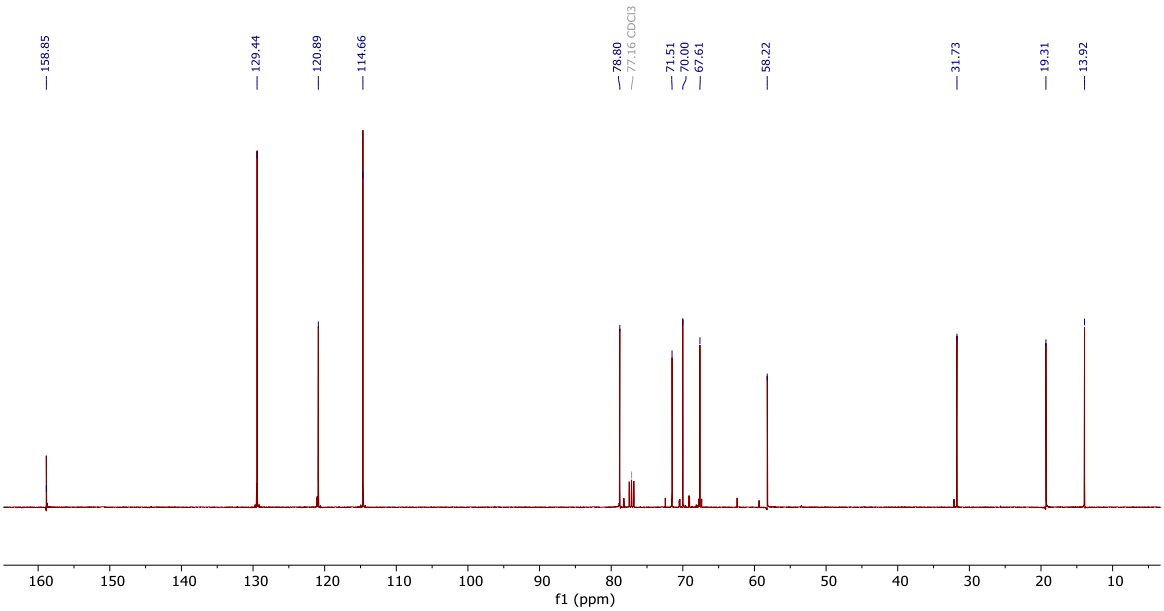

Figure S61. ^{13}CNMR of Model 2 in $CDCl_3$.

^{13}C NMR (100 MHz, cdcl3) δ 158.86, 129.44, 120.89, 114.66, 78.80, 71.51, 70.00, 67.61, 58.22, 31.73, 19.31, 13.92.

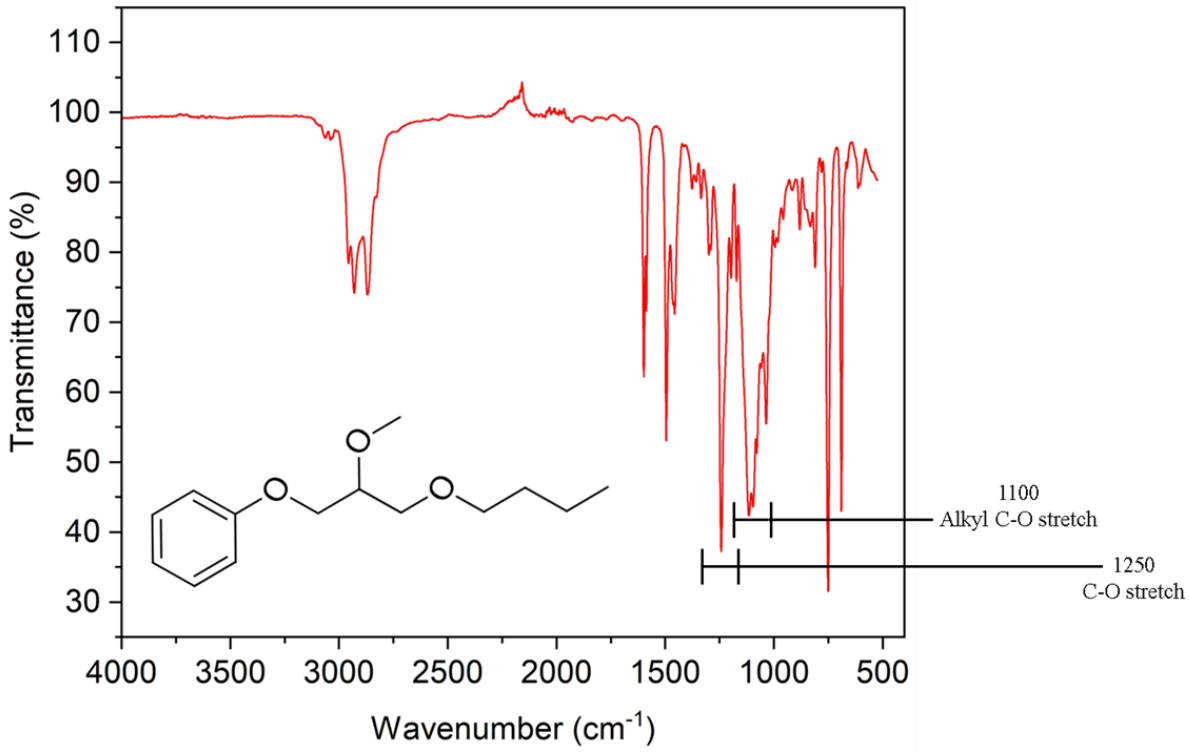

Figure S62. FTIR of Model 2.

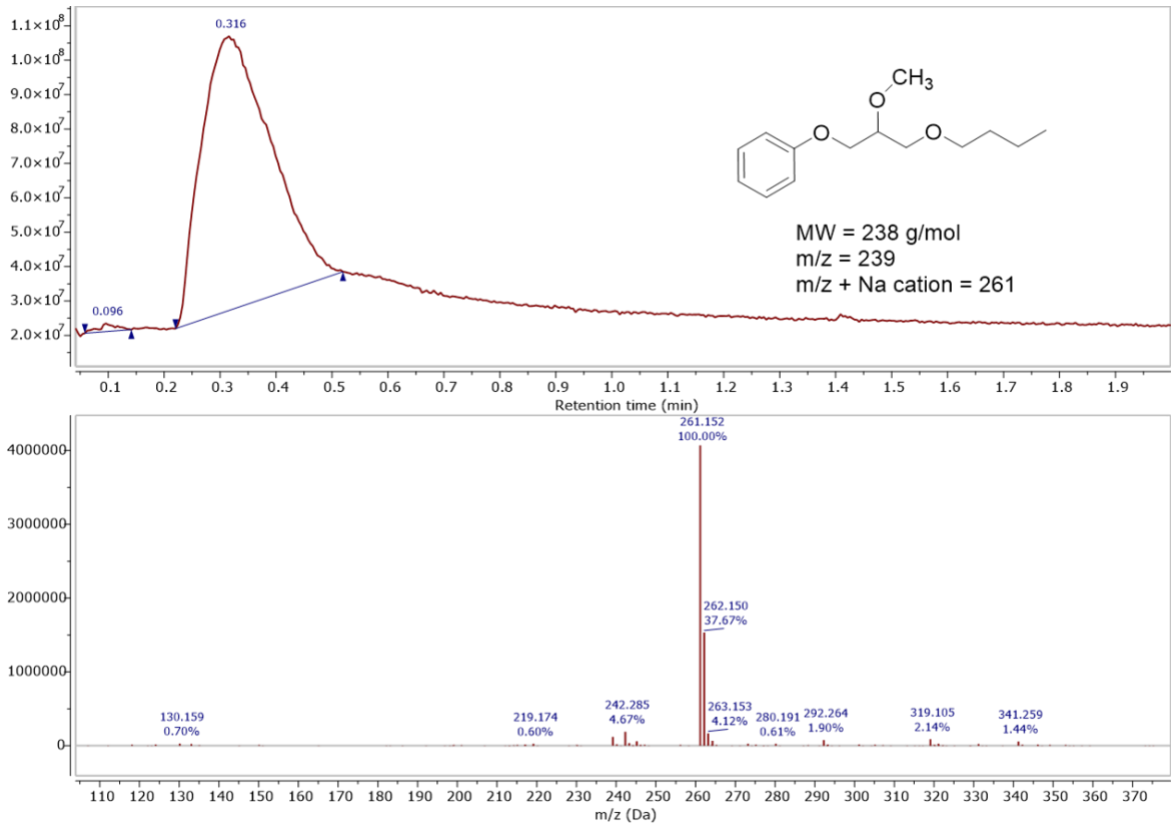

Figure S63. LC-QTOF of Model 2 at retention time = 0.32 min.

b. Model 2 degradation reaction at 180 ˚C

Scheme S7. Degradation reaction of Model 2 at 180 ˚C

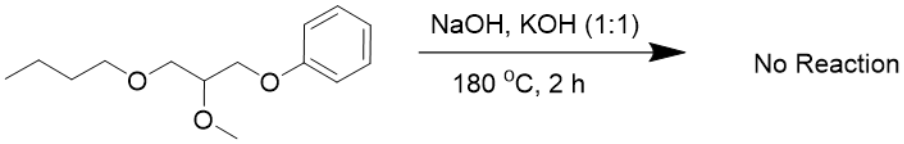

Model 2

Finely ground NaOH (0.1 g, 2.5 mmol), and KOH (0.14 g, 2.5 mmol) was added to a 50 mL Schlenk flask. Then Model 2 (200 mg, 0.84 mmol) was transferred into the flask. Finally, the flask was carefully flushed with nitrogen gas and placed in an oil bath set to 180 ˚C for two hours. After the reaction, 50 mL of saturated sodium bicarbonate was added to the Schlenk flask to dissolve the solid residue. The aqueous mixture was then transferred to a 250 mL separatory funnel. The organic material was then extracted with DCM (3 x 30 mL). The organic layers were then combined, and the solvent was removed under reduced pressure. The ^{1}H and ^{13}C NMR spectra can be found in Figures S64 and S65.

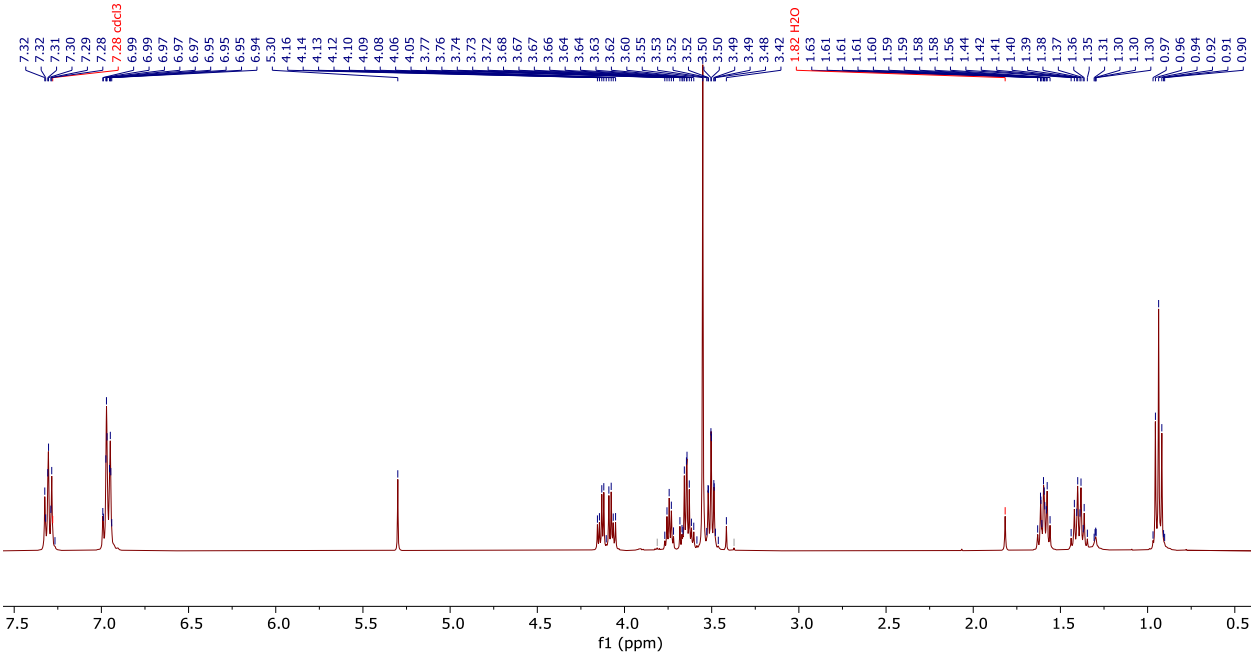

Figure S64. ^{1}HNMR of Model 2 180˚C degradation reaction extract $CDCl_3$.

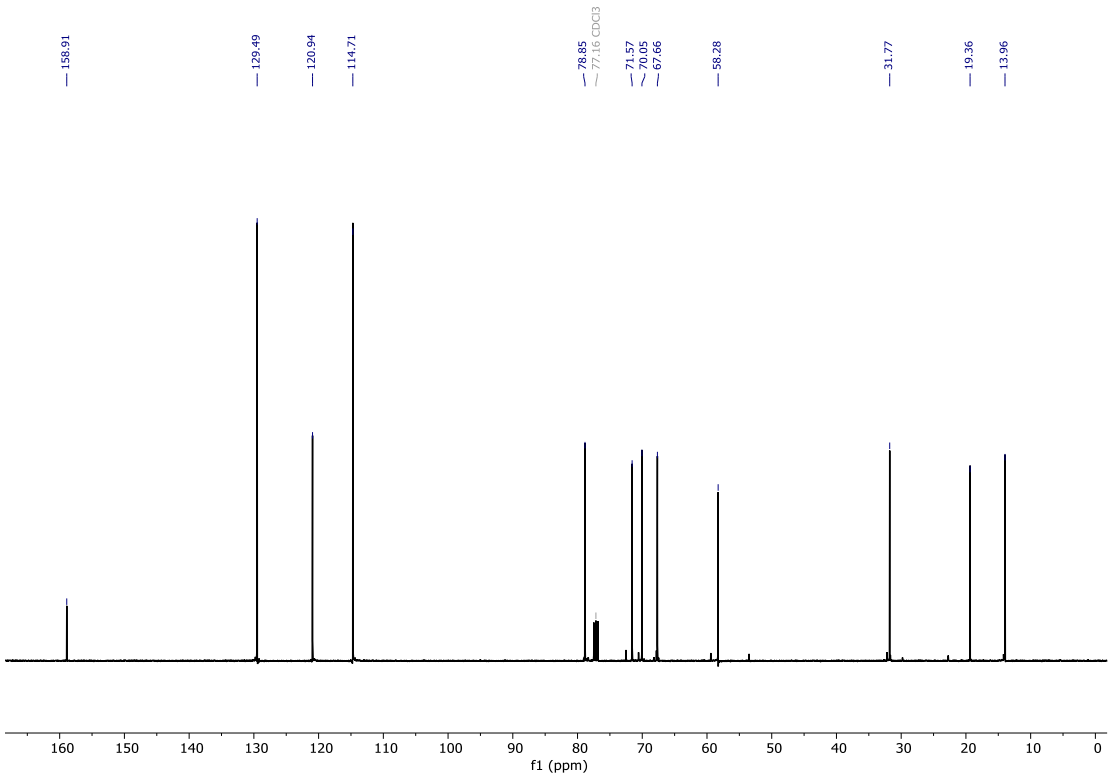

Figure S65. $^{13}C\{^{1}H\}$ NMR of Model 2 180˚C degradation reaction extract $CDCl_3$.

c. Model 2 Degradation reaction at 150˚C

Scheme S8. Degradation reaction of Model 2 at 150 ˚C.

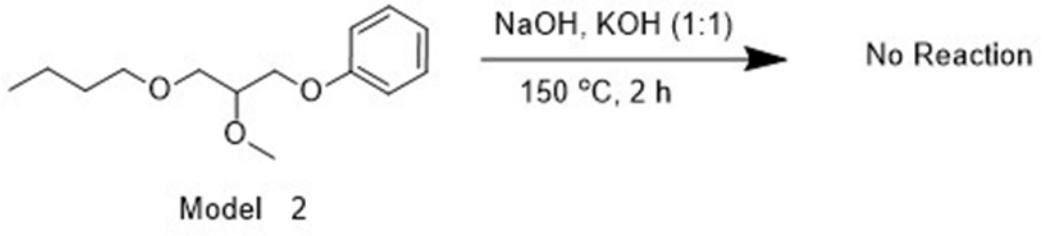

Finely ground NaOH (0.1 g, 2.5 mmol) and KOH (0.14 g, 2.5 mmol) were added to a 50 mL Schlenk flask. Then Model 2 (0.2 g, 0.84 mmol) was transferred into the flask. Finally, the flask was carefully flushed with nitrogen gas and placed in an oil bath set to 150 ˚C for two hours. After the reaction, aqueous sodium bicarbonate (saturated, 50 mL) was added to the Schlenk flask to dissolve the solid residue. The aqueous mixture was then transferred to a 250 mL separatory funnel. The organic material was then extracted with DCM (3 x 30 mL). The organic layers were then combined, and the solvent was removed under reduced pressure. The ^{1}HNMR can be found in Figure S66.

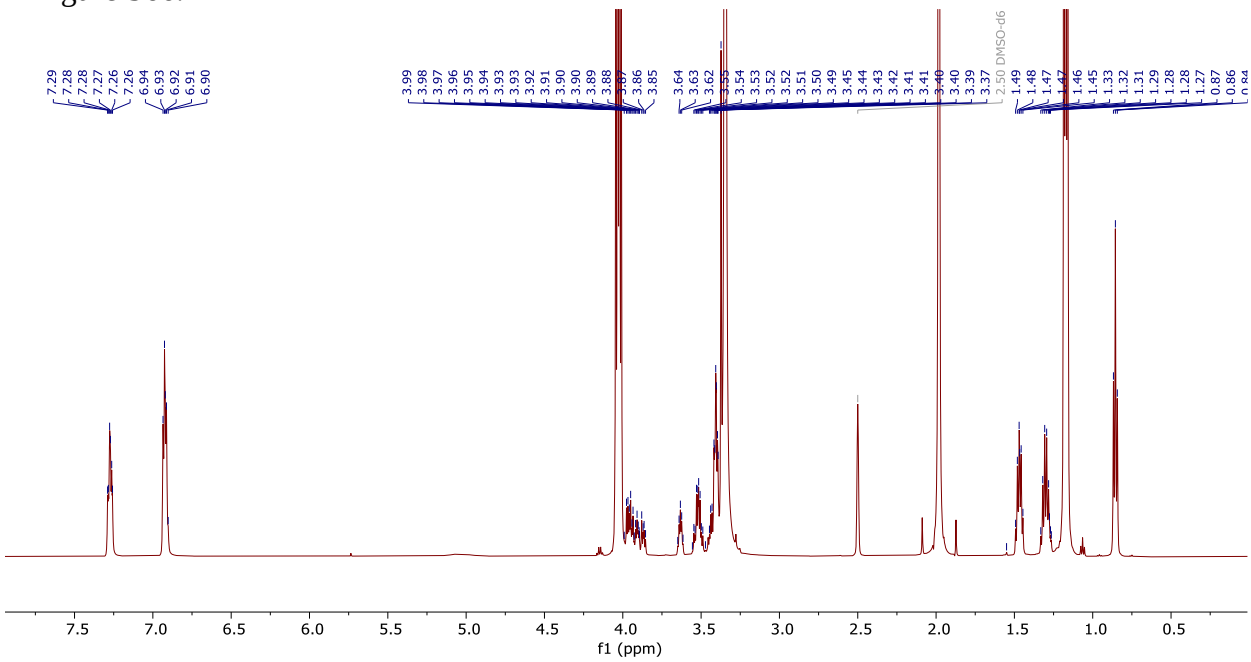

Figure S66. ^{1}HNMR of Model 2 150˚C degradation reaction extract in DMSO-d_6.

13. 3,3’-DDS degradation experiments

To evaluate the stability of sulfones under hot hydroxide conditions, we attempted to degrade 3,3’-DDS under various conditions shown below.

Scheme S9. Degradation of 3,3’-DDS

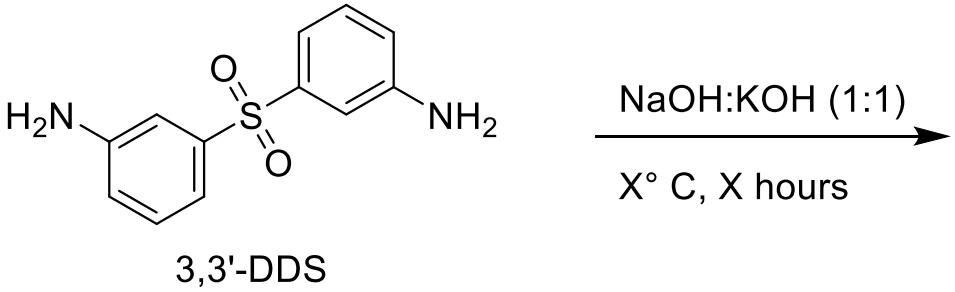

In a 50 mL Schlenk flask, a finely ground powder of NaOH (0.15 g, 3.75 mmol) and KOH (0.21 g, 3.75 mmol) were combined. Afterwards, 3,3’-DDS (0.1 g, 0.4 mmol) was added into the flask. Finally, the flask was carefully flushed with nitrogen gas and placed in a heated oil bath for X hours. Table S23 below shows the conditions used in each trial. Entries 1 and 2 were determined to have not reacted based on ^{1}H NMR and ^{13}C NMR. The ^{1}H NMR spectra of entry 3 does show a reaction and is shown in Figure S 67. Due to the transformation of 3,3’-DDS in entry 3, we state that the sulfone is unstable under these conditions.

Table S23. Summary of 3,3'-DDS degradation experiment.

Entry	Temperature (˚C)	Time (hours)	Reaction
1	150	2	No reaction
2	180	2	No reaction
3	190	6	Reaction

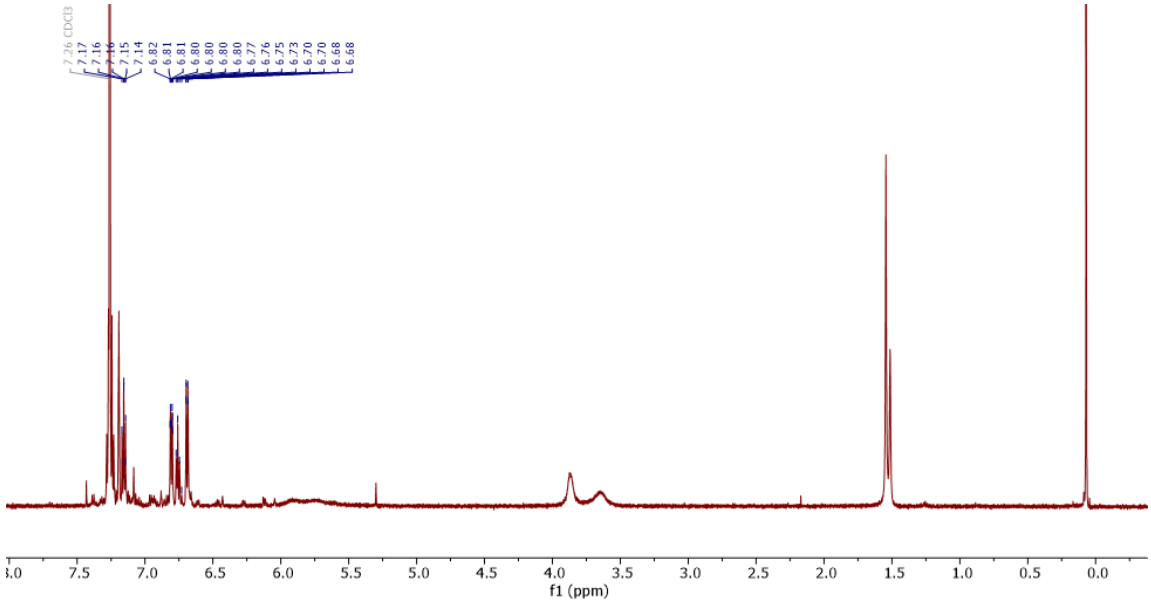

Figure S67. ^{1}HNMR of 3,3’-DDS degradation reaction extract in $CDCl_3$.

References:

1. H. Yan, C. Lu, D. Jing and X. Hou, *Polymer degradation and stability*, 2013, **98**, 2571-2582.
2. Y. Liu, J. Liu, Z. Jiang and T. Tang, *Polymer degradation and stability*, 2012, **97**, 214-220.
3. J. Jiang, G. Deng, X. Chen, X. Gao, Q. Guo, C. Xu and L. Zhou, *Composites Science and Technology*, 2017, **151**, 243-251.
4. Q. Zhao, J. Jiang, C. Li and Y. Li, *Polymer Degradation and Stability*, 2020, **179**, 109268.
5. R. C. DiPucchio, K. R. Stevenson, C. W. Lahive, W. E. Michener and G. T. Beckham, *ACS Sustainable Chemistry & Engineering*, 2023, **11**, 16946-16954.
6. A. Ahrens, A. Bonde, H. Sun, N. K. Wittig, H. C. D. Hammershøj, G. M. F. Batista, A. Sommerfeldt, S. Frølich, H. Birkedal and T. Skrydstrup, *Nature*, 2023, **617**, 730-737.
7. H. Sun, A. Ahrens, G. M. F. Batista, B. S. Donslund, A. K. Ravn, E. V. Schwibinger, A. Nova and T. Skrydstrup, *Green Chemistry*, 2024, **26**, 815-824.
8. J. TAKAHASHI and T. WAJIMA, *International Journal of the Society of Materials Engineering for Resources*, 2022, **25**, 85-89.
9. T. Wu, W. Zhan, X. Jia, H. Li, G. Sui and X. Yang, *Polymer Degradation and Stability*, 2022, **196**, 109849.
10. Y. Ren, H. Hu, Z. Lin, C. Cao, H. Liu, X. Li and H. Yao, *Chemical Engineering Journal*, 2024, **496**, 153792.
11. W. Nie, J. Liu, W. Liu, J. Wang and T. Tang, *Polymer Degradation and Stability*, 2015, **111**, 247-256.
12. X. Chen, X. Wang and D. Fang, *Fullerenes, Nanotubes and Carbon Nanostructures*, 2020, **28**, 1048-1058.